



## Research paper

## A highly potent CDK4/6 inhibitor was rationally designed to overcome blood brain barrier in glioblastoma therapy

Lei Yin<sup>a</sup>, Heng Li<sup>b</sup>, Wenjian Liu<sup>b</sup>, Zhenglin Yao<sup>b</sup>, Zhenzhen Cheng<sup>b</sup>, Huabei Zhang<sup>a,\*</sup>, Hui Zou<sup>b,\*\*</sup>

<sup>a</sup> Key Laboratory of Radiopharmaceuticals of Ministry of Education, College of Chemistry, Beijing Normal University, Beijing 100875, China

<sup>b</sup> Gan & Lee Pharmaceuticals, China

## ARTICLE INFO

## Article history:

Received 1 November 2017

Received in revised form

29 November 2017

Accepted 1 December 2017

Available online 6 December 2017

## Keywords:

Glioblastoma

CNS

CDK4/6 inhibitor

U87MG

Pharmacokinetics

Structure-activity relationship

## ABSTRACT

Glioblastoma multiforme (GBM) is the most common and deadliest of malignant brain tumors in adults. Disease development is associated with dysregulation of the cyclin D-CDK4/6-INK4-Rb pathway, resulting in increased proliferation; thus, CDK4/6 kinase inhibitors are promising candidates for GBM treatment. The recently developed CDK4/6 inhibitors, palbociclib, ribociclib, and abemaciclib, are effective in subcutaneous glioma models, but their blood-brain barrier (BBB) permeability is poor, limiting drug delivery to the central nervous system. Here, we designed and synthesized a series of novel CDK4/6 inhibitors with favorable BBB permeability for the treatment of GBM. Compound **11** exhibited a favorable pharmacological profile and significant penetration of the BBB with the  $K_p$  value of 4.10 and the  $K_{p,uu}$  value of 0.23 in mice after an oral dose of 10 mg/kg.  $IC_{50}$  values for CDK4/cyclin D1 and CDK6/cyclin D3 were 3 nM and 1 nM, respectively. *In vivo* studies with an orthotopic xenograft mouse model of GBM showed that **11** had tumor growth inhibition values ranging from 62% to 99% for doses ranging from 3.125 to 50 mg/kg, and no significant body weight loss was observed. The increase in life span based on the median survival time of vehicle-treated animals in mice administered a dose of 50 mg/kg was significant at 162% ( $p < 0.0001$ ). These results suggest that compound **11** is a promising candidate for further investigation as an effective drug for the treatment of GBM.

© 2017 Published by Elsevier Masson SAS.

## 1. Introduction

Glioblastoma multiforme (GBM) is the most common and aggressive malignant brain tumor in adults. Patients with this disease have a very poor prognosis, with an estimated median survival between 12 and 18 months with maximal treatment, a 5-year survival rate <10%, and a mortality rate close to 100% [1]. Currently, the standard-of-care for GBM consists of surgical resection followed by radiotherapy in combination with temozolomide [2,3] (approved by the U.S. Food and Drug Administration [FDA] in 1999), which together with the carmustine-based Gliadel wafer [4] (approved in 1996), are the only FDA-approved chemotherapeutic drugs for the treatment of newly diagnosed GBM. Considering the lack of recent progress in the treatment of this devastating disease,

novel therapeutic options are urgently needed.

The normal cell cycle is divided into four phases, G1, S, G2, and M, with checkpoints that are vital cellular components guarding the integrity of genetic information [5]. The cyclin D-CDK4/6-INK4/Rb pathway regulates G1 progression to the S phase of the cell cycle [6,7]. CDK4/6 mediates the transition from G1 to S phase by binding to D-type cyclins; the resulting CDK4/6-cyclin D complex phosphorylates the negative growth regulator Rb, causing it to dissociate from E2F transcription factors, which allows them to participate in DNA replication and cell division. Increased CDK4/6-cyclin D activity [8–10], which leads to dysregulation of the cyclin D-CDK4/6-INK4/Rb pathway and uncontrolled cell proliferation, has been observed in most cases of GBM [11]. Furthermore, CDK4/6 amplification is frequently observed in diffuse intrinsic pontine gliomas [12]. These considerations make CDK4/6 kinase inhibitors promising candidates for cancer treatment, including GBM [13].

Palbociclib (trade name: Ibrance, approved by FDA in February 2015 to treat HR+/HER2-breast cancer) [14], amebaciclib [15] and ribociclib (trade name: Kisqali, approved by FDA in March 2017 to

\* Corresponding author.

\*\* Corresponding author.

E-mail addresses: [hbzhang@bnu.edu.cn](mailto:hbzhang@bnu.edu.cn) (H. Zhang), [hzou@phanesbio.com](mailto:hzou@phanesbio.com) (H. Zou).

treat HR+/HER2-breast cancer) [16] are recently developed CDK4/6 inhibitors currently undergoing clinical testing as potential chemotherapeutics for the treatment of primary or secondary brain tumors [17]. Palbociclib was shown to promote survival in a genetic mouse model of brainstem glioma [18], but its unbound brain-to-plasma partition coefficient ( $K_{p,uu}$ ) was only 0.01, 5 min after intravenous administration of 1 mg/kg [19,20]. Amebaciclib had a  $K_{p,uu}$  value of 0.03 in mice after an oral dose of 30 mg/kg, indicative of active efflux [19]. The  $K_{p,uu}$  value for ribociclib was 0.12 in CD1 nude mice after oral administration of 100 mg/kg using cerebral microdialysis [16]. Therefore, there is a clear and pressing need to develop a potent and selective CDK4/6 inhibitor with high BBB permeability that is capable of acting on its target at therapeutically beneficial concentrations in the CNS without impacting the safety of the drug by limiting systemic exposure [18,19,21–23].

In this study, we prepared a series of CDK4/6 inhibitor analogues, from which structure-activity relationships were derived based on CDK4/6 inhibitory potency and selectivity against CDK1. After structure optimization, compound **11** was chosen to investigate its selectivity against another 83 kinases, anti-proliferation properties in the U87MG GBM cell line, physicochemical properties, pharmacokinetics (PK) including BBB permeability and Rb phosphorylation in mice bearing human colon cancer COLO 205 cell xenografts. In addition, *in vivo* studies investigating the effectiveness of compound **11** for tumor inhibition in an U87MG-Luc orthotopic xenograft mouse model of GBM were performed.

## 2. Results and discussion

### 2.1. Drug design

It is inherently important for drug candidates to freely cross the BBB to achieve the required concentrations in the brain. Therefore, a key consideration in drug design is the affinity of the drug candidate for the efflux transport proteins, P-glycoprotein (P-gp) and breast cancer resistance protein (BCRP), which are highly expressed in the BBB [24]. Molecules that are significant substrates for P-gp and BCRP have limited BBB permeability [21]. A number of physicochemical properties such as topological polar surface area (TPSA) and/or the number of hydrogen bond donors (HBDs) are considered to be important factors for determining the degree of transport-mediated efflux [25]. For example, an analysis conducted at Eli Lilly on an internal dataset of 2000 compounds found that molecules with a TPSA <60 Å<sup>2</sup> exhibited a high likelihood (94%) of not being P-gp substrates, whereas more than 75% of P-gp substrates had a TPSA >60 Å<sup>2</sup> [26]. A review of the medicinal chemistry literature by Hitchcock in 2012 provided general guidelines for minimizing P-gp recognition, which included having less than two HBDs and a TPSA <90 Å<sup>2</sup> (preferably <70 Å<sup>2</sup>) [27]. Fig. 1 [28] shows

the part of pyridyl-NH-pyrimidyl that is necessary for selective CDK4/6 inhibitors. As Fig. 2 further shows, NH-pyrimidyl forms hydrogen bonds with Val-101 in the CDK6 hinge region, and the pyridyl forms a favorable electrostatic interaction with His-100 in CDK6, but the corresponding residue is Phe-82 in CDK1/2, so the pyridyl is important for CDK1/2 selectivity [29,30]. Therefore, we anticipated that modifying the groups connected to pyrimidyl and pyridyl would meet the criterion of BBB permeability and selective CDK4/6 inhibitors. To this end, we initially obtained compound **5** (Fig. 3) with a PSA of 60 Å<sup>2</sup> (calculated with Sybyl-X.v2.0). For comparison, the CDK4/6 inhibitors abemaciclib, palbociclib, and ribociclib have PSAs of 62, 101, and 82 Å<sup>2</sup> (calculated with Sybyl-X.v2.0), respectively, and the median TPSA of the 119 marketed CNS drugs is 45 Å<sup>2</sup> [31]. Therefore, **5** was the lead compound with a PSA indicative of appropriate BBB permeability. Its IC<sub>50</sub> for inhibition of CDK6/cyclin D3 was encouraging at 2 nM, but it had a poor hepatic intrinsic clearance ( $CL_{int}$ ) value of 171.4 µL/min/mg in cluster of differentiation 1 (CD-1) mouse liver microsomes (Table 1). A wide variety of drugs and other foreign compounds undergo N-dealkylation by enzyme systems localized in the microsomal fraction of the liver [32]. Thus, we prepared the N-dealkylated analogue of compound **5**, which was missing the methylene bridge between the pyridine and piperazine rings (**8**). It was encouraging to find that the modified analogue had an acceptable and reduced  $CL_{int}$  value of 49.2 µL/min/mg (Table 1), which was proof of concept that the structure could be modified to obtain more satisfactory ADME properties. Next, we synthesized a

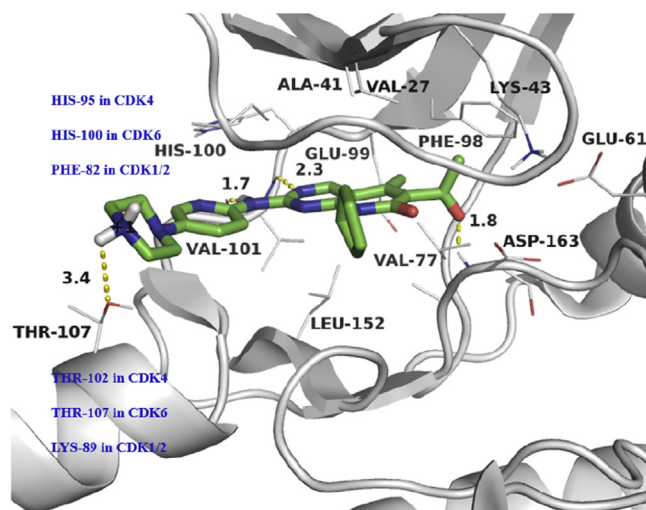


Fig. 2. The interaction between palbociclib and human CDK6-Vcyclin: PDB ID: 2EUF; prepared by Sybyl X V2.0, presented by PyMOL V1.1.

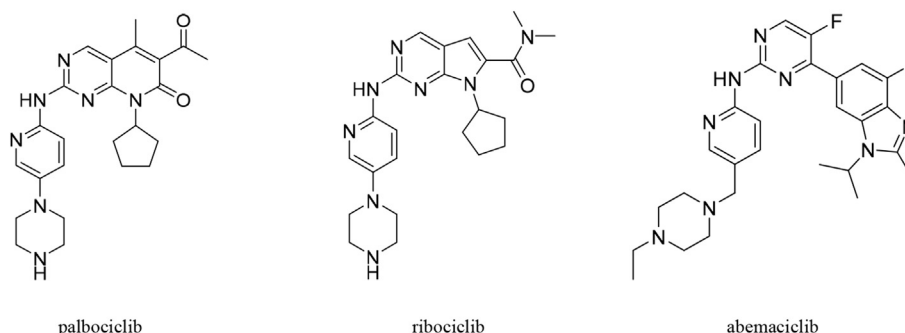


Fig. 1. Chemical structure of palbociclib, ribociclib, and abemaciclib.

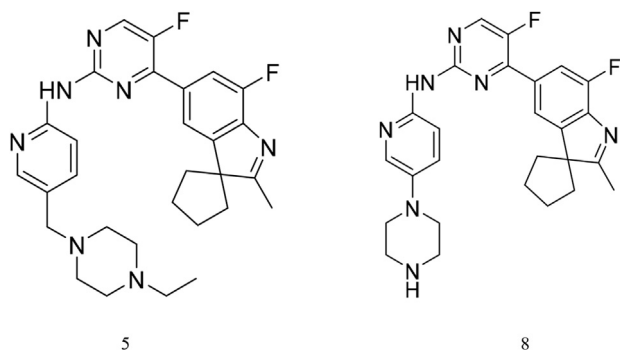


Fig. 3. Chemical structure of compounds **5** and **8**.

series of analogues based on the core structure of **5**, and investigated the structure–activity relationship to identify a compound with good CDK4/6 inhibitory activity, good selectivity for CDK4/6 over CDK1/2, and excellent BBB permeability.

## 2.2. Structure–activity relationship

After the core was determined, more analysis about the interaction between the selective CDK4/6 inhibitor and CDK1/2/4/6 was performed. As Fig. 2 shows, the terminal amine of piperazinyl may make a favorable polar interaction with Thr-107 in CDK6 (Thr-102 in CDK4), but it may make an unfavorable electrostatic repulsion with Lys-89 in CDK1/2, which will significantly improve the CDK4/6 inhibitors' selectivity over CDK1/2 [29,30], and the interaction between the terminal amine and Thr-107 was supported based on the molecular docking simulation study between compound **11** and CDK6 (Fig. 4d). On the basis of the molecular docking simulation study (Fig. 4a), we can see that the fluorine atom at the C-7' position of benzoheterocycle formed an F–H bond with Lys-43 in CDK6, which may be helpful in improving the activity against CDK6. However, those residues that interacted with the fluorine atom are highly hydrophilic, such as Asp-163, Lys-43, Glu-61, Phe-164, and Gly-65. The introduced hydrophilic group in this region may be favorable to activity against CDK6, but more introduced heteroatoms and longer side chains may produce higher PSAs and molecular weights, which are unfavorable to CNS drugs. The fluorine atom at the C-5 position of the pyrimidine moiety formed a favorable hydrophobic interaction with Ala-41, Val-27, Phe-98, and Val-77 in CDK6, which may be important to improve the activity over CDK6, while the region occupied by cyclopentane can hold a variety of hydrophobic groups (Fig. 4a). Based on the analysis above, more compounds were rationally designed to meet the criterion of BBB permeability and selective CDK4/6 inhibitors. To elucidate the importance of the R<sub>2</sub> or R<sub>3</sub> group for potent CDK4/6 inhibition, we prepared several analogues (compounds **1–7**, Table 2). Compounds where both R<sub>2</sub> and R<sub>3</sub> were methyl or formed part of a cyclobutyl ring (**1** and **4**) weakly inhibited CDK6/cyclin D3. However, compounds **2**, **3**, and **5–7**, in which R<sub>2</sub> and R<sub>3</sub> were methyl, ethyl, ethyl, ethyl, and cyclopentyl, respectively, had significantly higher inhibitory activity against CDK6/cyclin D3, suggesting that the steric bulkiness of R<sub>2</sub> and R<sub>3</sub> substituents is

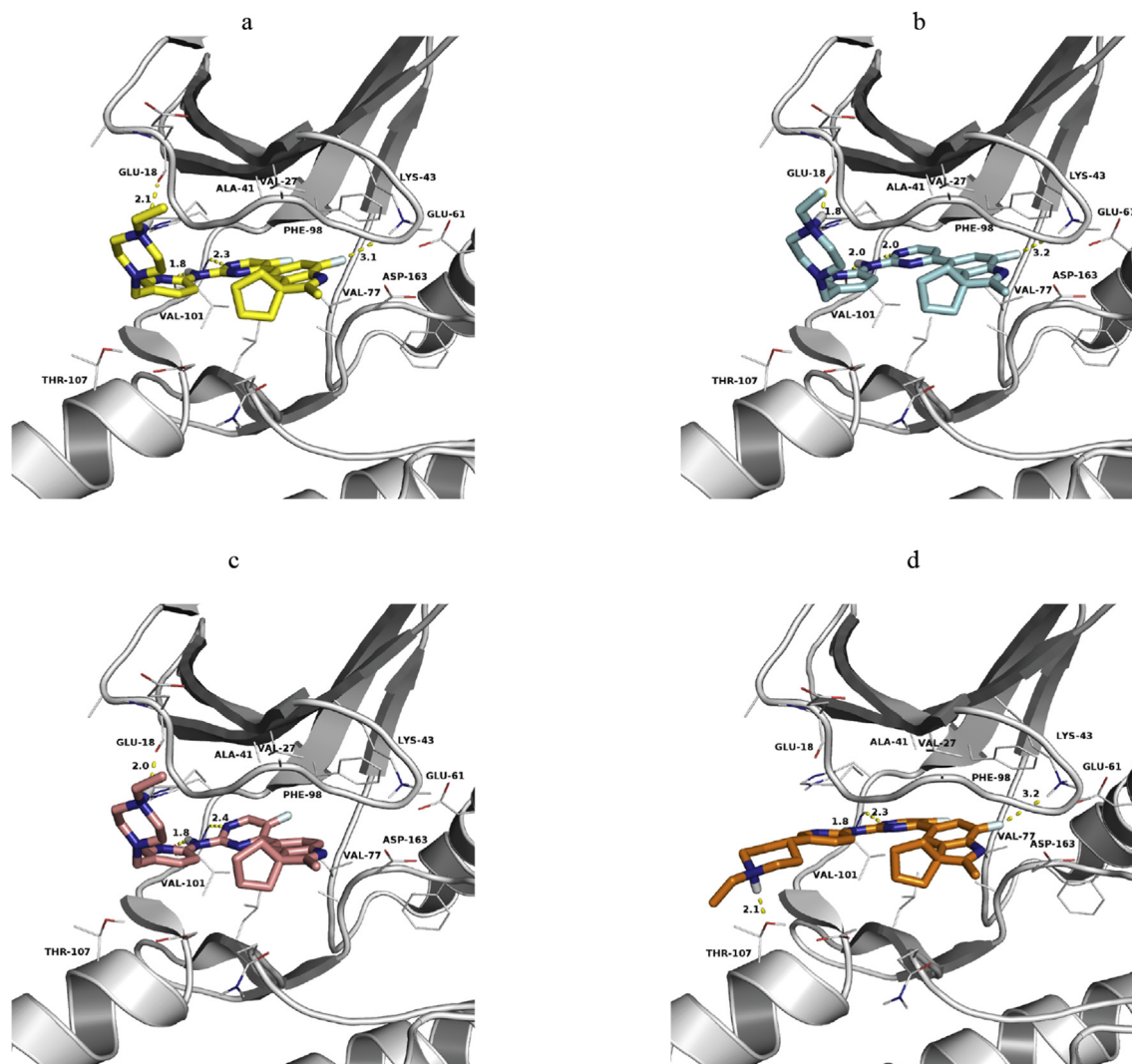
important for kinase inhibition. As we expected, fluorine substitution at the C-5 position led to a remarkable decrease in the IC<sub>50</sub> for CDK6/cyclin D3 from 86 nM to 2 nM for compounds **6** and **5**, respectively, which showed that the hydrophobic interaction is important between the fluorine atom and Ala-41, Val-27, Phe-98, and Val-77 in CDK6. The second reason may be that the fluorine atom at the C-5 position of the pyrimidine moiety formed a favorable interaction with a hydrogen atom at the C-6' of the adjacent benzoheterocycle, which may be important to stabilize the active conformation. The third reason may be due to the introduction of a fluorine atom at the C-5 position that increases the acidity of the bridging N–H between pyridine and pyrimidine moieties, which increases the strength of hydrogen bonding with the backbone carbonyl of the kinase hinge region [33]. The three factors together determined the difference in the activity of the two compounds, and the docking score of compound **6** is 8.97, which is significantly lower than 11.66 (the docking score of compound **5**, Fig. 4a). As Fig. 4c shows, the F–H bond between the fluorine atom at the C-7' position of benzoheterocycle and Lys-43 in CDK6 is in the hydrophilic subpocket formed by Asp-163, Lys-43, Glu-61, Phe-164, and Gly-65, so the favorable interaction may be not significant, which was confirmed by the IC<sub>50</sub> for CDK6/cyclin D3 only decreasing from 7 nM in **7** to 2 nM in **5**. However, a marked increase in the selectivity over CDK1 was observed in compound **5** (IC<sub>50</sub> = 2239 nM) with a fluorine atom (R<sub>1</sub> = F) compared to the analogue **5** (IC<sub>50</sub> = 268 nM; CDK1/CDK6 = 1120 and 38, for **5** and **7**, respectively), which showed that the fluorine atom is important to selectivity over CDK1 (Table 2).

Having ascertained the importance of fluorine substitution in X<sub>1</sub> and R<sub>1</sub>, and the presence of the sterically bulky and conformationally restricted cyclopentyl moiety in R<sub>2</sub> and R<sub>3</sub> to maximize the inhibition potency of CDK6/cyclin D3 (i.e., **5**), this compound was used as a lead for the synthesis of additional analogues with different substitutions in R (piperazine or piperidine moieties) linked to the core pyridine group. We investigated the inhibitory activity against CDK6/cyclin D3, CDK4/cyclin D1, and CDK1/cyclin A2 (Table 3), and the CDK1/CDK6 selectivity of these new analogues (compounds **8–16**, Table 3). Regarding CDK6/cyclin D3 activity, the greatest inhibition was observed in **10** bearing a simple unsubstituted piperidine moiety (0.4 nM), and the least inhibition was observed in **12** with an N-methyl piperazine moiety (88 nM). We were also interested in identifying CDK4/6 inhibitors with high selectivity over other off-target kinases; however, because of evolutionary conservation of the ATP-binding site, the discovery of highly selective CDK inhibitors remains a formidable challenge [34]. The substitution pattern also had a considerable effect on CDK1/CDK6 selectivity, with the (CDK1/cyclin A2) to (CDK6/cyclin D3) IC<sub>50</sub> ratio ranging from 16 (**12**) to 2707 (**11**). The piperazine substituted analogue with the greatest CDK6/cyclin D3 inhibitory potency was **14** with a terminal alcohol linked via an ethyl chain to the piperazine ring (IC<sub>50</sub> = 6 nM). Interestingly, the analogous piperidine analogue **15** not only had higher inhibitory potency (IC<sub>50</sub> = 0.5 nM) but also had more than 6-fold selectivity (CDK1/CDK6) over **14**. These results highlight the importance of controlling the number of hydrogen bond acceptors in the ring linked to the core pyridine to achieve both optimal kinase inhibitor properties and good selectivity.

Table 1  
Stability of compounds **5** and **8** in mouse liver microsomes.

Compound	t <sub>1/2</sub> (min)	CL (μL/min/mg)	Remaining (t = 60 min)	Remaining (NCF <sup>a</sup> = 60 min)
<b>5</b>	8.1	171.4	1.0%	81.1%
<b>8</b>	28.2	49.2	24.0%	94.4%

<sup>a</sup> Test compound incubated with microsomes without the NADPH-regenerating system for 60 min.

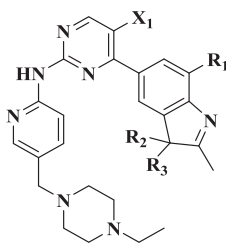


**Fig. 4.** The interaction between compounds **5**, **6**, **7** and **11** and human CDK6-Vcyclin; presented by PyMOL V1.1: a) on the basis of the molecular docking simulation study between compound **5** and human CDK6-Vcyclin, the docking score is 11.66. b) On the basis of the molecular docking simulation study between compound **6** and human CDK6-Vcyclin, the docking score is 8.97. c) On the basis of the molecular docking simulation study between compound **7** and human CDK6-Vcyclin, the docking score is 9.90. d) On the basis of the molecular docking simulation study between compound **11** and human CDK6-Vcyclin, the docking score is 11.53.

We screened more compounds (**17–38**, Table 4) for *in vitro* inhibitory activity against CDK6/cyclin D3 and CDK4/cyclin D1, and for CDK1/CDK6 selectivity. A decrease in the inhibitory potency, particularly the selectivity, was also observed in the piperidine analogue **27** ( $IC_{50} = 4$  nM and 8 nM) with a missing fluorine ( $R_1 = H$ ) compared to the analogue **11** ( $IC_{50} = 1$  nM and 3 nM; CDK1/CDK6 = 2707 and 12, for **11** and **27** respectively). This once again highlights the importance of the fluorine atom in the  $R_1$  position for achieving both satisfactory inhibitory activity and selectivity. But the PK properties of most of the compounds were poor in the rats (Table S1), interestingly, compound **11**, which had the most satisfactory properties in terms of CDK6 inhibitory activity and CDK1/CDK6 selectivity, also showed acceptable PK properties in the rats compared to other compounds. Its bioavailability is 66%, and  $AUC_{0-24hr}$  is 1531 ng h/mL after administration of P.O. 5 mg/kg (Table S1), which encouraged us to conduct more studies of this compound. Some general observations were derived from these structure-activity relationships. First, maintaining both  $X_1$  and  $R_1 = F$  was crucial for achieving optimal *in vitro* results. Second,

increasing the bulkiness and decreasing the conformational freedom of the aliphatic group in the  $R_2$  and  $R_3$  positions resulted in marked improvements in potency and selectivity (compare **11** with a bulky cyclopentyl to **28**, where  $R_2 = methyl$  and  $R_3 = ethyl$ , respectively). Third, the number of hydrogen acceptors in the ring linked to the core pyrimidine was very important (compare **11** to **12**, with an N-methyl piperidine and N-methyl piperazine moieties, respectively). Overall, compound **11** had the most satisfactory properties in terms of CDK6 inhibitory activity, CDK1/CDK6 selectivity (Table 3), and acceptable PK properties in rats. In addition, **11** inhibited CDK4/cyclin D1 with an  $IC_{50}$  value of 3 nM, and also exhibited good CDK2/CDK6 selectivity (2321 fold, Table 5). Therefore, **11** was chosen for additional *in vivo* investigations. In comparison, the  $IC_{50}$  value of palbociclib, ribociclib, and abemaciclib for CDK6 inhibition was 19 nM, 28 nM, and 5 nM, respectively (assayed using the protocol in the Experimental section). Thus, **11** represents the discovery of a compound with particularly potent CDK6 inhibition ( $IC_{50} = 1$  nM), good CDK1/CDK6 selectivity (2707 fold), and acceptable PK properties in rats.



**Table 2**CDK4/6/1 inhibitory potency (IC<sub>50</sub>) and CDK1/CDK6 selectivity with different R<sub>1</sub>, R<sub>2</sub>, R<sub>3</sub> and X<sub>1</sub> substituents.

Cpd	X <sub>1</sub>	R <sub>1</sub>	R <sub>2</sub>	R <sub>3</sub>	CDK6 <sup>b</sup> IC <sub>50</sub> (nM)	CDK4 <sup>c</sup> IC <sub>50</sub> (nM)	CDK1 <sup>d</sup> IC <sub>50</sub> (nM)	CDK1/CDK6 <sup>e</sup>
<b>1</b>	F	F	methyl	methyl	159	NA <sup>a</sup>	NA <sup>a</sup>	NA <sup>a</sup>
<b>2</b>	F	F	methyl	ethyl	26	33	966	37
<b>3</b>	F	F	ethyl	ethyl	47	NA <sup>a</sup>	436	9
<b>4</b>	F	F	cyclobutyl		2147	NA <sup>a</sup>	NA <sup>a</sup>	NA <sup>a</sup>
<b>5</b>	F	F	cyclopentyl		2	12	2239	1120
<b>6</b>	H	F	cyclopentyl		86	NA <sup>a</sup>	NA <sup>a</sup>	NA <sup>a</sup>
<b>7</b>	F	H	cyclopentyl		7	13	268	38

<sup>a</sup> Data not available.<sup>b</sup> CDK6/cyclin D3.<sup>c</sup> CDK4/cyclin D1.<sup>d</sup> CDK1/cyclin A2.<sup>e</sup> Ratio of CDK1/cyclin A2 IC<sub>50</sub> (nM) to CDK6/cyclin D3 IC<sub>50</sub> (nM).

### 2.3. Selective inhibitory activity of compound **11** against 83 kinases

Compound **11** was tested against several serine-threonine and tyrosine kinases in single-point binding at 0.1 μM and 1 μM. The highest inhibition ratio was 56% against janus kinase 3 (JAK3) and NF-κB-inducing kinase (NIK) at 0.1 μM (Table S2), and their IC<sub>50</sub> values were determined. The IC<sub>50</sub> value was 154 nM for JAK3 and the selectivity against CDK6/cyclin D3 was 154-fold, while the IC<sub>50</sub> value was 45 nM for NIK and the selectivity against CDK6/cyclin D3 was 45-fold (Table 5), which showed the selectivity against JAK3 and NIK was moderate with an IC<sub>50</sub> of 1 nM for CDK6/cyclin D3 and of 3 nM for CDK4/cyclin D1.

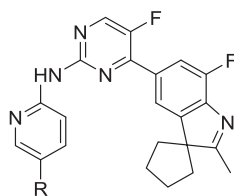
### 2.4. Compound **11** is a potent anti-proliferative agent that arrests U87MG cell line exclusively in G<sub>1</sub>

Compound **11**, which was found to be the most potent and selective CDK4/6 inhibitor, was further tested in the U87MG GBM cell line. Its IC<sub>50</sub> was 15.3 ± 2.9 nM (Fig. 5a) in the anti-proliferation assay, which was indicative of significant anti-proliferation activity in these cells compared to the positive control compound abemaciclib (IC<sub>50</sub> = 48.1 ± 11.3 nM), so we concluded it is more likely that compound **11** has greater efficacy in treating brain tumors compared to abemaciclib. U87MG cells exposed to varying concentrations of compound **11** for 24 h showed a dose-related increase in G<sub>1</sub> arrest, and a significant increase in the percentage of cells in G<sub>1</sub> was found in as little as 13.72 nM of compound **11** (Fig. 5b). Maximum effects were attained at 41.15 nM, and an exclusive G<sub>1</sub> arrest was maintained even at concentrations as high as 10 μM, which was consistent with high selectivity for CDK4/6 versus CDK1/2 (Table 5).

### 2.5. Physicochemical properties of compound **11**

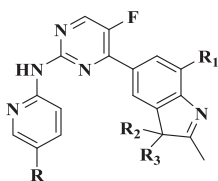
The human brain is a uniquely complex and sophisticated organ, and the blood-brain barrier protects the CNS from being invaded by external substances. Thus, it is difficult for compounds to enter the

brain for therapeutic purposes compared to other organs. Regarding the physicochemical properties of CNS drugs, there are some special requirements compared to the rule of 5 [35]; a key consideration is that the compound can not be a substrate of P-gp and BCRP, which are highly expressed in the BBB [24]. In 1998, Van der Waterbeemd et al. summarized the physicochemical properties of 125 CNS and non-CNS drugs and found that CNS penetration improved if the molecular weight (MW) was <450 Da [36]. In 2009, Waring [37] summarized 9571 Caco-2 measurements and found that passive permeability was influenced by both MW and lipophilicity (logD); as the MW increased, the logD needed to also increase to achieve good passive permeability in Caco-2 cells and to avoid becoming a P-gp substrate. When the MW was 450–500, AZLogD (the AZlogD algorithm is an in-house protocol for calculating logD in AstraZeneca, and in their experience, is the most accurate method for calculating the logD of drug candidates) needed be higher than >3.4 to achieve permeability into the brain. As shown in Table 6, the MW of compound **11** was 488.59 Da, and the logD<sub>7.4</sub> was 3.49; these values are consistent with the description by Waring. In 2002, Hitchcock [38] reviewed the medicinal chemistry literature and proposed general guidelines for minimize P-gp-mediated efflux including a hydrogen bond donor (HBD) count <2 and polar surface area (PSA) < 90 Å<sup>2</sup> (preferably <70 Å<sup>2</sup>). The number of HBDs of compound **11** was 1, which is similar to the mean HBD (1.1) of CNS drugs [31]. The PSA of compound **11** was 58 Å<sup>2</sup>, which is within the preferred PSA (<70 Å<sup>2</sup>) of CNS drugs (Table 6). In 2005, Pajouhesh and Lenz [39] reviewed marketed CNS drugs, and found that the properties of a successful CNS drug candidate included a logarithm of its partition coefficient (clogP) < 5 and a dissociation constant (pKa) ranging from 7.5 to 10.5. The clogP of compound **11** was calculated to be 5.52 by the Sybyl-X v2.0 computer program, which was slightly higher than 5 mentioned above and the higher clogP may be caused by the different computer program; the pKa of compound **11** was 8.19, which is within the 7.5–10.5 range (Table 6). Therefore, we concluded compound **11** had the properties of a successful CNS drug.

**Table 3**CDK4/6/1 inhibitory potency (IC<sub>50</sub>) and CDK1/CDK6 selectivity with different R substituents.

Cpd	R	CDK6/cyclin D3 IC <sub>50</sub> (nM)	CDK4/cyclin D1 IC <sub>50</sub> (nM)	CDK1/cyclin A2 IC <sub>50</sub> (nM)	CDK1/CDK6 <sup>a</sup>
8		6	8	152	25
9		4	6	1071	268
10		0.4	8	327	818
11		1	3	2707	2707
12		88	NA <sup>b</sup>	1444	16
13		16	18	1160	72
14		6	17	328	55
15		0.5	NA <sup>b</sup>	176	352
16		10	78	1056	106

<sup>a</sup> Ratio of CDK1/cyclin A2 IC<sub>50</sub> (nM) to CDK6/cyclin D3 IC<sub>50</sub> (nM).<sup>b</sup> Data not available.

**Table 4**CDK4/6/1 inhibitory potency (IC<sub>50</sub>) and CDK1/CDK6 selectivity with different R<sub>1</sub>, R<sub>2</sub>, R<sub>3</sub>, R substituents.

Cpd	R	R <sub>1</sub>	R <sub>2</sub>	R <sub>3</sub>	CDK6 <sup>a</sup> IC <sub>50</sub> (nM)	CDK4 <sup>b</sup> IC <sub>50</sub> (nM)	CDK1 <sup>c</sup> IC <sub>50</sub> (nM)	CDK1/CDK6 <sup>d</sup>
17		F	methyl	methyl	43	NA <sup>e</sup>	2224	52
18		F	methyl	ethyl	3	44	84	28
19		F	ethyl	ethyl	3	3	82	27
20		H	cyclopentyl		4	4	234	58
21		H	cyclopentyl		4	4	27	7
22		F	ethyl	ethyl	9	10	96	11
23		F	methyl	ethyl	1	6	153	153
24		F	methyl	ethyl	65	NA <sup>e</sup>	65	1
25		H	cyclopentyl		28	NA <sup>e</sup>	135	5

(continued on next page)

Table 4 (continued)

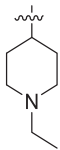
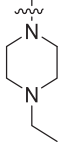
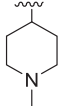
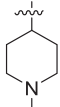
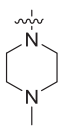
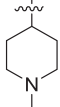
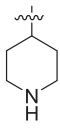
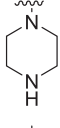
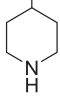
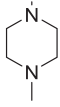
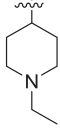
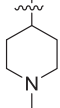
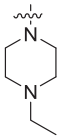
Cpd	R	R <sub>1</sub>	R <sub>2</sub>	R <sub>3</sub>	CDK6 <sup>a</sup> IC <sub>50</sub> (nM)	CDK4 <sup>b</sup> IC <sub>50</sub> (nM)	CDK1 <sup>c</sup> IC <sub>50</sub> (nM)	CDK1/CDK6 <sup>d</sup>
26		H	cyclopentyl		52	NA <sup>e</sup>	915	18
27		H	cyclopentyl		4	8	50	12
28		F	methyl	ethyl	9	16	131	14
29		H	cyclopentyl		9	15	417	46
30		F	methyl	ethyl	12	16	216	18
31		F	methyl	ethyl	6	NA <sup>e</sup>	110	18
32		F	methyl	methyl	59	NA <sup>e</sup>	NA <sup>b</sup>	NA <sup>b</sup>
33		H	methyl	ethyl	10	28	142	14
34		H	methyl	ethyl	16	NA <sup>e</sup>	166	10
35		H	methyl	ethyl	5	35	112	22
36		H	methyl	ethyl	19	42	125	6
37		H	methyl	ethyl	9	18	54	6



Table 4 (continued)

Cpd	R	R <sub>1</sub>	R <sub>2</sub>	R <sub>3</sub>	CDK6 <sup>a</sup> IC <sub>50</sub> (nM)	CDK4 <sup>b</sup> IC <sub>50</sub> (nM)	CDK1 <sup>c</sup> IC <sub>50</sub> (nM)	CDK1/CDK6 <sup>d</sup>
38		H	methyl	ethyl	4	NA <sup>e</sup>	101	25

<sup>a</sup> CDK6/cyclin D3.<sup>b</sup> CDK4/cyclin D1.<sup>c</sup> CDK1/cyclinA2.<sup>d</sup> Ratio of CDK1/cyclin A2 IC<sub>50</sub> (nM) to CDK6/cyclin D3 IC<sub>50</sub> (nM).<sup>e</sup> Data not available.

Table 5

Inhibitory activity and selectivity of compound **11** against CDK, JAK3, and NIK.

CDK1/cyclin A2 IC <sub>50</sub> (nM)	2707
CDK2/cyclin E1 IC <sub>50</sub> (nM)	2321
CDK4/cyclin D1 IC <sub>50</sub> (nM)	3
CDK6/cyclin D3 IC <sub>50</sub> (nM)	1
JAK3 (nM)	154
NIK (nM)	45
CDK1/CDK6 <sup>a</sup>	2707
CDK2/CDK6 <sup>b</sup>	2321
JAK3/CDK6 <sup>c</sup>	154
NIK/CDK6 <sup>d</sup>	45

<sup>a</sup> Ratio of CDK1/cyclin A2 IC<sub>50</sub> (nM) to CDK6/cyclin D3 IC<sub>50</sub> (nM).<sup>b</sup> Ratio of CDK2/cyclinE1 IC<sub>50</sub> (nM) to CDK6/cyclinD3 IC<sub>50</sub> (nM).<sup>c</sup> Ratio of JAK3 IC<sub>50</sub> (nM) to CDK6/cyclin D3 IC<sub>50</sub> (nM).<sup>d</sup> Ratio of NIK IC<sub>50</sub> (nM) to CDK6/cyclin D3 IC<sub>50</sub> (nM).

## 2.6. Bidirectional flux studies in transfected MDCK and Caco2 cell lines

The bidirectional flux of compound **11** was evaluated in wild-type MDCK II cells and MDR1-MDCK II cells overexpressing human P-gp (Table 7). In wild-type MDCK II cells, in the absence of a P-gp inhibitor (GF120918), the mean apparent passive permeability coefficient  $P_{app}(A-B)$  was  $0.17 \times 10^{-6}$  cm/s; the  $P_{app}(A-B)$  in the presence of the P-gp inhibitor was  $0.36 \times 10^{-6}$  cm/s. According to the internal standard (IS), the permeability was poor when  $P_{app}(A-B)$  was lower than  $1.0 \times 10^{-6}$  cm/s. However, the  $P_{app}(A-B)$  may be significantly underestimated because their recovery is only 4.85% and 6.36% respectively, but their total recovery is 87.19% and 103.63%, respectively, which showed that there is the propensity to partition into the cell monolayer for compound **11**. The low recovery and high total recovery (A–B) were also found in the MDR1-MDCK II cells overexpressing human P-gp. In the absence of the P-gp inhibitor, the  $P_{app}(A-B)$  in MDR1-MDCK II cells was  $0.71 \times 10^{-6}$  cm/s; the  $P_{app}(A-B)$  in the presence of the P-gp inhibitor in MDR1-MDCK II cells was  $0.81 \times 10^{-6}$  cm/s, which showed that the P-gp inhibitor had almost no influence on the  $P_{app}(A-B)$  of compound **11** in MDR1-MDCK II cells overexpressing human P-gp. In addition, in the absence of the P-gp inhibitor, the efflux ratio (ER) in MDR1-MDCK II cells was 0.71 and the net efflux ratio (NER) was 0.18, which showed that compound **11** was not a substrate of P-gp. This conclusion was further confirmed by the ER (0.59) and NER (0.21) in the presence of the P-gp inhibitor, which showed that inhibiting P-gp had almost no influence on the ER and NER of compound **11** in MDR1-MDCK II cells overexpressing human P-gp. The bidirectional flux of compound **11** was also evaluated in the

Caco-2 cell line with or without a BCRP inhibitor (Table 8). In the absence of a BCRP inhibitor, the  $P_{app}(A-B)$  was  $0.89 \times 10^{-6}$  cm/s, according to the IS, the permeability was moderate when  $P_{app}(A-B)$  was between  $0.5 \times 10^{-6}$  cm/s and  $2.5 \times 10^{-6}$  cm/s. But the  $P_{app}(A-B)$  may be significantly underestimated because their recovery is only 6.88%, but their total recovery is 72.00%, which showed there is the propensity to partition into the cell monolayer for the compound **11**. This trend was also found in Caco-2 cells treated with a BCRP inhibitor (Novobiocin). In the absence of the BCRP inhibitor, the ER was 0.82, which showed that compound **11** is not a substrate of transporters expressed in Caco-2 cells; for example, P-gp and BCRP. In the presence of the BCRP inhibitor, the  $P_{app}(A-B)$  was  $0.65 \times 10^{-6}$  cm/s, which was close to the  $P_{app}(A-B)$  in the absence of the BCRP inhibitor, and the ER was 0.77, which further confirmed that compound **11** was not a substrate of BCRP. As a comparison, abemaciclib and palbociclib are substrates of P-gp and BCRP [19].

## 2.7. PK and blood-brain distribution studies

The PK profile of compound **11** was investigated in ICR mice (Table 9), which were given an intravenous (i.v.) dose of 2 mg/kg and a per os (p.o.) dose of 5 mg/kg. The half-life ( $T_{1/2}$ ) following i.v. infusion was 9.1 h. The large steady-state volume of distribution of 17.8 L/kg suggested extravascular distribution. The CL of 25.2 mL/min/kg was moderate relative to the hepatic blood flow rate in ICR mice, and the maximum serum concentration ( $C_{max}$ ) and area under plasma drug concentration-time curve ( $AUC_{0-24 h}$ ) following a p.o. dose of 5 mg/kg were 134.0 ng/mL and 2134.0 ng h/mL respectively, which were acceptable, and the oral bioavailability ( $F = 75\%$ ) was ideal. Compound **11** exhibited significant penetration of the BBB, with a total brain/plasma ratio ( $K_p$ ) of 4.10 and a free brain/plasma ratio ( $K_{p,uu}$ ) of 0.23 (Table 10) in mice after a 10 mg/kg p.o. dose. For comparison, abemaciclib had a  $K_p$  of 0.21 and  $K_{p,uu}$  of 0.03 in mice after a 30 mg/kg p.o. dose [19]. The  $C_{max}$  in the plasma and brain were 818 ng/mL and 2582 ng/mL respectively, which were attained ( $T_{max}$ ) after 2 h (Table 10). The  $T_{1/2}$  in the plasma was 6.03 h, which was similar to that in the brain (6.38 h). Based on the similar  $T_{max}$  and  $T_{1/2}$  of compound **11** in the plasma and brain, we concluded that it could freely cross the BBB, which contributed to its efficacy in the brain.

## 2.8. Compound **11** inhibits Rb phosphorylation in nude mice bearing subcutaneous COLO 205 human colon tumor xenografts

Rb phosphorylation by CDK4/6 is required for the progression of cells through the G1 phase of the cell cycle. Therefore, inhibition of CDK4/6 prevents Rb phosphorylation and inhibits cell proliferation, resulting in anti-tumor activity *in vivo*. In this study, cellular

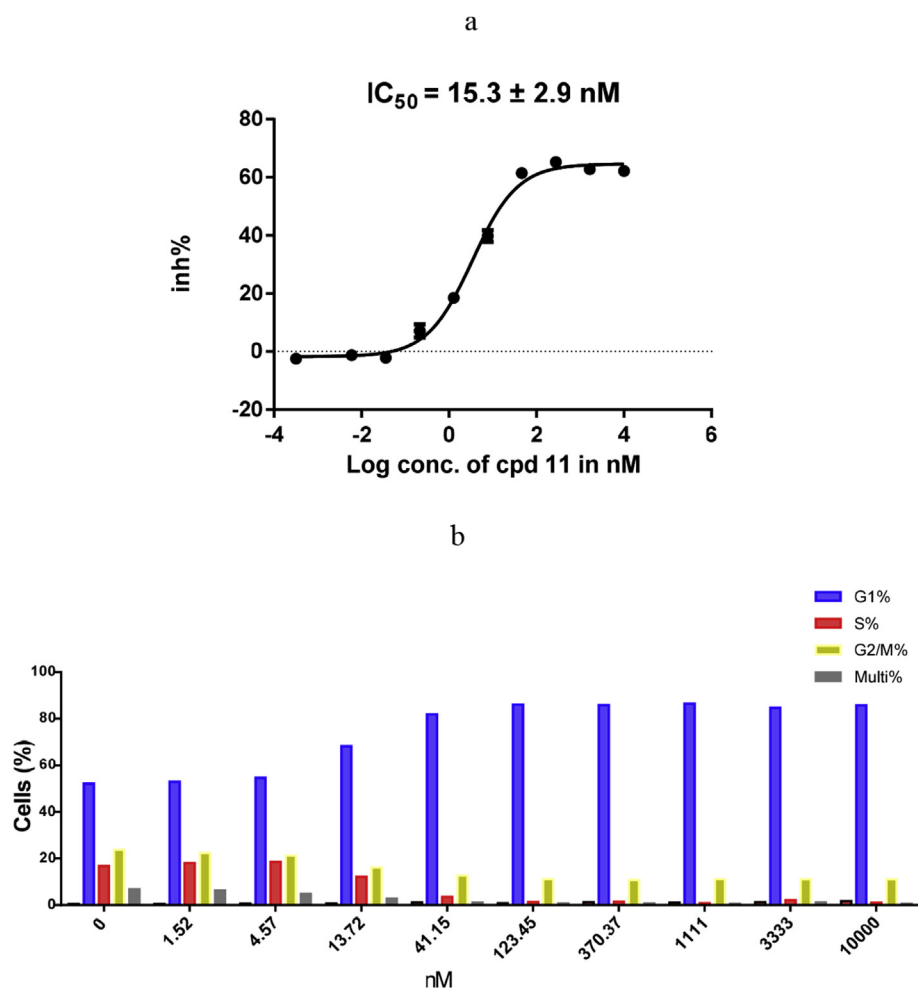


**Fig. 5.** a) Anti-proliferation activity of compound **11** in U87MG cells. b) U87MG cells treated with increasing concentrations of compound **11** for 24 h and cell cycle activity profiled by flow cytometry.

**Table 6**

Physicochemical properties of compound **11**.

Property	Result
MW	488.59 Da
HBD	1
PSA <sup>a</sup>	58 Å <sup>2</sup>
clogP <sup>a</sup>	5.38
logD <sub>7.4</sub> <sup>b</sup>	3.49
pKa <sup>c</sup>	8.19

<sup>a</sup> Calculated by Sybyl-X.v2.0.

<sup>b</sup> measured by multiple reaction monitoring (MRM).

<sup>c</sup> Determined by pH metrics at pH = 3–11.

inhibition associated with CDK4/6 was determined by using Western blotting to evaluate Rb phosphorylation at serine 780 (p-Rb), which is specific for CDK4/6. As shown in Fig. 6a, *in vivo* inhibition of p-Rb was dose-dependent and significant at 24 h after oral administration of 12.5 mg/kg, which was the minimum dose given to mice bearing COLO 205 human xenografts, and time course studies showed that maximum inhibition occurred 24 h after administration (Fig. 6b). These data show that compound **11** caused sustained suppression of tumor Rb phosphorylation, which corresponded with its long  $T_{1/2}$  (8.38 h after 5 mg/kg P.O.) in mice (Table 9).

## 2.9. *In vivo* anti-cancer activity of compound **11** in a U87MG-Luc orthotopic xenograft mouse model of GBM

Based on the desirable pharmacological profile of **11**, its high CDK4/6 inhibitory activity, good selectivity against other kinases, high anti-proliferation activity in the U87MG GBM cell line, and ability to inhibit Rb phosphorylation in nude mice bearing subcutaneous COLO 205 xenograft tumors, we next investigated the therapeutic efficacy of **11** in an U87MG-Luc orthotopic mouse model. *In vivo* anti-tumor effects were evaluated by bioluminescence imaging, and the level of tumor growth at the orthotopic site was indicated by the strength of the bioluminescence signal at different time points after tumor inoculation. Tumor-bearing mice were treated orally with **11** at doses ranging from 3.125 to 50 mg/kg for 35 consecutive days. As shown in Fig. 7 and Table 11, administration of **11** resulted in significant inhibition of tumor growth, with tumor growth inhibition (TGI) values of 62–99% for the range of administered doses. No significant body weight loss was observed in the groups, indicating that treatment was well tolerated, although weight loss of 4.20% was observed at day 28 in mice treated with 50 mg/kg. Survival was monitored for the entire treatment period of 35 days. As shown in Fig. 8, treatment with **11** resulted in a marked prolongation of survival, with higher doses leading to longer survival periods. The median survival time (MST) of vehicle-treated mice was 30 days, and the increase in life span

**Table 7**Bidirectional flux studies of compound **11** using wild type MDCK II and MDR1-MDCK II cells that overexpress human P-gp.

Cell line	Inhibitor <sup>a</sup>	$P_{app}$ <sup>b</sup>		Recovery(%) <sup>c</sup>		Total recovery (%) <sup>d</sup>		ER <sup>e</sup>	NER <sup>f</sup>
		A-B	B-A	A-B	B-A	A-B	B-A		
MDCK II	—	0.17	0.71	4.85	47.03	87.19	59.61	4.06	0.18
MDR1-MDCK II	—	0.71	0.50	8.23	48.35	105.33	58.95	0.71	
MDCK II	+	0.36	1.01	6.36	65.87	103.63	80.47	2.81	0.21
MDR1-MDCK II	+	0.81	0.47	6.05	59.13	93.83	75.64	0.59	

<sup>a</sup> GF120918.<sup>b</sup>  $10^{-6}$  cm/s.<sup>c</sup> Ratio of the mass that was added to the donor and recovered in the donor and receiver chambers.<sup>d</sup> Ratio of the mass that was added to the donor and recovered in the donor, receiver chambers and the cell lysate solution.<sup>e</sup>  $B-A P_{app}/A-B P_{app}$ .<sup>f</sup>  $ER (MDR1-MDCK II)/ER (MDCK II)$ .**Table 8**Bidirectional flux studies of compound **11** in Caco2 cells with or without the BCRP inhibitor.

Inhibitor <sup>a</sup>	$P_{app}$ <sup>b</sup>		Recovery (%) <sup>c</sup>		Total recovery (%) <sup>d</sup>		ER <sup>e</sup>
	A-B	B-A	A-B	B-A	A-B	B-A	
—	0.89	0.73	6.88	57.51	72.00	61.55	0.82
+	0.65	0.50	4.84	48.11	56.07	50.64	0.77

<sup>a</sup> Novobiocin.<sup>b</sup>  $10^{-6}$  cm/s.<sup>c</sup> Ratio of the mass that was added to the donor and recovered in the donor and receiver chambers.<sup>d</sup> Ratio of the mass that was added to the donor and recovered in the donor, receiver chambers and cell lysate solution.<sup>e</sup>  $B-A P_{app}/A-B P_{app}$ .**Table 10**Blood-brain distribution of compound **11** in mice after p.o. dose at 10 mg/kg.

	Plasma	Brain
$C_{max}$ (ng/mL or ng/g)	818	2582
$T_{max}$ (h)	2.00	2.00
$T_{1/2}$ (h)	6.03	6.38
$AUC_{0-48 h}$ (ng·h/mL or ng·h/g)	9064	37178
$AUC_{0-inf}$ (ng·h/mL or ng·h/g)	9109	37438
$f_u$ (Percentage of unbound fraction) <sup>a</sup>	0.7	0.04
Unbound $C_{max}$ <sup>b</sup>	5.73	1.03
Unbound $AUC_{0-24 h}$ <sup>c</sup>	63.45	14.87
$AUC_{0-48 h}$ ratio	4.10	
Unbound $AUC_{0-48 h}$ ratio	0.23	

<sup>a</sup> Measured at equilibrium dialysis.<sup>b</sup>  $C_{max} \times f_u$ .<sup>c</sup>  $AUC_{0-24h} \times f_u$ .

based on the MST for mice administered doses of 12.5 mg/kg, 25 mg/kg, and 50 mg/kg was significant at 48% ( $p = 0.0004$ ), 103% ( $p < 0.0001$ ), and 162% ( $p < 0.0001$ ) respectively (Table 12).

### 3. Conclusions

In summary, we prepared a novel CDK inhibitor (compound **11**), which had good inhibitory activity against both CDK4/cyclin D1 and CDK6/cyclin D3 ( $IC_{50} = 3$  nM and 1 nM, respectively). Structure-activity studies showed that the presence of a fluorine atom at the C-5 position of the pyrimidine ring and on the C-7' position of benzoheterocycle was critical for obtaining the highest inhibitory activity against CDK4/6 and optimal CDK6/CDK1 selectivity. In addition, the nature of the N-alkyl substituent and the number of hydrogen bond acceptors in the piperidine or piperazine ring linked to the core pyridine moiety had a strong impact on kinase inhibition and selectivity properties. Compound **11** exhibited favorable PK, significant penetration into the BBB, and *in vitro* anti-proliferation activity in the U87MG GBM cell line; it was also not a substrate of P-gp or BCRP. Inhibition of p-Rb *in vivo* by compound **11** in subcutaneous COLO 205 tumor xenografts was dose-dependent and sustained. *In vivo* studies were performed in a U87MG-Luc orthotopic xenograft mouse model, demonstrating the anti-cancer efficacy of compound **11**, as it had a higher TGI and survival rate compared to vehicle-treated animals. These data showed

that compound **11** was able to cross the BBB and reach the brain at levels that effectively inhibited CDK4 and CDK6 activity. Based on these results, we believe further investigations on compound **11** as a candidate for clinical studies are warranted.

### 4. Experimental section

#### 4.1. Materials and methods for chemistry

All of the reagents and solvents were obtained from commercial suppliers and used without further purification. Solvents were dried using standard procedures. Proton nuclear magnetic resonance ( $^1H$  NMR) spectra and  $^{13}C$  NMR were recorded using a Bruker 400M AVANCE II (Billerica, MA, USA). Chemical shifts were reported in parts per million ( $\delta$ ) downfield using tetramethylsilane ( $SiMe_4$ ) as the IS. Spin multiplicities were given as s (singlet), d (doublet), t (triplet), q (quartet), dd (double doublet), bs (broad singlet), and m (multiplet); the coupling constants ( $J$  values) were in Hz. All liquid chromatography/mass spectrometry (LC/MS) data were acquired on the Agilent 1260 LC with Agilent 6120 mass spectrometer detectors (Savage, MD, USA) or Thermo Scientific QE-UHPLC (Waltham, MA, USA). Purity was determined using the Agilent column with the following parameters: Phase A, 0.1% trifluoroacetic acid (TFA) in water; Phase B, 0.1% TFA in water; linear gradient, 0/10, 2/95, 4/95 [T (min)]/% B; flow rate, 1.0 mL/min; and ultraviolet (UV)

**Table 9**Pharmacokinetic parameters of compound **11** in ICR mice.

Route	Dose (mg/kg)	CL (mL/min/kg)	$V_{ss}$ (L/kg)	$C_{max}$ (ng/mL)	$AUC_{0-24hr}$ (ng·hr/mL)	$AUC_{0-\infty}$ (ng·hr/mL)	$T_{1/2}$ (hr)	F (%)
i.v.	2 mg/kg	25.2 $\pm$ 1.7	17.8 $\pm$ 1.1		1137 $\pm$ 77.8	1327 $\pm$ 88.4	9.1 $\pm$ 0.3	
p.o.	5 mg/kg			134.0 $\pm$ 11.8	2134.0 $\pm$ 96.9	2504.0 $\pm$ 387.0	8.38 $\pm$ 3.2	75

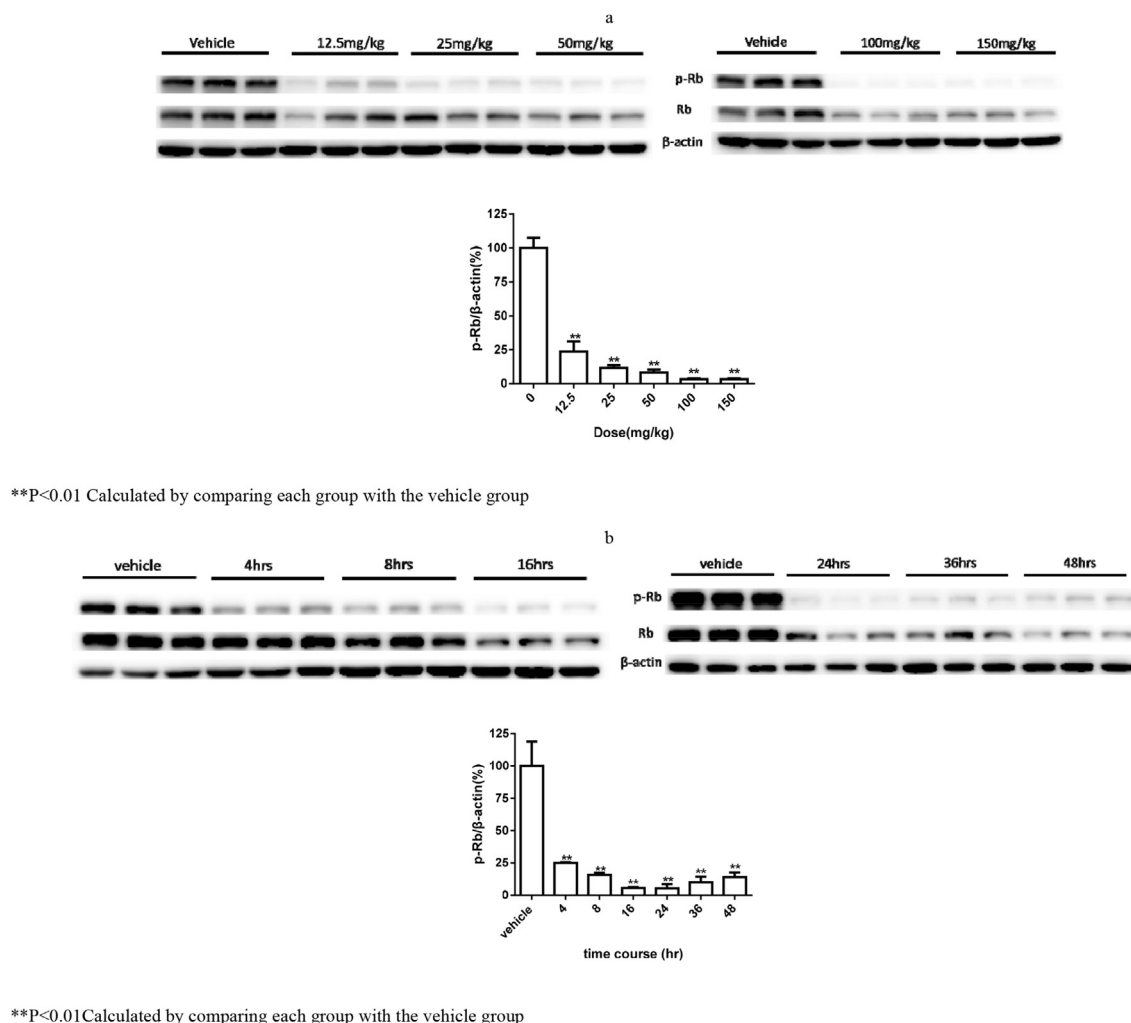


**Fig. 6.** Target inhibition in tumor tissue by compound **11**. **a)** Tumors harvested 24 h after dosing for analysis of the p-Rb marker (pRb ser 780); β-actin was used as the loading control. **b)** Time course of 100 mg/kg of compound **11** and tumors harvested at the indicated times (n = 3 per treatment and vehicle).

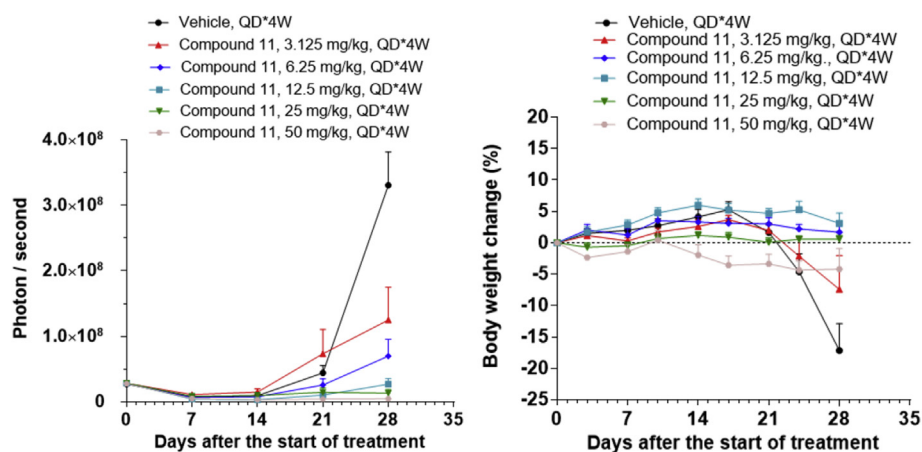


**Fig. 7.** *In vivo* antitumor activity of compound **11** in an orthotopic U87MG-Luc xenograft model of glioblastoma.

visualization at 254 nm. All melting points were collected on a melting point apparatus (YRT-3 produced by Jing Tuo in China). All yields reported were isolated yields.

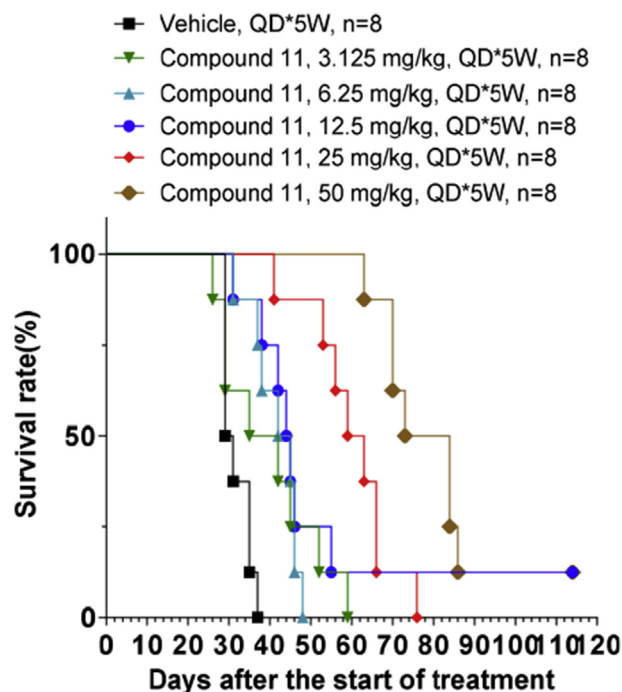
#### 4.2. Synthesis of CDK4/6 inhibitor analogues

The general methodology used to synthesize the CDK4/6 inhibitor analogues is outlined in [Scheme 1–4](#). Starting from different

**Table 11**

Tumor growth inhibition in the U87MG-Luc orthotopic xenograft mouse model after 28 days of once-daily treatment.

Treatment	Bioluminescence at day 28( $\times 10^7$ ) <sup>a</sup>	TGI (%) <sup>b</sup>	p value <sup>c</sup>
Vehicle	33.1 $\pm$ 5.1	–	–
3.125 mg/kg QD compound <b>11</b>	12.5 $\pm$ 5.0	62	0.268
6.25 mg/kg QD compound <b>11</b>	7.0 $\pm$ 2.6	79	0.028
12.5 mg/kg QD compound <b>11</b>	2.7 $\pm$ 0.9	92	0.012
25 mg/kg QD compound <b>11</b>	1.3 $\pm$ 0.6	96	0.010
50 mg/kg QD compound <b>11</b>	0.5 $\pm$ 0.1	99	0.009

<sup>a</sup> Mean  $\pm$  SEM ( $\times 10^7$  photons/second); number of animals in all groups: n = 8, 7, 8, 8, 8, 8.<sup>b</sup> TGI (%) = [(Bioluminescence of vehicle group on day 28 – Bioluminescence of treatment group on day 28)/Bioluminescence of vehicle group on day 28]  $\times$  100%.<sup>c</sup> Calculated based on bioluminescence, compared with the vehicle group.**Fig. 8.** Kaplan–Meier analysis of animal survival following treatment with compound **11** or vehicle control.**Table 12**Survival of tumor-bearing mice treated q.d. for 35 days with compound **11**.

Group	MST (days) <sup>b</sup>	ILS (%) <sup>c</sup>	P value <sup>d</sup>
Vehicle	30 (29–37) <sup>a</sup>	–	–
3.125 mg/kg qd compound <b>11</b>	38.5 (26–59)	28	0.0822
6.25 mg/kg qd compound <b>11</b>	43.5 (31–48)	45	0.0007
12.5 mg/kg qd compound <b>11</b>	44.5 (31–114)	48	0.0004
25 mg/kg qd compound <b>11</b>	61 (41–76)	103	<0.0001
50 mg/kg qd compound <b>11</b>	78.5 (63–>114)	162	<0.0001

<sup>a</sup> Range of survival times.<sup>b</sup> MST = Median survival time.<sup>c</sup> ILS = Increase in life-span based on MST of vehicle group.<sup>d</sup> Calculated by comparing each group with the vehicle group.

commercially available hydrazine reagents **A** and ketone reagents **B**, a range of different precursor intermediates **1–5C**, **7C**, and **33C** were obtained. Then the bromine was converted to a borate ester, affording intermediates **1–5D**, **7D**, and **33D**. Following Suzuki coupling, **1–7E** and **33E** were obtained. Introduction of R<sub>4</sub> or R<sub>5</sub> groups was achieved via Buchwald–Hartwig amination, affording compounds **1–7**, **9**, **11–13**, **22–32**, **35–38**, **8F**, **10F**, **17–21F**, **31F**, and **33–34F**. After removal of the Boc group from **8F**, **10F**, **17–21F**, **31F**, and **33–34F**, analogues **8**, **10**, **17–21**, **31**, and **33–34**, respectively,

were obtained. For N-alkylated analogues, reaction with the appropriate reagent afforded analogues **14–16** [40,41].

#### 4.2.1. 5-(4-Methylpiperazin-1-yl)pyridin-2-amine (**INT-1**)

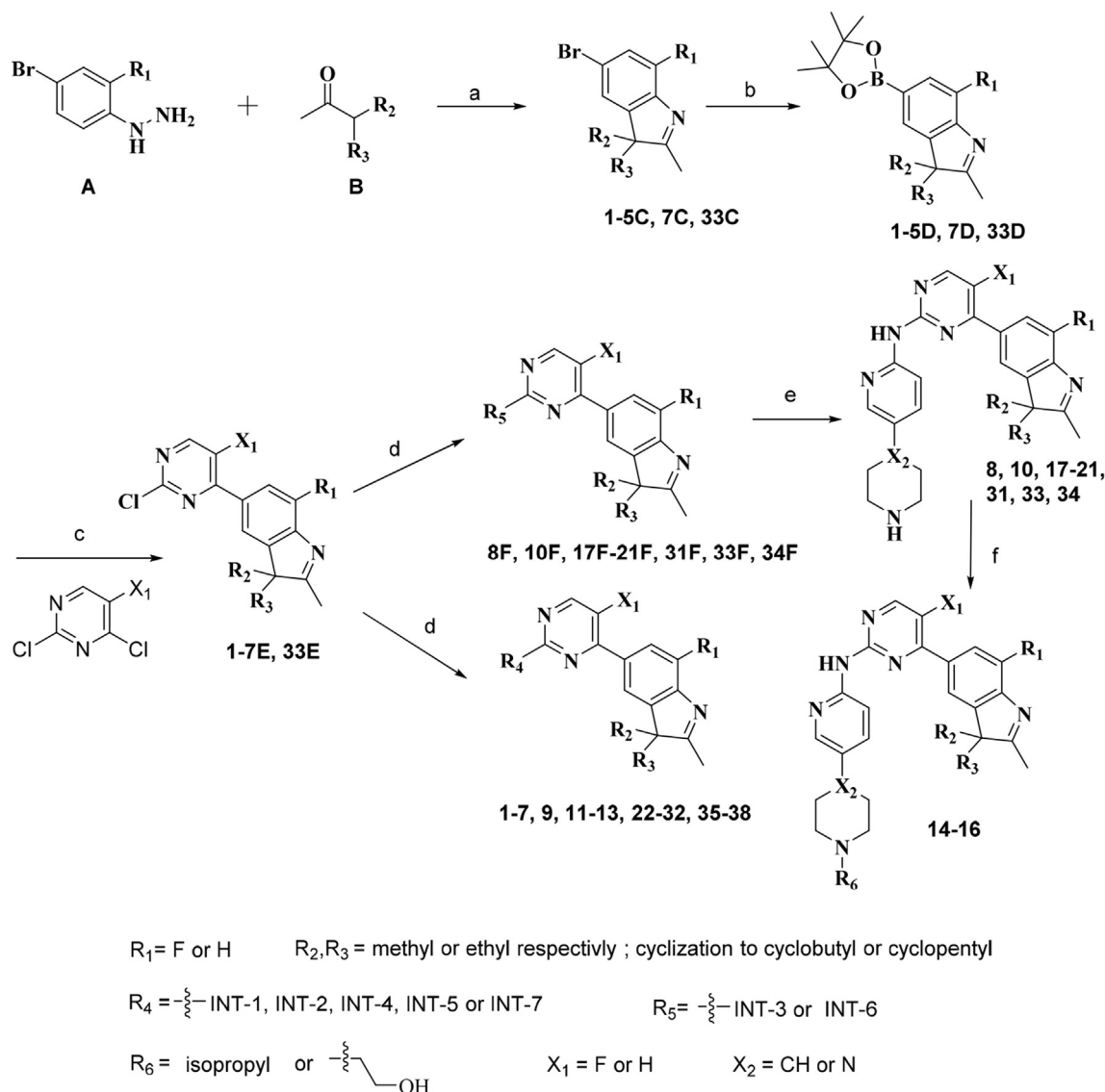
1-methylpiperazine (3.00 g, 29.6 mmol), potassium carbonate ([K<sub>2</sub>CO<sub>3</sub>] 4.10 g, 29.6 mmol), and tetrabutylammonium iodide ([TBAI] 0.42 g, 1.2 mmol) were added to a solution of 5-bromo-2-nitropyridine (4.00 g, 19.7 mmol) in dimethyl sulfoxide ([DMSO] 50 mL). The mixture was heated at 80 °C for 16 h, and the reaction was poured into ice water and extracted with dichloromethane (DCM). The combined organic layers were washed with water, dried over anhydrous sodium sulfate (Na<sub>2</sub>SO<sub>4</sub>), concentrated under a vacuum, and purified by silica gel column chromatography (DCM/methanol [MeOH] = 50:1–10:1) to obtain 1-methyl-4-(6-nitropyridin-3-yl)piperazine (2.45 g; yield, 56%) as a yellow solid. Then palladium on carbon ([Pd/C], 0.10 g) was added to the 1-methyl-4-(6-nitropyridin-3-yl)piperazine (1.00 g, 4.5 mmol) in ethanol (EA)/MeOH (10 mL/10 mL) solution. The mixture was degassed by flushing with hydrogen (H<sub>2</sub>), stirred at room temperature (RT) under a H<sub>2</sub> atmosphere for 2 h, and filtered and concentrated under vacuum to obtain **INT-1** (825 mg; yield, 95%) as a white solid. ESI-MS: *m/z* 193.3 [M+H]<sup>+</sup>.

#### 4.2.2. 5-(4-Ethylpiperazin-1-yl)pyridin-2-amine (**INT-2**)

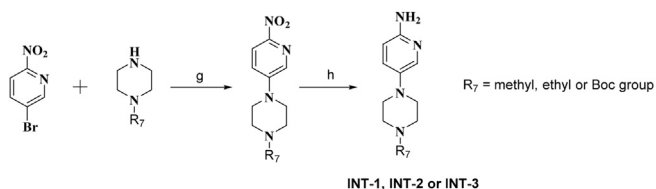
1-ethylpiperazine (3.40 g, 29.8 mmol), K<sub>2</sub>CO<sub>3</sub> (4.10 g, 29.6 mmol), and TBAI (0.42 g, 1.2 mmol) were added to a solution of 5-bromo-2-nitropyridine (4.00 g, 19.7 mmol) in DMSO (40 mL). The mixture was heated at 80 °C for 16 h, and the reaction was poured into ice water, and extracted with DCM. The combined organic layers were washed with water, dried over anhydrous Na<sub>2</sub>SO<sub>4</sub>, concentrated under a vacuum, and purified by silica gel column chromatography (DCM/MeOH = 100:1–10:1) to obtain 1-ethyl-4-(6-nitropyridin-3-yl)piperazine (3.59 g; yield, 56%) as a yellow solid. Pd/C (0.10 g) was added to the 1-ethyl-4-(6-nitropyridin-3-yl)piperazine (0.90 g, 3.8 mmol) in EA/MeOH (9 mL/9 mL) solution. The mixture was degassed by H<sub>2</sub>, stirred at RT under a H<sub>2</sub> atmosphere for 2 h, and filtered and concentrated under a vacuum to obtain **INT-2** (720.0 mg; yield, 92%) as an off-white solid. ESI-MS: *m/z* 207.2 [M+H]<sup>+</sup>.

#### 4.2.3. *tert*-butyl 4-(6-aminopyridin-3-yl)piperazine-1-carboxylate (**INT-3**)

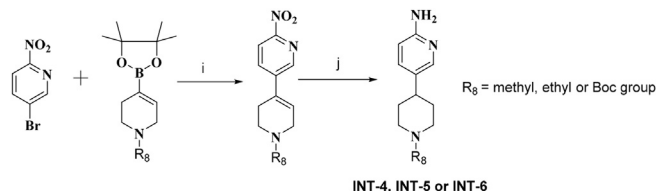
N,N-Diisopropylethylamine (4.77 g, 36.94 mmol) was added to a solution of 5-bromo-2-nitropyridine (5.00 g, 24.63 mmol) and *tert*-butyl piperazine-1-carboxylate (5.10 g, 27.09 mmol) in acetonitrile ([ACN] 30 mL). The mixture was refluxed for 2 h, cooled to RT, concentrated under a vacuum, and purified by silica gel column chromatography (from PE/EA = 1:1 to DCM/MeOH = 20:1) to obtain *tert*-butyl 4-(6-nitropyridin-3-yl)piperazine-1-carboxylate (3.80 g; yield, 50%) as a yellow solid. Pd/C (100.0 mg) was added to a solution of *tert*-butyl 4-(6-nitropyridin-3-yl)piperazine-1-



**Scheme 1.** General scheme for synthesis of 3H-indole CDK inhibitor analogues; Reagents and conditions: (a) HOAc, reflux, 4 h, yield 19–95%; (b) Bis(pinacolato)diboron, Pd(dppf)Cl<sub>2</sub>, AcOK, dioxane, 90 °C, 5 h, yield 58–78%; (c) Pd(PPh)<sub>4</sub>, K<sub>3</sub>PO<sub>4</sub>, 100 °C, dioxane/H<sub>2</sub>O, 4 h, yield 21–99%; (d) Cs<sub>2</sub>CO<sub>3</sub>, Pd<sub>2</sub>(dba)<sub>3</sub>, XantPhos, 1,4-dioxane, microwave 120 °C, 1 h, yield 10–47%; (e) RT, CF<sub>3</sub>COOH, 2 h, yield 25–91%; (f) Cs<sub>2</sub>CO<sub>3</sub>, 80 °C, ACN, 1 h, yield 20–55%.



**Scheme 2.** Synthesis of INT-1, INT-2, and INT-3; Reagents and conditions: (g) K<sub>2</sub>CO<sub>3</sub>, TBAI, 100 °C, DMSO, 16 h, yield 50–56%; (h) Pd/C, H<sub>2</sub>, EA/MeOH, RT, 2 h, yield 92–95%.



**Scheme 3.** Synthesis of INT-4, INT-5, and INT-6; Reagents and conditions: (i) Cs<sub>2</sub>CO<sub>3</sub>, Pd(dppf)Cl<sub>2</sub>, 1,4-dioxane/H<sub>2</sub>O, 85 °C, 12 h, yield 26–36%; (j) Pd/C, H<sub>2</sub>, EA/MeOH, RT, 12 h, yield 95–95%.

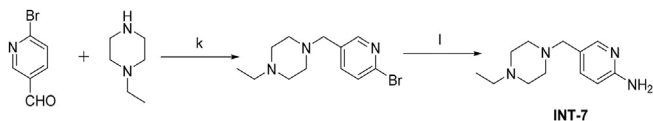
carboxylate (925.0 mg, 3.0 mmol) in EA/MeOH (10 mL/10 mL). The mixture was degassed by flushing with H<sub>2</sub>, stirred at RT under a H<sub>2</sub> atmosphere for 2 h, and filtered and concentrated under a vacuum to obtain **INT-3** (792.0 mg; yield, 95%) as an off-white solid. ESI-MS:  $m/z$  279.2 [M+H]<sup>+</sup>.

#### 4.2.4. 5-(1-Methylpiperidin-4-yl)pyridin-2-amine (**INT-4**)

Cesium carbonate ([Cs<sub>2</sub>CO<sub>3</sub>] 66.00 g, 0.2 mol) and Pd(dppf)Cl<sub>2</sub>

(7.33 g, 0.01 mol) were added to a solution of 5-bromo-2-nitropyridine (20.30 g, 0.1 mol) and 1-methyl-4-(4,4,5,5-tetramethyl-1,3,2-dioxaborolan-2-yl)-1,2,3,6-tetrahydropyridine (22.30 g, 0.1 mol) in dioxane/H<sub>2</sub>O (250 mL/30 mL). The mixture was allowed to stir at 85 °C for 12 h under nitrogen (N<sub>2</sub>). Then the solution was cooled to RT, concentrated under a vacuum, and purified by silica gel column chromatography (from PE/EA = 1:1 to DCM/





**Scheme 4.** Synthesis of INT-7; Reagents and conditions: (k) NaHB(OAc)<sub>3</sub>, DCM, RT, overnight, yield 71%; (l) Cy-John-Phos, Pd<sub>2</sub>(dba)<sub>3</sub>, toluene, LHMDs(1N), N<sub>2</sub>, 85 °C, overnight, yield 69%.

MeOH = 20:1) to obtain 1'-methyl-6-nitro-1',2',3',6'-tetrahydro-3,4'-bipyridine (5.70 g; yield, 26%) as a white solid. Next, Pd/C (0.10 g) was added to the solution of 1'-methyl-6-nitro-1',2',3',6'-tetrahydro-3,4'-bipyridine (657.0 mg, 3.0 mmol) in EA/MeOH (10 mL/10 mL). The mixture was degassed by flushing with H<sub>2</sub>, stirred at RT under a H<sub>2</sub> atmosphere for 2 h, and then filtered and concentrated under a vacuum to obtain **INT-4** (550.0 mg; yield, 96%) as a white solid. ESI-MS: *m/z* 192.2 [M+H]<sup>+</sup>.

#### 4.2.5. 5-(1-Ethylpiperidin-4-yl)pyridin-2-amine (**INT-5**)

Cs<sub>2</sub>CO<sub>3</sub> (66.00 g, 0.2 mol), and Pd(dppf)Cl<sub>2</sub> (7.33 g, 0.01 mol) were added to a solution of 5-bromo-2-nitropyridine (20.30 g, 0.1 mol) and *tert*-butyl 4-(4,4,5,5-tetramethyl-1,3,2-dioxaborolan-2-yl)-5,6-dihydropyridine-1(2H)-carboxylate (31.00 g, 0.1 mol) in dioxane/H<sub>2</sub>O (250 mL/30 mL). The mixture was allowed to stir at 85 °C for 12 h under N<sub>2</sub>, cooled to RT and concentrated under a vacuum, and purified by silica gel column chromatography (from PE/EA = 1:1 to DCM/MeOH = 20:1) to obtain *tert*-butyl 6-nitro-5',6'-dihydro-[3,4'-bipyridine]-1'(2'H)-carboxylate (11.00 g; yield, 36%) as a yellow solid. Then TFA (20 mL) was added to the solution of *tert*-butyl 6-nitro-5',6'-dihydro-[3,4'-bipyridine]-1'(2'H)-carboxylate (5.00 g, 24.4 mmol) in DCM (100 mL). The mixture was stirred at RT for 1 h, after which the reaction mixture was concentrated, washed with sodium carbonate (Na<sub>2</sub>CO<sub>3</sub>) (aq.), and extracted with DCM. The combined organic layers were washed with brine, dried over anhydrous Na<sub>2</sub>SO<sub>4</sub>, concentrated under a vacuum, and purified by silica gel column chromatography (PE/EA = 5:1) to obtain 6-nitro-1',2',3',6'-tetrahydro-3,4'-bipyridine (2.61 g; yield, 52%) as a yellow solid. Sodium hydride (270.0 mg, 11.2 mmol) in dimethyl fluoride ([DMF] 6 mL) was added at 0 °C to a solution of 6-nitro-1',2',3',6'-tetrahydro-3,4'-bipyridine (2.11 g, 10.2 mmol), and the reaction was stirred at 0 °C for 0.5 h. Then iodoethane (2.39 g, 15.28 mmol) was added and stirred for 2 h. The mixture was poured into water and extracted with DCM. The combined organic layers were washed with brine, dried over anhydrous Na<sub>2</sub>SO<sub>4</sub>, concentrated under a vacuum, and purified by silica gel column chromatography (PE/EA = 5:1) to obtain 1'-ethyl-6-nitro-1',2',3',6'-tetrahydro-3,4'-bipyridine (800.2 mg; yield, 33.7%) as a yellow solid. Then Pd/C (0.10 g) was added to a solution of 1'-ethyl-6-nitro-1',2',3',6'-tetrahydro-3,4'-bipyridine (699.0 mg, 3.0 mmol) in EA/MeOH (10 mL/10 mL). The mixture was degassed by flushing with H<sub>2</sub>, stirred at RT under a H<sub>2</sub> atmosphere for 2 h, and filtered and concentrated under a vacuum to obtain **INT-5** (284.0 mg; yield, 95%) as a white solid. ESI-MS: *m/z* 206.2 [M+H]<sup>+</sup>.

#### 4.2.6. *tert*-butyl 4-(6-aminopyridin-3-yl)piperidine-1-carboxylate (**INT-6**)

Cs<sub>2</sub>CO<sub>3</sub> (66.00 g, 0.2 mol), and Pd(dppf)Cl<sub>2</sub> (7.33 g, 0.01 mol) were added to a solution of 5-bromo-2-nitropyridine (20.30 g, 0.1 mol) and *tert*-butyl 4-(4,4,5,5-tetramethyl-1,3,2-dioxaborolan-2-yl)-5,6-dihydropyridine-1(2H)-carboxylate (30.90 g, 0.1 mol) in dioxane/H<sub>2</sub>O (250 mL/30 mL). The mixture was allowed to stir at 85 °C for 12 h under N<sub>2</sub>, after which it was cooled to RT, concentrated under a vacuum, and purified by silica gel column chromatography (from PE/EA = 1:1 to DCM/MeOH = 20:1) to obtain *tert*-

butyl 6-nitro-5',6'-dihydro-[3,4'-bipyridine]-1'(2'H)-carboxylate (11.01 g, yield: 36%) as a yellow solid. Pd/C (100.0 mg) was added to a solution of *tert*-butyl 6-nitro-5',6'-dihydro-[3,4'-bipyridine]-1'(2'H)-carboxylate (915.0 mg, 3.0 mmol) in EA/MeOH (10 mL/10 mL). The mixture was degassed by flushing with H<sub>2</sub>, stirred at RT under a H<sub>2</sub> atmosphere for 2 h, and filtered and concentrated under a vacuum to obtain **INT-6** (790.0 mg; yield, 95%) as an off-white solid. ESI-MS: *m/z* 278.2 [M+H]<sup>+</sup>.

#### 4.2.7. 4-((4-Ethylpiperazin-1-yl)methyl)aniline (**INT-7**)

NaHB(OAc)<sub>3</sub> (2.60 g, 12.23 mmol) was added to a solution of 6-bromonicotinaldehyde (1.50 g, 8.15 mmol) and 1-ethylpiperazine (0.90 g, 8.15 mmol) in DCM (15 mL). The mixture was allowed to stir at RT overnight, after which it was filtered and concentrated under a vacuum, and purified by silica gel column chromatography (DCM/MeOH = 100:1–10:1) to obtain 1-((6-bromopyridin-3-yl)methyl)-4-ethylpiperazine (1.65 g; yield, 71%) as a yellow oil. Lithium bis(trimethylsilyl)amide (1 N) (20 mL, 20.0 mmol) under N<sub>2</sub> was added to a solution of 1-((6-bromopyridin-3-yl)methyl)-4-ethylpiperazine (2.80 g, 10.0 mmol), Cy-John-Phos (700.0 mg, 2.0 mmol), and Pd<sub>2</sub>(dba)<sub>3</sub> (915.0 mg, 1.0 mmol) in dry toluene (30 mL). Then the mixture was heated to 80 °C overnight, cooled to RT, filtered and concentrated under a vacuum, and purified by silica gel column chromatography (DCM/MeOH = 100:1–10:1) to give **INT-7** (1.52 g; yield, 69%) as a brown solid. ESI-MS: *m/z* 221.2 [M+H]<sup>+</sup>.

#### 4.2.8. 5-Bromo-7-fluoro-2,3,3-trimethyl-3H-indole (**1C**)

3-methylbutan-2-one (353.3 mg, 4.09 mmol) was added to a solution of (4-bromo-2-fluorophenyl)hydrazinehydrochloride (900.0 mg, 3.73 mmol) in acetic acid (5 mL), and the mixture was refluxed for 5 h. The solvent was removed, diluted with water (20 mL) and extracted with ethyl acetate (EtOAc) (20 mL × 3). The combined organic layers were washed with brine (25 mL), dried over anhydrous Na<sub>2</sub>SO<sub>4</sub>, concentrated under a vacuum, and purified by silica gel column chromatography (EA:PE = 1:50–1:25) to obtain 5-bromo-7-fluoro-2,3,3-trimethyl-3H-indole (910.0 mg; yield, 95%) as a yellow solid. ESI-MS: *m/z* found 256.0 [M+H]<sup>+</sup>.

#### 4.2.9. 7-Fluoro-2,3,3-trimethyl-5-(4,4,5,5-tetramethyl-1,3,2-dioxaborolan-2-yl)-3H-indole (**1D**)

Pd(dppf)Cl<sub>2</sub> (228.7 mg, 0.32 mmol) was added under N<sub>2</sub> to a solution of **1C** (400.0 mg, 1.57 mmol), 4,4,4',4',5,5,5',5'-octamethyl-2,2'-bi(1,3,2-dioxaborolane) (436.5 mg, 1.71 mmol) and potassium acetate (306.3 mg, 3.12 mmol) in 1,4-dioxane (10 mL), and the mixture was heated to 90 °C overnight. The mixture was cooled to RT, filtered, diluted with water (10 mL), and extracted with EtOAc (20 mL × 3). The combined organic layers were washed with brine (25 mL), dried over anhydrous Na<sub>2</sub>SO<sub>4</sub>, concentrated under a vacuum, and purified by silica gel column chromatography (DCM:MeOH = 50:1–30:1) to obtain **1D** (306.5 mg; yield, 64%) as a yellow oil. ESI-MS: *m/z* 304.2 [M+H]<sup>+</sup>.

#### 4.2.10. 5-(2-Chloro-5-fluoropyrimidin-4-yl)-7-fluoro-2,3,3-trimethyl-3H-indole (**1E**)

Pd(PPh<sub>3</sub>)<sub>4</sub> (114.5 mg, 0.09 mmol) was added under N<sub>2</sub> to a solution of **1D** (300.0 mg, 0.99 mmol), 2,4-dichloro-5-fluoropyrimidine (181.8 mg, 1.08 mmol) and potassium phosphate (419.8 mg, 1.98 mmol) in 1,4-dioxane/water (4 mL/1 mL). Then the mixture was reacted in the microwave at 130 °C for 1 h. the mixture was cooled to RT, filtered, diluted with water (10 mL), and extracted with DCM (15 mL × 3). The combined organic layers were washed with brine (20 mL), dried over anhydrous Na<sub>2</sub>SO<sub>4</sub>, concentrated under a vacuum, and purified by silica gel column chromatography (DCM:MeOH = 100:1–50:1) to obtain **1E** (301.2 mg; yield, 99%) as a

yellow solid. ESI-MS:  $m/z$  308.1  $[M+H]^+$

#### 4.2.11. *N*-(5-((4-ethylpiperazin-1-yl)methyl)pyridin-2-yl)-5-fluoro-4-(7-fluoro-2,3,3-trimethyl-3H-indol-5-yl)pyrimidin-2-amine (**1**)

$Pd_2(dba)_3$  (86.4 mg, 0.09 mmol) and Xant-phos (109.2 mg, 0.19 mmol) were added under  $N_2$  to a solution of **1E** (290.0 mg, 0.94 mmol), **INT-7** (228.6 mg, 1.04 mmol), and potassium phosphate (400.5 mg, 1.88 mmol) in 1,4-dioxane (10 mL). Then the mixture was reacted in the microwave at 150 °C for 1 h. The mixture was cooled to RT, filtered, diluted with water (10 mL), and extracted with DCM (10 mL  $\times$  3). The combined organic layers were washed with brine (30 mL), dried over anhydrous  $Na_2SO_4$ , concentrated under a vacuum, and purified by preparative thin-layer chromatography to obtain compound **1** (140.3 mg; yield, 30%) as a yellow solid. Purity: 99.6%; retention time: 3.10 min. MP: 152.9–153.4 °C. High-resolution mass spectrometry (HRMS)-ESI:  $[M+H]^+$  observed 492.2677, calculated 492.2687.  $^1H$  NMR (400 MHz,  $CDCl_3$ )  $\delta$  8.72 (s, 1H), 8.49 (d, 1H,  $J = 3.2$  Hz), 8.38 (d, 1H,  $J = 8.4$  Hz), 8.31 (s, 1H), 7.92 (s, 1H), 7.89 (s, 1H), 7.73 (d, 1H,  $J = 8.4$  Hz), 3.52 (s, 2H), 2.54–2.41 (m, 10H), 2.38 (s, 3H), 1.40 (s, 6H), 1.10 (t, 3H,  $J = 7.2$  Hz).  $^{13}C$  NMR (100 MHz,  $CDCl_3$ )  $\delta$  191.29, 155.37 (d,  $J_{C-F} = 3.0$  Hz), 154.76 (d,  $J_{C-F} = 252.0$  Hz), 152.17, 152.00, 150.94 (d,  $J_{C-F} = 9.0$  Hz), 149.63 (d,  $J_{C-F} = 89.0$  Hz), 149.37 (d,  $J_{C-F} = 3.0$  Hz), 147.39 (d,  $J_{C-F} = 26.0$  Hz), 142.82 (d,  $J_{C-F} = 11.0$  Hz), 139.05, 132.05 (d,  $J_{C-F} = 6.0$  Hz), 127.27, 117.97 (dd,  $J_{C-F} = 3.0$  Hz), 116.32 (dd,  $J_{C-F} = 7.0$  Hz), 111.39, 59.84, 54.85, 52.91 (2C), 52.74 (2C), 52.28, 23.03 (2C), 15.84, 11.95.

#### 4.2.12. 5-Bromo-3-ethyl-7-fluoro-2,3-dimethyl-3H-indole (**2C**)

Starting from (4-bromo-2-fluorophenyl)hydrazine (5.00 g, 20.80 mmol) and 1-cyclopentylethanone (2.11 g, 20.80 mmol), 4.60 g of **2C** was obtained at 90% yield according to the method described for the synthesis of **1C**. ESI-MS:  $m/z$  found 270.0  $[M+H]^+$ .

#### 4.2.13. 3-Ethyl-7-fluoro-2,3-dimethyl-5-(4,4,5,5-tetramethyl-1,3,2-dioxaborolan-2-yl)-3H-indole (**2D**)

Starting from **2C** (4.60 g, 17.0 mmol) and bis(pinacolato)diboron (4.75 g, 18.7 mmol), 3.23 g of **2D** was obtained at 60% yield according to the method described for the synthesis of **1D**. ESI-MS:  $m/z$  318.2  $[M+H]^+$ .

#### 4.2.14. 5-(2-Chloro-5-fluoropyrimidin-4-yl)-3-ethyl-7-fluoro-2,3-dimethyl-3H-indole (**2E**)

Starting from **2D** (5.39 g, 17.0 mmol) and 2,4-dichloro-5-fluoropyrimidine (3.41 g, 20.4 mmol), 2.15 g of **2E** was obtained at 40% yield according to the method described for the synthesis of **1E**. ESI-MS:  $m/z$  322.1  $[M+H]^+$ .

#### 4.2.15. 4-(3-Ethyl-7-fluoro-2,3-dimethyl-3H-indol-5-yl)-*N*-(5-((4-ethylpiperazin-1-yl)methyl)pyridin-2-yl)-5-fluoropyrimidin-2-amine (**2**)

Starting from **2E** (0.50 g, 1.56 mmol) and **INT-7** (0.40 g, 1.82 mmol), 118.3 mg of **2** was obtained as a light yellow solid at 15% yield according to the method described for the synthesis of compound **1**. Purity: 95.7%; retention time: 3.12 min. MP: 168.4–169.7 °C. HRMS-ESI:  $[M+H]^+$  observed 506.2832, calculated 506.2844.  $^1H$  NMR (400 MHz,  $CDCl_3$ )  $\delta$  8.71 (s, 1H), 8.49 (d, 1H,  $J = 3.6$  Hz), 8.38 (d, 1H,  $J = 8.4$  Hz), 8.31 (s, 1H), 7.94 (d, 1H,  $J = 11.2$  Hz), 7.86 (s, 1H), 7.72 (dd, 1H,  $J = 8.0, 1.2$  Hz), 3.52 (s, 2H), 2.53–2.41 (m, 10H), 2.34 (s, 3H), 2.06–1.93 (m, 1H), 1.91–1.84 (m, 1H), 1.39 (s, 3H), 1.09 (t, 3H,  $J = 7.2$  Hz), 0.50 (t, 3H,  $J = 7.2$  Hz).  $^{13}C$  NMR (100 MHz,  $CDCl_3$ )  $\delta$  190.59, 155.36 (d,  $J_{C-F} = 3.0$  Hz), 154.71 (d,  $J_{C-F} = 252.0$  Hz), 151.99, 150.93 (d,  $J_{C-F} = 10.0$  Hz), 149.65 (d,  $J_{C-F} = 91.0$  Hz), 147.41, 147.15, 143.69 (d,  $J_{C-F} = 11.0$  Hz), 139.04, 131.87 (d,  $J_{C-F} = 6.0$  Hz), 127.29, 118.2 (d,  $J_{C-F} = 8.0$  Hz), 116.34 (dd,  $J_{C-F} = 7.0$  Hz), 111.39, 59.85, 59.70, 52.94 (2C), 52.76 (2C), 52.29, 30.20,

22.29, 16.12, 11.98, 8.59.

#### 4.2.16. 5-Bromo-3,3-diethyl-7-fluoro-2-methyl-3H-indole (**3C**)

Starting from (4-bromo-2-fluorophenyl)hydrazine hydrochloride (5.00 g, 20.75 mmol) and 3-ethylpentan-2-one (2.35 g, 20.75 mmol), 2.50 g of **3C** was obtained at 87% yield according to the method described for the synthesis of **1C**. ESI-MS:  $m/z$  284.0  $[M+H]^+$ .

#### 4.2.17. 3,3-Diethyl-7-fluoro-2-methyl-5-(4,4,5,5-tetramethyl-1,3,2-dioxaborolan-2-yl)-3H-indole (**3D**)

Starting from **3C** (2.00 g, 7.07 mmol) and bis(pinacolato)diboron (1.89 g, 7.77 mmol), 1.50 g of **3D** was obtained at 64% yield according to the method described for the synthesis of **1D**. ESI-MS:  $m/z$  332.2  $[M+H]^+$ .

#### 4.2.18. 5-(2-Chloro-5-fluoropyrimidin-4-yl)-3,3-diethyl-7-fluoro-2-methyl-3H-indole (**3E**)

Starting from **3D** (1.50 g, 4.88 mmol) and 2,4-dichloro-5-fluoropyrimidine (0.81 g, 5.00 mmol), 0.88 g of **3E** was obtained at 59% yield according to the method described for the synthesis of **1E**. ESI-MS:  $m/z$  336.1  $[M+H]^+$ .

#### 4.2.19. 4-(3,3-Diethyl-7-fluoro-2-methyl-3H-indol-5-yl)-*N*-(5-((4-ethylpiperazin-1-yl)methyl)pyridin-2-yl)-5-fluoropyrimidin-2-amine (**3**)

Starting from **3E** (100.0 mg, 0.29 mmol) and **INT-7** (65.6 mg, 0.29 mmol), 32.1 mg of **3** was obtained as a light yellow solid at 21% yield according to the method described for the synthesis of compound **1**. Purity: 97.7%; retention time: 3.36 min. MP: 183.6–184.3 °C. HRMS-ESI:  $[M+H]^+$  observed 520.2987, calculated 520.3000.  $^1H$  NMR (400 MHz,  $CDCl_3$ )  $\delta$  9.19 (brs, 1H), 8.53 (s, 1H), 8.39–8.34 (m, 2H), 7.95 (d, 1H,  $J = 11.2$  Hz), 7.83 (s, 1H), 7.72 (d, 1H,  $J = 8.0$  Hz), 3.51 (s, 2H), 2.52–2.41 (m, 10H), 2.31 (s, 3H), 2.06–2.01 (m, 2H), 1.90–1.85 (m, 2H), 1.08 (t, 3H,  $J = 6.8$  Hz), 0.46 (t, 6H,  $J = 6.8$  Hz).  $^{13}C$  NMR (100 MHz,  $CDCl_3$ )  $\delta$  189.80, 155.43, 154.63 (d,  $J_{C-F} = 258.0$  Hz), 152.11, 150.86 (d,  $J_{C-F} = 2.0$  Hz), 150.78 (d,  $J_{C-F} = 3.0$  Hz), 149.61 (d,  $J_{C-F} = 84.0$  Hz), 147.52 (d,  $J_{C-F} = 27.0$  Hz), 145.54 (d,  $J_{C-F} = 3.0$  Hz), 144.53 (d,  $J_{C-F} = 12.0$  Hz), 139.02, 131.91 (d,  $J_{C-F} = 5.0$  Hz), 127.18, 118.37 (dd,  $J_{C-F} = 3.0$  Hz), 116.33 (dd,  $J_{C-F} = 7.0$  Hz), 111.44, 65.10, 59.86, 52.97 (2C), 52.77 (2C), 52.28, 29.60 (2C), 16.41, 12.01, 8.31 (2C).

#### 4.2.20. 5'-bromo-7'-fluoro-2'-methylspiro[cyclobutane-1,3'-indole] (**4C**)

Starting from (4-bromo-2-fluorophenyl) hydrazine hydrochloride (2.00 g, 8.29 mmol) and 1-cyclobutylethanone (812.5 mg, 8.29 mmol), 408.4 mg of **4C** was obtained at 19% yield according to the method described for the synthesis of **1C**. ESI-MS:  $m/z$  268.0  $[M+H]^+$ .

#### 4.2.21. 7'-fluoro-2'-methyl-5'-(4,4,5,5-tetramethyl-1,3,2-dioxaborolan-2-yl)spiro[cyclobutane-1,3'-indole] (**4D**)

Starting from **4C** (400.0 mg, 1.49 mmol) and bis(pinacolato)diboron (417.0 mg, 1.64 mmol), 301.2 mg of **4D** was obtained at 64% yield according to the method described for the synthesis of **1D**. ESI-MS:  $m/z$  316.2  $[M+H]^+$ .

#### 4.2.22. 5'-(2-chloro-5-fluoropyrimidin-4-yl)-7'-fluoro-2'-methylspiro[cyclobutane-1,3'-indole] (**4E**)

Starting from **4D** (300.0 mg, 0.95 mmol) and 2,4-dichloro-5-fluoropyrimidine (174.9 mg, 3.63 mmol), 204.3 mg of **4E** was obtained at 67% yield according to the method described for the synthesis of **1E**. ESI-MS:  $m/z$  320.1  $[M+H]^+$ .

4.2.23. *N*-(5-((4-ethylpiperazin-1-yl)methyl)pyridin-2-yl)-5-fluoro-4-(7'-fluoro-2'-methylspiro[cyclobutane-1,3'-indol]-5'-yl)pyrimidin-2-amine (**4**)

Starting from **4E** (33.7 mg, 0.11 mmol) and **INT-7** (25.5 mg, 0.12 mmol), 10.4 mg of **4** was obtained as a yellow solid at 19% yield according to the method described for the synthesis of **1**. Purity: 97.2%; retention time: 3.37 min. MP: 166.4–167.5 °C. HRMS-ESI:  $[M+H]^+$  observed 504.2674, calculated 504.2687.  $^1H$  NMR (400 MHz,  $CDCl_3$ )  $\delta$  8.36–8.32 (m, 2H), 8.23 (s, 1H), 8.04 (s, 1H), 7.78–7.75 (m, 2H), 7.71 (d, 1H,  $J$  = 8.4 Hz), 5.84–5.83 (m, 1H), 5.63–5.62 (m, 1H), 4.39–4.38 (m, 1H), 3.66–3.64 (m, 1H), 3.51 (s, 2H), 3.06–3.00 (m, 1H), 2.71–2.38 (m, 11H), 1.55 (s, 3H), 1.11 (t, 3H,  $J$  = 7.2 Hz).  $^{13}C$  NMR (100 MHz,  $CDCl_3$ )  $\delta$  193.53, 155.05 (d,  $J_{C-F}$  = 2.0 Hz), 152.11 (d,  $J_{C-F}$  = 262.0 Hz), 151.44 (d,  $J_{C-F}$  = 10.0 Hz), 148.63 (d,  $J_{C-F}$  = 182.0 Hz), 146.36 (d,  $J_{C-F}$  = 20.0 Hz), 139.80 (d,  $J_{C-F}$  = 11.0 Hz), 138.99, 136.95 (d,  $J_{C-F}$  = 5.0 Hz), 135.40, 130.58, 127.00, 123.77, 121.54 (d,  $J_{C-F}$  = 7.0 Hz), 115.88 (dd,  $J_{C-F}$  = 8.0 Hz), 111.25, 78.01, 59.86, 52.92, 52.75, 52.29, 51.52, 39.65, 29.78, 29.32, 27.21, 26.12, 11.95.

4.2.24. 5'-bromo-7'-fluoro-2'-methylspiro[cyclopentane-1,3'-indole] (**5C**)

Starting from (4-bromo-2-fluorophenyl) hydrazine (2.00 g, 9.76 mmol) and 1-cyclopentylethanone (1.09 g, 9.76 mmol), 2.10 g of **5C** was obtained at 76% yield according to the method described for the synthesis of **1C**. ESI-MS:  $m/z$  282.0  $[M+H]^+$ .

4.2.25. 7'-fluoro-2'-methyl-5'-(4,4,5,5-tetramethyl-1,3,2-dioxaborolan-2-yl)spiro[cyclopentane-1,3'-indole] (**5D**)

Starting from **5C** (2.10 g, 9.76 mmol) and bis(pinacolato)diboron (2.08 g, 8.2 mmol), 1.39 g of **5D** was obtained at 58% yield according to the method described for the synthesis of **1D**. ESI-MS:  $m/z$  330.2  $[M+H]^+$ .

4.2.26. 5'-(2-chloro-5-fluoropyrimidin-4-yl)-7'-fluoro-2'-methylspiro[cyclopentane-1,3'-indole] (**5E**)

Starting from **5D** (1.39 g, 4.1 mmol) and 2,4-dichloro-5-fluoropyrimidine (0.87 g, 5.2 mmol), 700.1 mg of **5E** was obtained at 49% yield according to the method described for the synthesis of **1E**. ESI-MS:  $m/z$  334.1  $[M+H]^+$ .

4.2.27. *N*-(5-((4-ethylpiperazin-1-yl)methyl)pyridin-2-yl)-5-fluoro-4-(7'-fluoro-2'-methylspiro[cyclopentane-1,3'-indol]-5'-yl)pyrimidin-2-amine (**5**)

Starting from **5E** (100.0 mg, 0.30 mmol) and **INT-7** (66.0 mg, 0.30 mmol), 20.2 mg of **5** was obtained as light yellow solid at 13% yield according to the method described for the synthesis of **1**. Purity: 98.7%; retention time: 3.36 min. MP: 198.7–199.6 °C. HRMS-ESI:  $[M+H]^+$  observed 518.2833, calculated 518.2844.  $^1H$  NMR (400 MHz,  $CDCl_3$ )  $\delta$  9.75 (s, 1H), 8.54 (d, 1H,  $J$  = 3.2 Hz), 8.38–8.37 (m, 2H), 7.94 (s, 1H), 7.87 (d, 1H,  $J$  = 10.8 Hz), 7.68 (d, 1H,  $J$  = 8.4 Hz), 3.49 (s, 2H), 2.99–2.39 (m, 10H), 2.37 (s, 3H), 2.14–2.08 (m, 6H), 1.87–1.84 (m, 2H), 1.06 (t, 3H,  $J$  = 6.4 Hz).  $^{13}C$  NMR (100 MHz,  $CDCl_3$ )  $\delta$  190.41, 155.45 (d,  $J_{C-F}$  = 3.0 Hz), 154.41 (d,  $J_{C-F}$  = 215.0 Hz), 152.04, 151.90, 150.82 (d,  $J_{C-F}$  = 4.0 Hz), 150.64 (d,  $J_{C-F}$  = 10.0 Hz), 149.50 (d,  $J_{C-F}$  = 71.0 Hz), 147.62 (d,  $J_{C-F}$  = 27.0 Hz), 142.86 (d,  $J_{C-F}$  = 12.0 Hz), 138.94, 132.03 (d,  $J_{C-F}$  = 6.0 Hz), 127.02, 117.79 (dd,  $J_{C-F}$  = 2.0 Hz), 116.02 (dd,  $J_{C-F}$  = 8.0 Hz), 111.45, 64.99, 59.85, 52.92 (2C), 52.76 (2C), 52.28, 35.47 (2C), 26.78 (2C), 16.29, 12.00.

4.2.28. 5'-(2-chloropyrimidin-4-yl)-7'-fluoro-2'-methylspiro[cyclopentane-1,3'-indole] (**6E**)

Starting from **5D** (2.90 g, 8.8 mmol) and 2,4-dichloropyrimidine (2.00 g, 13.2 mmol), 883.6 mg of **6E** was obtained at 30% yield according to the method described for the synthesis of **1E**. ESI-MS:  $m/z$

$z$  316.2  $[M+H]^+$ .

4.2.29. *N*-(5-((4-ethylpiperazin-1-yl)methyl)pyridin-2-yl)-4-(7'-fluoro-2'-methylspiro[cyclopentane-1,3'-indol]-5'-yl)pyrimidin-2-amine (**6**)

Starting from **6E** (150.0 mg, 0.48 mmol) and **INT-7** (105.7 mg, 0.48 mmol), 28.7 mg of **6** was obtained as a white solid at 12% yield according to the method described for the synthesis of **1**. Purity: 96.6%; retention time: 3.33 min. MP: 170.8–171.9 °C. HRMS-ESI:  $[M+H]^+$  observed 500.2925, calculated 500.2938.  $^1H$  NMR (400 MHz,  $CDCl_3$ )  $\delta$  8.83 (s, 1H), 8.61 (d, 1H,  $J$  = 5.2 Hz), 8.49 (d, 1H,  $J$  = 8.8 Hz), 8.32 (d, 1H,  $J$  = 1.2 Hz), 7.91 (d, 1H,  $J$  = 1.2 Hz), 7.78 (d, 1H,  $J$  = 10.8 Hz), 7.78 (dd, 1H,  $J$  = 8.4, 1.6 Hz), 7.21 (d, 1H,  $J$  = 5.2 Hz), 3.52 (s, 2H), 2.54–2.41 (m, 10H), 2.38 (s, 3H), 2.19–2.08 (m, 6H), 1.90–1.87 (m, 2H), 1.10 (t, 3H,  $J$  = 6.8 Hz).  $^{13}C$  NMR (100 MHz,  $CDCl_3$ )  $\delta$  189.98, 163.75, 159.36, 158.78, 154.75 (d,  $J_{C-F}$  = 252.0 Hz), 152.11, 151.22 (d,  $J_{C-F}$  = 3.0 Hz), 148.69, 142.89 (d,  $J_{C-F}$  = 11.0 Hz), 138.89, 135.86 (d,  $J_{C-F}$  = 6.0 Hz), 127.18, 115.77, 113.89 (d,  $J_{C-F}$  = 20.0 Hz), 112.16, 108.86, 64.93, 59.84, 52.88 (2C), 52.76 (2C), 52.30, 35.5 (2C), 26.8 (2C), 16.28, 11.95.

4.2.30. 5'-bromo-2'-methylspiro[cyclopentane-1,3'-indole] (**7C**)

Starting from (4-bromophenyl) hydrazine (18.70 g, 100.0 mmol) and 1-cyclopentylethanone (11.22 g, 100.0 mmol), 13.21 g of **7C** was obtained at 50% yield according to the method described for the synthesis of **1C**. ESI-MS:  $m/z$  264.0  $[M+H]^+$ .

4.2.31. 2'-methyl-5'-(4,4,5,5-tetramethyl-1,3,2-dioxaborolan-2-yl)spiro[cyclopentane-1,3'-indole] (**7D**)

Starting from **7C** (2.64 g, 10.0 mmol) and bis(pinacolato)diboron (2.79 g, 11.0 mmol), 2.45 g of **7D** was obtained at 78% yield according to the method described for the synthesis of **1D**. ESI-MS:  $m/z$  312.2  $[M+H]^+$ .

4.2.32. 5'-(2-chloro-5-fluoropyrimidin-4-yl)-2'-methylspiro[cyclopentane-1,3'-indole] (**7E**)

Starting from **7D** (2.40 g, 7.6 mmol) and 2, 4-dichloro-5-fluoropyrimidine (1.50 g, 10.0 mmol), 1.15 g of **7E** was obtained at 49% yield according to the method described for the synthesis of **1E**. ESI-MS:  $m/z$  316.1  $[M+H]^+$ .

4.2.33. *N*-(5-((4-ethylpiperazin-1-yl)methyl)pyridin-2-yl)-5-fluoro-4-(2'-methylspiro[cyclopentane-1,3'-indol]-5'-yl)pyrimidin-2-amine (**7**)

Starting from **7E** (151.6 mg, 0.48 mmol) and **INT-7** (105.7 mg, 0.48 mmol), 55.1 mg of **7** was obtained as a white solid at 23% yield according to the method described for the synthesis of **1**. Purity: 99.1%; retention time: 3.08 min. MP: 161.3–162.0 °C. HRMS-ESI:  $[M+H]^+$  observed 500.2926, calculated 500.2938.  $^1H$  NMR (400 MHz,  $CDCl_3$ )  $\delta$  8.73 (brs, 1H), 8.47 (d, 1H,  $J$  = 3.6 Hz), 8.43 (d, 1H,  $J$  = 8.4 Hz), 8.30 (s, 1H), 8.15–8.13 (m, 2H), 7.70–7.64 (m, 2H), 3.52 (s, 2H), 2.53–2.37 (m, 10H), 2.31 (s, 3H), 2.21–2.06 (m, 6H), 1.89–1.86 (m, 2H), 1.10 (t, 3H,  $J$  = 7.2 Hz).  $^{13}C$  NMR (100 MHz,  $CDCl_3$ )  $\delta$  189.95, 156.34, 155.31 (d,  $J_{C-F}$  = 3.0 Hz), 152.30, 152.17 (d,  $J_{C-F}$  = 6.0 Hz), 149.76 (d,  $J_{C-F}$  = 105.0 Hz), 147.66, 147.07 (d,  $J_{C-F}$  = 27.0 Hz), 146.80, 138.94, 130.36 (d,  $J_{C-F}$  = 6.0 Hz), 129.15 (d,  $J_{C-F}$  = 9.0 Hz), 127.06, 121.95 (d,  $J_{C-F}$  = 6.0 Hz), 119.73, 111.33, 64.23, 59.84, 52.86 (2C), 52.76 (2C), 52.29, 35.39 (2C), 26.80 (2C), 16.18, 11.94.

4.2.34. *tert*-butyl 4-(6-((5-fluoro-4-(7'-fluoro-2'-methylspiro[cyclopentane-1,3'-indol]-5'-yl)pyrimidin-2-yl)amino)pyridin-3-yl)piperazine-1-carboxylate (**8F**)

Starting from **5E** (200.0 mg, 0.6 mmol) and **INT-3** (167.0 mg, 0.6 mmol), 103.5 mg of **8F** was obtained at 30% yield according to the method described for the synthesis of **1**. ESI-MS:  $m/z$  576.3  $[M+H]^+$ .

**4.2.35. 5-Fluoro-4-(7'-fluoro-2'-methylspiro[cyclopentane-1,3'-indol]-5'-yl)-N-(5-(piperazin-1-yl)pyridin-2-yl)pyrimidin-2-amine (8)**

TFA (2.5 mL) was added to **8F** (100.0 mg, 0.17 mmol) in DCM (10 mL). The mixture was stirred at RT for 3 h, concentrated under a vacuum, diluted with saturated aqueous Na<sub>2</sub>CO<sub>3</sub>, and extracted with DCM. The combined organic layers were washed with brine, dried over anhydrous Na<sub>2</sub>SO<sub>4</sub>, concentrated under a vacuum, and purified by silica gel column chromatography to obtain **8** (25.8 mg, yield: 32%) as a yellow solid. Purity: 99.1%; retention time: 3.09 min. MP: 222.7–223.5 °C. HRMS-ESI: [M+H]<sup>+</sup> observed 476.2357, calculated 476.2374. <sup>1</sup>H NMR (400 MHz, CDCl<sub>3</sub>) δ 8.67 (brs, 1H), 8.44 (d, 1H, *J* = 3.6 Hz), 8.29 (d, 1H, *J* = 9.2 Hz), 8.11 (d, 1H, *J* = 2.4 Hz), 7.95 (s, 1H), 7.89 (d, 1H, *J* = 10.8 Hz), 7.36 (dd, 1H, *J* = 9.2, 2.8 Hz), 3.12–3.06 (m, 8H), 2.39 (s, 3H), 2.16–2.10 (m, 6H), 1.89–1.86 (m, 2H). <sup>13</sup>C NMR (100 MHz, CDCl<sub>3</sub>) δ 190.35, 155.53 (d, *J*<sub>C-F</sub> = 3.0 Hz), 154.45 (d, *J*<sub>C-F</sub> = 251.0 Hz), 150.82 (d, *J*<sub>C-F</sub> = 4.0 Hz), 150.74 (d, *J*<sub>C-F</sub> = 9.0 Hz), 149.41 (d, *J*<sub>C-F</sub> = 201.0 Hz), 147.13, 146.28, 142.84 (d, *J*<sub>C-F</sub> = 12.0 Hz), 136.89, 132.13 (d, *J*<sub>C-F</sub> = 13.0 Hz), 132.07, 126.39, 117.80 (dd, *J*<sub>C-F</sub> = 3.0 Hz), 116.02 (dd, *J*<sub>C-F</sub> = 8.0 Hz), 112.35, 65.00, 51.02 (2C), 46.06 (2C), 35.48 (2C), 26.80 (2C), 16.30.

**4.2.36. N-(5-(1-ethylpiperidin-4-yl)pyridin-2-yl)-5-fluoro-4-(7'-fluoro-2'-methylspiro[cyclopentane-1,3'-indol]-5'-yl)pyrimidin-2-amine (9)**

Starting from **5E** (33.5 mg, 0.1 mmol) and **INT-5** (20.5 mg, 0.1 mmol), 11.0 mg of **9** was obtained as a light yellow solid at 22% yield according to the method described for the synthesis of **1**. Purity: 99.2%; retention time: 3.38 min. MP: 209.4–209.8 °C. HRMS-ESI: [M+H]<sup>+</sup> observed 503.2719, calculated 503.2735. <sup>1</sup>H NMR (400 MHz, CDCl<sub>3</sub>) δ 8.45 (d, 1H, *J* = 3.6 Hz), 8.38 (s, 1H), 8.33 (d, 1H, *J* = 8.8 Hz), 8.25 (s, 1H), 7.97 (s, 1H), 7.90 (d, 1H, *J* = 11.2 Hz), 7.62 (dd, 1H, *J* = 8.8, 2.0 Hz), 3.14–3.11 (m, 2H), 2.55–2.46 (m, 3H), 2.40 (s, 3H), 2.18–2.03 (m, 8H), 1.90–1.82 (m, 6H), 1.15 (t, 3H, *J* = 7.2 Hz). <sup>13</sup>C NMR (100 MHz, CDCl<sub>3</sub>) δ 190.38, 155.34 (d, *J*<sub>C-F</sub> = 3.0 Hz), 154.4 (d, *J*<sub>C-F</sub> = 252.0 Hz), 151.93 (d, *J*<sub>C-F</sub> = 79.0 Hz), 150.87 (d, *J*<sub>C-F</sub> = 5.0 Hz), 149.62 (d, *J*<sub>C-F</sub> = 224.0 Hz), 147.11, 146.81, 142.95 (d, *J*<sub>C-F</sub> = 11.0 Hz), 136.14, 135.55, 131.92 (d, *J*<sub>C-F</sub> = 12.0 Hz), 131.86, 117.72 (dd, *J*<sub>C-F</sub> = 3.0 Hz), 116.15 (dd, *J*<sub>C-F</sub> = 8.0 Hz), 111.70, 65.06, 53.83 (2C), 52.67, 39.73, 35.48 (2C), 33.45 (2C), 26.7 (2C), 16.28, 12.17.

**4.2.37. tert-butyl 4-(6-((5-fluoro-4-(7'-fluoro-2'-methylspiro[cyclopentane-1,3'-indol]-5'-yl)pyrimidin-2-yl)amino)pyridin-3-yl)piperidine-1-carboxylate (10F)**

Starting from **5E** (835.0 mg, 2.5 mmol) and **INT-6** (693.0 mg, 2.5 mmol), 500.3 mg of **10F** was obtained at 35% yield according to the method described for the synthesis of **1**. ESI-MS: *m/z* 575.3 [M+H]<sup>+</sup>.

**4.2.38. 5-Fluoro-4-(7'-fluoro-2'-methylspiro[cyclopentane-1,3'-indol]-5'-yl)-N-(5-(piperidin-4-yl)pyridin-2-yl)pyrimidin-2-amine (10)**

Starting from **10F** (500.0 mg, 0.87 mmol), 148.1 mg of **10** was obtained as a yellow solid at 36% yield according to the method described for the synthesis of **8**. Purity: 98.0%; retention time: 1.20 min. MP: 240.2–241.3 °C. HRMS-ESI: [M+H]<sup>+</sup> observed 475.2416, calculated 475.2422. <sup>1</sup>H NMR (400 MHz, CDCl<sub>3</sub>) δ 9.14 (brs, 1H), 8.48 (d, 1H, *J* = 3.2 Hz), 8.34–8.30 (m, 2H), 7.96 (s, 1H), 7.89 (d, 1H, *J* = 10.8 Hz), 7.58 (d, 1H, *J* = 8.4 Hz), 3.22–3.19 (m, 2H), 2.76 (t, 2H, *J* = 11.6 Hz), 2.66–2.60 (m, 1H), 2.38 (s, 3H), 2.16–2.02 (m, 6H), 1.88–1.83 (m, 4H), 1.69–1.61 (m, 2H). <sup>13</sup>C NMR (100 MHz, CDCl<sub>3</sub>) δ 190.36, 155.48 (d, *J*<sub>C-F</sub> = 3.0 Hz), 154.44 (d, *J*<sub>C-F</sub> = 236.0 Hz), 151.92 (d, *J*<sub>C-F</sub> = 58.0 Hz), 150.84 (d, *J*<sub>C-F</sub> = 4.0 Hz), 150.77 (d, *J*<sub>C-F</sub> = 1.0 Hz), 150.69 (d, *J*<sub>C-F</sub> = 2.0 Hz), 149.54 (d, *J*<sub>C-F</sub> = 208.0 Hz), 147.19, 146.72, 142.88 (d, *J*<sub>C-F</sub> = 12.0 Hz), 136.11 (d, *J*<sub>C-F</sub> = 40.0 Hz), 131.97, 117.77 (dd,

*J*<sub>C-F</sub> = 3.0 Hz), 116.07 (d, *J*<sub>C-F</sub> = 8.0 Hz), 111.79, 65.03, 47.07 (2C), 39.99, 35.47 (2C), 34.38 (2C), 26.77 (2C), 16.26.

**4.2.39. 5-Fluoro-4-(7'-fluoro-2'-methylspiro[cyclopentane-1,3'-indol]-5'-yl)-N-(5-(1-methylpiperidin-4-yl)pyridin-2-yl)pyrimidin-2-amine (11)**

Starting from **5E** (67.0 mg, 0.2 mmol) and **INT-4** (39.0 mg, 0.2 mmol), 12.2 mg of **11** was obtained as a white solid at 16% yield according to the method described for the synthesis of **1**. Purity: 97.9%; retention time: 3.37 min. MP: 230.7–231.4 °C. HRMS-ESI: [M+H]<sup>+</sup> observed 489.2570, calculated 489.2578. <sup>1</sup>H NMR (400 MHz, CDCl<sub>3</sub>) δ 9.38 (brs, 1H), 8.49 (d, 1H, *J* = 3.2 Hz), 8.34–8.33 (m, 2H), 7.96 (s, 1H), 7.88 (d, 1H, *J* = 11.2 Hz), 7.58 (dd, 1H, *J* = 8.8 Hz, 1.6 Hz), 3.01–2.98 (m, 2H), 2.52–2.44 (m, 1H), 2.38 (s, 3H), 2.34 (s, 3H), 2.25–2.04 (m, 8H), 1.87–1.76 (m, 6H). <sup>13</sup>C NMR (100 MHz, CDCl<sub>3</sub>) δ 190.35, 155.49 (d, *J*<sub>C-F</sub> = 3.0 Hz), 154.41 (d, *J*<sub>C-F</sub> = 236.0 Hz), 151.90 (d, *J*<sub>C-F</sub> = 45.0 Hz), 150.82 (d, *J*<sub>C-F</sub> = 8.0 Hz), 149.51 (d, *J*<sub>C-F</sub> = 200.0 Hz), 147.24, 146.86, 142.86 (d, *J*<sub>C-F</sub> = 11.0 Hz), 136.07, 135.18, 132.02 (d, *J*<sub>C-F</sub> = 12.0 Hz), 131.96, 117.75 (dd, *J*<sub>C-F</sub> = 3.0 Hz), 116.10 (dd, *J*<sub>C-F</sub> = 8.0 Hz), 111.80, 65.04, 56.22 (2C), 46.48, 38.94, 35.46 (2C), 33.42 (2C), 26.74 (2C), 16.28.

**4.2.40. 5-Fluoro-4-(7'-fluoro-2'-methylspiro[cyclopentane-1,3'-indol]-5'-yl)-N-(5-(4-methylpiperazin-1-yl)pyridin-2-yl)pyrimidin-2-amine (12)**

Starting from **5E** (100.0 mg, 0.30 mmol) and **INT-1** (57.6 mg, 0.3 mmol), 32.0 mg of **12** was obtained as a yellow solid at 16% yield according to the method described for the synthesis of **1**. Purity: 98.3%; retention time: 3.36 min. MP: 212.4–213.1 °C. HRMS-ESI: [M+H]<sup>+</sup> observed 490.2522, calculated 490.2531. <sup>1</sup>H NMR (400 MHz, DMSO-*d*<sub>6</sub>) δ 9.77 (brs, 1H), 8.63 (d, 1H, *J* = 4.0 Hz), 8.02–7.98 (m, 3H), 7.82 (d, 1H, *J* = 11.2 Hz), 7.41 (dd, 1H, *J* = 8.8 Hz, 2.8 Hz), 3.13–3.11 (m, 4H), 2.49–2.46 (m, 4H), 2.33 (s, 3H), 2.26 (s, 3H), 2.23–2.07 (m, 6H), 1.76–1.74 (m, 2H). <sup>13</sup>C NMR (100 MHz, DMSO-*d*<sub>6</sub>) δ 191.44, 156.20, 153.92 (d, *J*<sub>C-F</sub> = 206.0 Hz), 151.61 (d, *J*<sub>C-F</sub> = 4.0 Hz), 151.43, 149.90 (d, *J*<sub>C-F</sub> = 65.0 Hz), 148.32 (d, *J*<sub>C-F</sub> = 22.0 Hz), 146.02, 143.12, 142.71 (d, *J*<sub>C-F</sub> = 11.0 Hz), 135.91, 132.05 (d, *J*<sub>C-F</sub> = 6.0 Hz), 125.40, 118.31, 115.63 (dd, *J*<sub>C-F</sub> = 12.0 Hz), 113.61, 65.15, 54.91 (2C), 48.90 (2C), 46.21, 35.32 (2C), 26.75 (2C), 16.51.

**4.2.41. N-(5-(4-ethylpiperazin-1-yl)pyridin-2-yl)-5-fluoro-4-(7'-fluoro-2'-methylspiro[cyclopentane-1,3'-indol]-5'-yl)pyrimidin-2-amine (13)**

Starting from **5E** (100.0 mg, 0.3 mmol) and **INT-2** (61.8 mg, 0.3 mmol), 31.6 mg of **13** was obtained as a yellow solid at 22% yield according to the method described for the synthesis of **1**. Purity: 98.8%; retention time: 4.44 min. MP: 219.8–220.4 °C. HRMS-ESI: [M+H]<sup>+</sup> observed 504.2691, calculated 504.2687. <sup>1</sup>H NMR (400 MHz, CDCl<sub>3</sub>) δ 8.92 (brs, 1H), 8.44 (d, 1H, *J* = 3.6 Hz), 8.29 (d, 1H, *J* = 9.2 Hz), 8.15 (d, 1H, *J* = 2.8 Hz), 7.94 (s, 1H), 7.89 (d, 1H, *J* = 11.2 Hz), 7.36 (dd, 1H, *J* = 9.2 Hz, 2.8 Hz), 3.21–3.19 (m, 4H), 2.65–2.63 (m, 4H), 2.51 (q, 2H, *J* = 7.2 Hz), 2.38 (s, 3H), 2.22–2.07 (m, 6H), 1.89–1.86 (m, 2H), 1.15 (t, 3H, *J* = 7.2 Hz). <sup>13</sup>C NMR (100 MHz, CDCl<sub>3</sub>) δ 190.34, 155.55 (d, *J*<sub>C-F</sub> = 3.0 Hz), 154.44 (d, *J*<sub>C-F</sub> = 242.0 Hz), 150.80 (d, *J*<sub>C-F</sub> = 3.0 Hz), 150.68 (d, *J*<sub>C-F</sub> = 6.0 Hz), 149.38 (d, *J*<sub>C-F</sub> = 194.0 Hz), 147.44 (d, *J*<sub>C-F</sub> = 27.0 Hz), 146.31, 142.97, 142.81 (d, *J*<sub>C-F</sub> = 9.0 Hz), 136.85, 132.15 (d, *J*<sub>C-F</sub> = 6.0 Hz), 126.25, 117.81 (dd, *J*<sub>C-F</sub> = 3.0 Hz), 116.02 (dd, *J*<sub>C-F</sub> = 7.0 Hz), 112.34, 64.99, 52.69 (2C), 52.36, 49.76 (2C), 35.48 (2C), 26.79 (2C), 16.31, 12.02.

**4.2.42. 2-(4-(6-((5-fluoro-4-(7'-fluoro-2'-methylspiro[cyclopentane-1,3'-indol]-5'-yl)pyrimidin-2-yl)amino)pyridin-3-yl)piperazin-1-yl)ethanol (14)**

Cs<sub>2</sub>CO<sub>3</sub> (39.1 mg, 0.12 mmol) was added to a solution of compound **8** (19.0 mg, 0.04 mmol) and 2-bromoethanol-1-ol (15.0 mg,

0.12 mmol) in DMF (2 mL). The mixture was heated at 80 °C for 1 h, cooled to RT, diluted with water (10 mL), and extracted with EtOAc (40 mL  $\times$  3). The combined organic layers were washed with brine (40 mL), dried over anhydrous Na<sub>2</sub>SO<sub>4</sub>, concentrated under a vacuum, and purified by silica gel column chromatography (DCM/MeOH = 10:1) to obtain **14** (10.2 mg, yield: 55%) as a yellow solid. Purity: 97.3%; retention time: 3.11 min. MP: 220.8–221.2 °C. HRMS-ESI: [M+H]<sup>+</sup> observed 520.2625, calculated 520.2636.<sup>1</sup>H NMR (400 MHz, CDCl<sub>3</sub>)  $\delta$  8.52 (brs, 1H), 8.43 (d, 1H, *J* = 2.8 Hz), 8.29 (d, 1H, *J* = 9.2 Hz), 8.09 (s, 1H), 7.94 (s, 1H), 7.89 (d, 1H, *J* = 10.8 Hz), 7.36 (d, 1H, *J* = 8.8 Hz), 3.70–3.68 (m, 2H), 3.19–3.18 (m, 4H), 2.71–2.63 (m, 7H), 2.39 (s, 3H), 2.25–2.00 (m, 6H), 1.90–1.87 (m, 2H). <sup>13</sup>C NMR (100 MHz, CDCl<sub>3</sub>)  $\delta$  190.33, 155.50 (d, *J*<sub>C-F</sub> = 3.0 Hz), 154.47 (d, *J*<sub>C-F</sub> = 252.0 Hz), 150.84 (d, *J*<sub>C-F</sub> = 4.0 Hz), 150.72 (d, *J*<sub>C-F</sub> = 126.0 Hz), 147.35 (d, *J*<sub>C-F</sub> = 27.0 Hz), 146.30, 142.91 (d, *J*<sub>C-F</sub> = 16.0 Hz), 142.86, 136.80, 132.11 (d, *J*<sub>C-F</sub> = 12.0 Hz), 132.05, 126.34, 117.79 (dd, *J*<sub>C-F</sub> = 3.0 Hz), 116.02 (dd, *J*<sub>C-F</sub> = 8.0 Hz), 112.36, 65.01, 59.34, 57.84, 52.76 (2C), 49.85 (2C), 35.48 (2C), 26.80 (2C), 16.27.

4.2.43. 2-(4-(6-((5-fluoro-4-(7'-fluoro-2'-methylspiro [cyclopentane-1,3'-indol]-5'-yl)pyrimidin-2-yl)amino)pyridin-3-yl) piperidin-1-yl)ethan-1-ol (**15**)

Starting from **10** (19.0 mg, 0.04 mmol) and bromine ethanol (14.9 mg, 0.12 mmol), 11.3 mg of **15** was obtained as a light yellow solid at 55% yield according to the method described for the synthesis of **14**. Purity: 97.9%; retention time: 3.26 min. MP: 216.7–217.3 °C. HRMS-ESI:  $[M+H]^+$  observed 519.2670, calculated 519.2684.  $^1H$  NMR (400 MHz,  $CDCl_3$ )  $\delta$  8.63 (brs, 1H), 8.46 (d, 1H,  $J = 3.2$  Hz), 8.34 (d, 1H,  $J = 8.4$  Hz), 8.26 (s, 1H), 7.96 (s, 1H), 7.90 (d, 1H,  $J = 10.8$  Hz), 7.60 (d, 1H,  $J = 8.0$  Hz), 3.67–3.66 (m, 2H), 3.08–3.06 (m, 2H), 2.60–2.52 (m, 4H), 2.39 (s, 3H), 2.25–2.11 (m, 8H), 1.89–1.83 (m, 4H), 1.80–1.77 (m, 2H).  $^{13}C$  NMR (100 MHz,  $CDCl_3$ )  $\delta$  190.40, 155.37, 154.47 (d,  $J_{C-F} = 230.0$  Hz), 151.96 (d,  $J_{C-F} = 68.0$  Hz), 150.87 (d,  $J_{C-F} = 8.0$  Hz), 149.62 (d,  $J_{C-F} = 222.0$  Hz), 147.13, 146.71, 142.95 (d,  $J_{C-F} = 12.0$  Hz), 136.12, 135.21, 131.97 (d,  $J_{C-F} = 12.0$  Hz), 131.91, 117.77 (dd,  $J_{C-F} = 3.0$  Hz), 116.08 (dd,  $J_{C-F} = 7.0$  Hz), 111.75, 65.04, 59.55, 57.98, 53.97 (2C), 39.49, 35.48 (2C), 33.46 (2C), 26.79 (2C), 16.28.

4.2.44. 5-Fluoro-4-(7'-fluoro-2'-methylspiro[cyclopentane-1,3'-indol]-5'-yl)-N-(5-(4-isopropylpiperazin-1-yl)pyridin-2-yl)pyrimidin-2-amine (**16**)

Starting from **8** (100.0 mg, 0.21 mmol) and 2-iodopropane (43.0 mg, 0.31 mmol), 21.2 mg of **16** was obtained as a light yellow solid at 20% yield according to the method described for the synthesis of **14**. Purity: 96.9%; retention time: 3.18 min. MP: 236.1–237.2 °C. HRMS-ESI:  $[M+H]^+$  observed 518.2830, calculated 518.2844.<sup>1</sup>H NMR (400 MHz, CDCl<sub>3</sub>)  $\delta$  8.47 (brs, 1H), 8.43 (d, 1H,  $J$  = 3.2 Hz), 8.28 (d, 1H,  $J$  = 9.2 Hz), 8.11 (d, 1H,  $J$  = 2.4 Hz), 7.95 (s, 1H), 7.90 (d, 1H,  $J$  = 11.2 Hz), 7.60 (dd, 1H,  $J$  = 8.8 Hz, 2.4 Hz), 3.21–3.20 (m, 4H), 2.79–2.74 (m, 5H), 2.39 (s, 3H), 2.17–2.08 (m, 6H), 1.90–1.86 (m, 2H), 1.14 (d, 6H,  $J$  = 6.4 Hz). <sup>13</sup>C NMR (100 MHz, CDCl<sub>3</sub>)  $\delta$  190.29, 155.50 (d,  $J_{C-F}$  = 2.0 Hz), 154.46 (d,  $J_{C-F}$  = 248.0 Hz), 151.95 (d,  $J_{C-F}$  = 13.0 Hz), 149.44 (d,  $J_{C-F}$  = 107.0 Hz), 147.10, 146.16, 143.10, 142.87 (d,  $J_{C-F}$  = 12.0 Hz), 136.86, 132.11 (d,  $J_{C-F}$  = 12.0 Hz), 132.05, 126.22, 117.77 (dd,  $J_{C-F}$  = 3.0 Hz), 116.05 (dd,  $J_{C-F}$  = 8.0 Hz), 112.32, 65.02, 54.61, 50.05, 48.57 (2C), 35.48 (2C), 26.79 (3C), 18.53 (2C), 16.27.

4.2.45. *tert*-butyl 4-(6-((5-fluoro-4-(7-fluoro-2,3,3-trimethyl-3H-indol-5-yl)pyrimidin-2-yl)amino)pyridin-3-yl)piperazine-1-carboxylate (**17F**)

Starting from **1E** (150.0 mg, 0.49 mmol) and **INT-3** (135.8 mg, 0.49 mmol), 53.4 mg of **17F** was obtained at 20% yield according to the method described for the synthesis of **1**. ESI-MS:  $m/z$  550.3

 $[M+H]^+$ .

4.2.46. 5-Fluoro-4-(7-fluoro-2,3,3-trimethyl-3H-indol-5-yl)-N-(5-(piperazin-1-yl)pyridin-2-yl)pyrimidin-2-amine (**17**)

Starting from **17F** (30.0 mg, 0.054 mmol), 10.5 mg of **17** was obtained as a yellow solid at 25% yield according to the method described for the synthesis of **8**. Purity: 97.6%; retention time: 3.30 min. MP: 198.5–199.7 °C. HRMS-ESI:  $[M+H]^+$  observed 450.2211, calculated 450.2218.<sup>1</sup>H NMR (400 MHz, DMSO-*d*<sub>6</sub>)  $\delta$  9.75 (brs, 1H), 8.65 (d, 1H, *J* = 3.2 Hz), 8.02–7.94 (m, 3H), 7.82 (d, 1H, *J* = 10.8 Hz), 7.43 (d, 1H, *J* = 8.8 Hz), 3.09–3.02 (m, 4H), 2.84–2.83 (m, 4H), 2.31 (s, 3H), 1.34 (s, 6H). <sup>13</sup>C NMR (100 MHz, DMSO-*d*<sub>6</sub>)  $\delta$  192.39, 156.24, 154.20 (d, *J*<sub>C-F</sub> = 243.0 Hz), 151.77 (d, *J*<sub>C-F</sub> = 7.0 Hz), 150.42 (d, *J*<sub>C-F</sub> = 3.0 Hz), 149.26 (d, *J*<sub>C-F</sub> = 109.0 Hz), 147.90, 145.90, 143.81, 142.52 (d, *J*<sub>C-F</sub> = 11.0 Hz), 135.84, 132.06, 125.60, 118.79, 115.89 (d, *J*<sub>C-F</sub> = 6.0 Hz), 113.50, 55.15, 50.25 (2C), 45.95 (2C), 22.77 (2C), 16.06.

4.2.47. *tert*-butyl 4-(6-((4-(3-ethyl-7-fluoro-2,3-dimethyl-3H-indol-5-yl)-5-fluoropyrimidin-2-yl)amino)pyridin-3-yl)piperazine-1-carboxylate (**18F**)

Starting from **2E** (200.0 mg, 0.62 mmol) and **INT-3** (172.6 mg, 0.62 mmol), 23.7 mg of **18F** was obtained at 21% yield according to the method described for the synthesis of **1**. ESI-MS:  $m/z$  564.3  $[M+H]^+$ .

4.2.48. 4-(3-Ethyl-7-fluoro-2,3-dimethyl-3H-indol-5-yl)-5-fluoro-N-(5-(piperazin-1-yl)pyridin-2-yl)pyrimidin-2-amine (**18**)

Starting from **18F** (100.0 mg, 0.18 mmol), 45.7 mg of **18** was obtained as a yellow solid at 26% yield according to the method described for the synthesis of **8**. Purity: 95.2%; retention time: 3.10 min. MP: 160.5–161.3 °C. HRMS-ESI:  $[M+H]^+$  observed 464.2361, calculated 464.2374.  $^1\text{H}$  NMR (400 MHz,  $\text{CDCl}_3$ )  $\delta$  9.33 (brs, 1H), 8.46 (d, 1H,  $J$  = 3.6 Hz), 8.28 (d, 1H,  $J$  = 8.8 Hz), 8.16 (d, 1H,  $J$  = 2.4 Hz), 7.90 (d, 1H,  $J$  = 10.8 Hz), 7.82 (s, 1H), 7.35 (dd, 1H,  $J$  = 8.8 Hz, 2.8 Hz), 3.10–3.03 (m, 8H), 2.31 (s, 3H), 2.03–1.80 (m, 3H), 1.36 (s, 3H), 0.47 (t, 6H,  $J$  = 7.6 Hz).  $^{13}\text{C}$  NMR (100 MHz,  $\text{CDCl}_3$ )  $\delta$  190.49, 155.68 (d,  $J_{\text{C-F}}$  = 3.0 Hz), 154.66 (d,  $J_{\text{C-F}}$  = 251.0 Hz), 151.85, 150.71 (d,  $J_{\text{C-F}}$  = 9.0 Hz), 149.32 (d,  $J_{\text{C-F}}$  = 190.0 Hz), 147.35 (d,  $J_{\text{C-F}}$  = 19.0 Hz), 146.47, 143.49 (d,  $J_{\text{C-F}}$  = 11.0 Hz), 136.86, 132.20 (d,  $J_{\text{C-F}}$  = 11.0 Hz), 123.14, 126.51, 118.26 (dd,  $J_{\text{C-F}}$  = 2.0 Hz), 116.22 (dd,  $J_{\text{C-F}}$  = 6.0 Hz), 112.38, 59.64, 51.01 (2C), 46.04 (2C), 30.16, 22.24, 16.10, 8.58.

4.2.49. *tert*-butyl 4-(6-((4-(3,3-diethyl-7-fluoro-2-methyl-3H-indol-5-yl)-5-fluoropyrimidin-2-yl)amino)pyridin-3-yl)piperazine-1-carboxylate (**19F**)

Starting from **3E** (100.0 mg, 0.29 mmol) and **INT-3** (80.6 mg, 0.29 mmol), 80.2 mg of **19F** was obtained at 47% yield according to the method described for the synthesis of **1**. ESI-MS:  $m/z$  578.3  $[M+H]^+$ .

**4.2.50. 4-(3,3-Diethyl-7-fluoro-2-methyl-3H-indol-5-yl)-5-fluoro-N-(5-(piperazin-1-yl)pyridin-2-yl)pyrimidin-2-amine (19)**

Starting from **19F** (50.0 mg, 0.086 mmol), 25.5 mg of **19** was obtained as a light yellow solid at 25% yield according to the method described for the synthesis of **8**. Purity: 98.2%; retention time: 3.40 min. MP: 144.1–145.3 °C. HRMS-ESI: [M+H]<sup>+</sup> observed 478.2515, calculated 478.2531.<sup>1</sup>H NMR (400 MHz, CDCl<sub>3</sub>) δ 8.66 (brs, 1H), 8.45 (d, 1H, *J* = 3.6 Hz), 8.29 (d, 1H, *J* = 9.2 Hz), 8.11 (d, 1H, *J* = 2.8 Hz), 7.94 (d, 1H, *J* = 11.2 Hz), 7.81 (s, 1H), 7.37 (dd, 1H, *J* = 8.8 Hz, 2.4 Hz), 3.13–3.12 (m, 4H), 3.08–3.07 (m, 4H), 2.30 (s, 3H), 2.08–1.99 (m, 2H), 1.91–1.82 (m, 3H), 0.46 (t, 6H, *J* = 7.6 Hz). <sup>13</sup>C NMR (100 MHz, CDCl<sub>3</sub>) δ 189.73, 155.56 (d, J<sub>C-F</sub> = 3.0 Hz), 154.63 (d, J<sub>C-F</sub> = 252.0 Hz), 150.79 (d, J<sub>C-F</sub> = 7.0 Hz), 149.45 (d, J<sub>C-F</sub> = 106.0 Hz), 147.13, 146.26, 145.49 (d, J<sub>C-F</sub> = 4.0 Hz), 144.44 (d, J<sub>C-</sub>

F = 11.0 Hz), 143.51, 136.86, 132.04 (d,  $J_{C-F}$  = 22.0 Hz), 126.50, 118.39 (dd,  $J_{C-F}$  = 3.0 Hz), 116.28 (dd,  $J_{C-F}$  = 7.0 Hz), 112.36, 65.09, 51.05 (2C), 46.07 (2C), 29.59 (2C), 16.40, 8.31 (2C).

**4.2.51. tert-butyl 4-(6-((5-fluoro-4-(7'-fluoro-2'-methylspiro[cyclopentane-1,3'-indol]-5'-yl)pyrimidin-2-yl)amino)pyridin-3-yl)piperazine-1-carboxylate (20F)**

Starting from **7E** (200.0 mg, 0.63 mmol) and **INT-3** (176.1 mg, 0.63 mmol), 105.6 mg of **20F** was obtained at 31% yield according to the method described for the synthesis of **1**. ESI-MS:  $m/z$  558.2 [M+H]<sup>+</sup>.

**4.2.52. 5-Fluoro-4-(7'-fluoro-2'-methylspiro[cyclopentane-1,3'-indol]-5'-yl)-N-(5-(piperazin-1-yl)pyridin-2-yl)pyrimidin-2-amine (20)**

Starting from **20F** (100.0 mg, 0.18 mmol), 25.8 mg of **20** was obtained as a yellow solid at 32% yield according to the method described for the synthesis of **8**. Purity: 97.3%; retention time: 3.37 min. MP: 213.8–214.5 °C. HRMS-ESI: [M+H]<sup>+</sup> observed 458.2465, calculated 458.2468. <sup>1</sup>H NMR (400 MHz, CDCl<sub>3</sub>) δ 9.28 (brs, 1H), 8.43 (d, 1H,  $J$  = 3.6 Hz), 8.33 (d, 1H,  $J$  = 9.2 Hz), 8.16–8.09 (m, 3H), 7.63 (d, 1H,  $J$  = 8.0 Hz), 7.32 (dd, 1H,  $J$  = 9.2 Hz, 2.8 Hz), 3.08–3.06 (m, 4H), 3.03–3.02 (m, 4H), 2.34 (s, 3H), 2.29–2.04 (m, 7H), 1.86–1.83 (m, 2H). <sup>13</sup>C NMR (100 MHz, CDCl<sub>3</sub>) δ 189.78, 156.13, 155.65, 152.05 (d,  $J_{C-F}$  = 7.0 Hz), 151.98, 149.46 (d,  $J_{C-F}$  = 193.0 Hz), 147.01, 146.73, 143.23, 136.94, 130.60 (d,  $J_{C-F}$  = 6.0 Hz), 129.07 (d,  $J_{C-F}$  = 8.0 Hz), 126.43, 121.98 (d,  $J_{C-F}$  = 6.0 Hz), 119.65, 112.34, 64.20, 51.01 (2C), 46.00 (2C), 35.35 (2C), 26.7 (2C), 16.13.

**4.2.53. 5-Fluoro-4-(2'-methylspiro[cyclopentane-1,3'-indol]-5'-yl)-N-(5-(piperidin-4-yl)pyridin-2-yl)pyrimidin-2-amine (21F)**

Starting from **7E** (315.7 mg, 1 mmol) and **INT-6** (277.3 mg, 1 mmol), 239.2 mg of **21F** was obtained at 43% yield according to the method described for the synthesis of **1**. ESI-MS:  $m/z$  557.3 [M+H]<sup>+</sup>.

**4.2.54. 5-Fluoro-4-(2'-methylspiro[cyclopentane-1,3'-indol]-5'-yl)-N-(5-(piperidin-4-yl)pyridin-2-yl)pyrimidin-2-amine (21)**

Starting from **21F** (200.0 mg, 0.36 mmol), 61.4 mg of **21** was obtained as a yellow solid at 36% yield according to the method described for the synthesis of **8**. Purity: 97.0%; retention time: 1.02 min. MP: 142.5–143.1 °C. HRMS-ESI: [M+H]<sup>+</sup> observed 457.2507, calculated 457.2516. <sup>1</sup>H NMR (400 MHz, CDCl<sub>3</sub>) δ 8.99 (brs, 1H), 8.46 (d, 1H,  $J$  = 3.6 Hz), 8.39 (d, 1H,  $J$  = 8.4 Hz), 8.29 (d, 1H,  $J$  = 1.6 Hz), 8.15–8.11 (m, 2H), 7.65 (d, 1H,  $J$  = 8.0 Hz), 7.58 (dd, 1H,  $J$  = 8.8 Hz, 2.0 Hz), 3.22–3.19 (m, 2H), 2.76 (t, 2H,  $J$  = 10.4 Hz), 2.65–2.59 (m, 1H), 2.36 (s, 3H), 2.18–2.05 (m, 7H), 1.88–1.83 (m, 4H), 1.70–1.60 (m, 2H). <sup>13</sup>C NMR (100 MHz, CDCl<sub>3</sub>) δ 189.88, 156.26, 155.47 (d,  $J_{C-F}$  = 3.0 Hz), 152.21 (d,  $J_{C-F}$  = 15.0 Hz), 152.15, 151.46, 149.68 (d,  $J_{C-F}$  = 207.0 Hz), 147.06, 146.79 (d,  $J_{C-F}$  = 10.0 Hz), 136.07, 135.57, 130.44 (d,  $J_{C-F}$  = 6.0 Hz), 129.14 (d,  $J_{C-F}$  = 8.0 Hz), 121.95 (d,  $J_{C-F}$  = 6.0 Hz), 119.68, 111.76, 64.24, 47.09 (2C), 39.99, 35.37 (2C), 34.41 (2C), 26.75 (2C), 16.14.

**4.2.55. 4-(3,3-Diethyl-7-fluoro-2-methyl-3H-indol-5-yl)-5-fluoro-N-(5-(4-methylpiperazin-1-yl)pyridin-2-yl)pyrimidin-2-amine (22)**

Starting from **3E** (200.0 mg, 0.59 mmol) and **INT-1** (114.6 mg, 0.59 mmol), 101.5 mg of **22** was obtained as a yellow solid at 35% yield according to the method described for the synthesis of **1**. Purity: 98.5%; retention time: 3.17 min. MP: 202.8–203.1 °C. HRMS-ESI: [M+H]<sup>+</sup> observed 492.2673, calculated 492.2687. <sup>1</sup>H NMR (400 MHz, CDCl<sub>3</sub>) δ 9.57 (brs, 1H), 8.47 (d, 1H,  $J$  = 3.2 Hz), 8.28 (d, 1H,  $J$  = 8.8 Hz), 8.18 (d, 1H,  $J$  = 2.0 Hz), 7.91 (d, 1H,  $J$  = 11.2 Hz), 7.78 (s, 1H), 7.33 (d, 1H,  $J$  = 8.8 Hz), 3.16–3.15 (m, 4H), 2.58–2.57 (m, 4H), 2.33 (s, 3H), 2.26 (s, 3H), 2.04–1.95 (m, 2H), 1.85–1.78 (m, 7H), 0.43

(t, 6H,  $J$  = 7.2 Hz). <sup>13</sup>C NMR (100 MHz, CDCl<sub>3</sub>) δ 189.65, 155.70 (d,  $J_{C-F}$  = 2.0 Hz), 154.59 (d,  $J_{C-F}$  = 252.0 Hz), 151.84, 150.63 (d,  $J_{C-F}$  = 4.0 Hz), 149.30 (d,  $J_{C-F}$  = 180.0 Hz), 146.52, 145.45 (d,  $J_{C-F}$  = 3.0 Hz), 144.34 (d,  $J_{C-F}$  = 11.0 Hz), 142.80, 136.83, 132.15 (d,  $J_{C-F}$  = 12.0 Hz), 126.37, 118.40 (dd,  $J_{C-F}$  = 3.0 Hz), 116.21 (dd,  $J_{C-F}$  = 6.0 Hz), 112.38, 65.03, 54.94 (2C), 49.70 (2C), 46.11, 29.52 (2C), 16.36, 8.30 (2C).

**4.2.56. 4.2.56.4-(3-ethyl-7-fluoro-2,3-dimethyl-3H-indol-5-yl)-5-fluoro-N-(5-(4-methylpiperazin-1-yl)pyridin-2-yl)pyrimidin-2-amine (23)**

Starting from **2E** (321.7 mg, 1.0 mmol) and **INT-1** (192.3 mg, 1.0 mmol), 47.1 mg of **23** was obtained as a yellow solid at 10% yield according to the method described for the synthesis of **1**. Purity: 97.8%; retention time: 3.38 min. MP: 130.2–131.9 °C. HRMS-ESI: [M+H]<sup>+</sup> observed 478.2516, calculated 478.2531. <sup>1</sup>H NMR (400 MHz, CDCl<sub>3</sub>) δ 9.48 (brs, 1H), 8.47 (d, 1H,  $J$  = 3.2 Hz), 8.28 (d, 1H,  $J$  = 9.2 Hz), 8.17 (s, 1H), 7.90 (d, 1H,  $J$  = 10.8 Hz), 7.82 (s, 1H), 7.34 (d, 1H,  $J$  = 8.4 Hz), 3.17–3.16 (m, 4H), 2.59–2.58 (m, 4H), 2.35 (s, 3H), 2.31 (s, 3H), 2.01–1.96 (m, 1H), 1.87–1.82 (m, 1H), 1.35 (s, 3H), 0.47 (t, 3H,  $J$  = 7.2 Hz). <sup>13</sup>C NMR (100 MHz, CDCl<sub>3</sub>) δ 190.42, 155.67, 154.67 (d,  $J_{C-F}$  = 252.0 Hz), 151.85, 150.69, 149.31 (d,  $J_{C-F}$  = 188.0 Hz), 147.17, 146.45, 143.49 (d,  $J_{C-F}$  = 11.0 Hz), 142.84, 136.81, 132.15, 126.38, 118.22 (d,  $J_{C-F}$  = 6.0 Hz), 116.22 (d,  $J_{C-F}$  = 21.0 Hz), 112.37, 59.63, 54.95 (2C), 49.70 (2C), 46.11, 30.15, 22.22, 16.08, 8.57.

**4.2.57. 4-(3-Ethyl-7-fluoro-2,3-dimethyl-3H-indol-5-yl)-N-(5-(4-ethylpiperazin-1-yl)pyridin-2-yl)-5-fluoropyrimidin-2-amine (24)**

Starting from **2E** (321.5 mg, 1.0 mmol) and **INT-2** (206.3 mg, 1.0 mmol), 49.1 mg of **24** was obtained as yellow solid at 10% yield according to the method described for the synthesis of **1**. Purity: 97.9%; retention time: 3.19 min. MP: 135.1–136.8 °C. HRMS-ESI: [M+H]<sup>+</sup> observed 492.2674, calculated 492.2687. <sup>1</sup>H NMR (400 MHz, CDCl<sub>3</sub>) δ 9.25 (brs, 1H), 8.46 (d, 1H,  $J$  = 3.2 Hz), 8.28 (d, 1H,  $J$  = 9.2 Hz), 8.17 (d, 1H,  $J$  = 2.0 Hz), 7.90 (d, 1H,  $J$  = 11.2 Hz), 7.82 (s, 1H), 7.35 (dd, 1H,  $J$  = 9.2 Hz, 2.8 Hz), 3.20–3.18 (m, 4H), 2.64–2.61 (m, 4H), 2.51 (q, 2H,  $J$  = 6.8 Hz), 2.31 (s, 3H), 2.03–1.94 (m, 1H), 1.89–1.82 (m, 1H), 1.36 (s, 3H), 1.13 (t, 3H,  $J$  = 7.2 Hz), 0.48 (t, 3H,  $J$  = 7.2 Hz). <sup>13</sup>C NMR (100 MHz, CDCl<sub>3</sub>) δ 190.42, 155.68 (d,  $J_{C-F}$  = 3.0 Hz), 154.68 (d,  $J_{C-F}$  = 252.0 Hz), 151.87, 150.73 (d,  $J_{C-F}$  = 10.0 Hz), 149.33 (d,  $J_{C-F}$  = 192.0 Hz), 147.36 (d,  $J_{C-F}$  = 4.0 Hz), 146.41, 143.51 (d,  $J_{C-F}$  = 12.0 Hz), 142.93, 136.80, 132.20 (d,  $J_{C-F}$  = 12.0 Hz), 126.34, 118.24 (dd,  $J_{C-F}$  = 3.0 Hz), 116.23 (dd,  $J_{C-F}$  = 6.0 Hz), 112.37, 59.64, 52.66 (2C), 52.33, 49.74 (2C), 30.16, 22.22, 16.08, 11.96, 8.57.

**4.2.58. N-(5-(1-ethylpiperidin-4-yl)pyridin-2-yl)-5-fluoro-4-(2'-methylspiro[cyclopentane-1,3'-indol]-5'-yl)pyrimidin-2-amine (25)**

Starting from **7E** (315.7 mg, 1.0 mmol) and **INT-5** (205.3 mg, 1.0 mmol), 53.2 mg of **25** was obtained as a light yellow solid at 11% yield according to the method described for the synthesis of **1**. Purity: 99.3%; retention time: 3.17 min. MP: 150.1–150.9 °C. HRMS-ESI: [M+H]<sup>+</sup> observed 485.2818, calculated 485.2829. <sup>1</sup>H NMR (400 MHz, DMSO-*d*<sub>6</sub>) δ 9.91 (brs, 1H), 8.65 (d, 1H,  $J$  = 4.0 Hz), 8.28–8.14 (m, 3H), 8.04 (d, 1H,  $J$  = 8.4 Hz), 7.43 (dd, 1H,  $J$  = 8.4 Hz, 2.0 Hz), 7.60 (d, 1H,  $J$  = 8.0 Hz), 3.00–2.97 (m, 4H), 2.38–2.33 (m, 2H), 2.30 (s, 3H), 2.08–2.07 (m, 6H), 1.99–1.94 (m, 2H), 1.77–1.64 (m, 6H), 1.02 (t, 3H,  $J$  = 7.2 Hz). <sup>13</sup>C NMR (100 MHz, DMSO-*d*<sub>6</sub>) δ 190.34, 156.60, 155.93, 152.19, 151.93, 151.38 (d,  $J_{C-F}$  = 8.0 Hz), 149.67 (d,  $J_{C-F}$  = 149.0 Hz), 148.00 (d,  $J_{C-F}$  = 26.0 Hz), 146.72, 136.09, 135.45, 130.20, 129.16 (d,  $J_{C-F}$  = 9.0 Hz), 122.13, 119.65, 112.59, 64.17, 53.59 (2C), 52.29, 39.14, 35.21 (2C), 33.18 (2C), 26.71 (2C), 16.25, 12.46.



#### 4.2.59. *N*-(5-(4-ethylpiperazin-1-yl)pyridin-2-yl)-5-fluoro-4-(2'-methylspiro[cyclopentane-1,3'-indol]-5'-yl)pyrimidin-2-amine (**26**)

Starting from **7E** (100.0 mg, 0.32 mmol) and **INT-2** (66.0 mg, 0.32 mmol), 31.2 mg of **26** was obtained as a yellow solid at 20% yield according to the method described for the synthesis of **1**. Purity: 96.9%; retention time: 3.24 min. MP: 188.4–189.6 °C. HRMS-ESI:  $[M+H]^+$  observed 486.2767, calculated 486.2781.  $^1H$  NMR (400 MHz,  $CDCl_3$ )  $\delta$  8.87 (brs, 1H), 8.42 (d, 1H,  $J = 3.6$  Hz), 8.33 (d, 1H,  $J = 9.2$  Hz), 8.13–8.10 (m, 3H), 7.65 (d, 1H,  $J = 8.0$  Hz), 7.35 (dd, 1H,  $J = 8.8$  Hz, 2.4 Hz), 3.19–3.18 (m, 4H), 2.64–2.63 (m, 4H), 2.53 (q, 2H,  $J = 6.8$  Hz), 2.35 (s, 3H), 2.27–2.06 (m, 6H), 1.88–1.85 (m, 2H), 1.14 (t, 3H,  $J = 6.8$  Hz).  $^{13}C$  NMR (100 MHz,  $CDCl_3$ )  $\delta$  189.78, 156.20, 155.58 (d,  $J_{C-F} = 2.0$  Hz), 152.10 (d,  $J_{C-F} = 6.0$  Hz), 152.01, 149.52 (d,  $J_{C-F} = 196.0$  Hz), 146.99 (d,  $J_{C-F} = 25.0$  Hz), 146.57, 142.85, 136.90, 130.56 (d,  $J_{C-F} = 6.0$  Hz), 129.09 (d,  $J_{C-F} = 8.0$  Hz), 126.29, 121.96 (d,  $J_{C-F} = 5.0$  Hz), 119.67, 112.31, 64.22, 52.67 (2C), 52.34, 49.78 (2C), 35.37 (2C), 26.77 (2C), 16.14, 11.94.

#### 4.2.60. 5-Fluoro-*N*-(5-(1-methylpiperidin-4-yl)pyridin-2-yl)-4-(2'-methylspiro[cyclopentane-1,3'-indol]-5'-yl)pyrimidin-2-amine (**27**)

Starting from **7E** (315.7 mg, 1.0 mmol) and **INT-4** (191.3 mg, 1.0 mmol), 47.0 mg of **27** was obtained as a yellow solid at 10% yield according to the method described for the synthesis of **1**. Purity: 98.6%; retention time: 3.11 min. MP: 201.9–202.6 °C. HRMS-ESI:  $[M+H]^+$  observed 471.2657, calculated 471.2672.  $^1H$  NMR (400 MHz,  $CDCl_3$ )  $\delta$  9.24 (brs, 1H), 8.47 (d, 1H,  $J = 3.2$  Hz), 8.38 (d, 1H,  $J = 8.8$  Hz), 8.31 (s, 1H), 8.14–8.09 (m, 2H), 7.64 (d, 1H,  $J = 8.4$  Hz), 7.57 (dd, 1H,  $J = 8.4$  Hz, 2.4 Hz), 3.00–2.98 (m, 2H), 2.49–2.46 (m, 1H), 2.35 (s, 3H), 2.33 (s, 3H), 2.16–1.99 (m, 8H), 1.85–1.76 (m, 6H).  $^{13}C$  NMR (100 MHz,  $CDCl_3$ )  $\delta$  189.83, 156.22, 155.49 (d,  $J_{C-F} = 3.0$  Hz), 152.18 (d,  $J_{C-F} = 8.0$  Hz), 152.01, 151.60, 149.64 (d,  $J_{C-F} = 206.0$  Hz), 147.10, 146.81, 136.00, 134.96, 130.46 (d,  $J_{C-F} = 6.0$  Hz), 129.15 (d,  $J_{C-F} = 9.0$  Hz), 121.92 (d,  $J_{C-F} = 5.0$  Hz), 119.66, 111.78, 64.25, 56.20 (2C), 46.42, 38.90, 35.35 (2C), 33.37 (2C), 26.73 (2C), 16.11.

#### 4.2.61. 4-(3-Ethyl-7-fluoro-2,3-dimethyl-3H-indol-5-yl)-5-fluoro-*N*-(5-(1-methylpiperidin-4-yl)pyridin-2-yl)pyrimidin-2-amine (**28**)

Starting from **2E** (321.6 mg, 1.0 mmol) and **INT-4** (191.3 mg, 1 mmol), 71.3 mg of **28** was obtained as a light yellow solid at 15% yield according to the method described for the synthesis of **1**. Purity: 98.6%; retention time: 3.43 min. MP: 179.8–180.6 °C. HRMS-ESI:  $[M+H]^+$  observed 477.2563, calculated 477.2578.  $^1H$  NMR (400 MHz,  $CDCl_3$ )  $\delta$  9.74 (brs, 1H), 8.50 (d, 1H,  $J = 3.6$  Hz), 8.35–8.32 (m, 2H), 7.88–7.82 (m, 2H), 7.57 (d, 1H,  $J = 8.8$  Hz), 2.97–2.95 (m, 2H), 2.49–2.42 (m, 1H), 2.30 (s, 6H), 2.24–1.93 (m, 3H), 1.88–1.74 (m, 5H), 1.35 (s, 3H), 0.47 (t, 3H,  $J = 7.2$  Hz).  $^{13}C$  NMR (100 MHz,  $CDCl_3$ )  $\delta$  190.48, 155.62 (d,  $J_{C-F} = 2.0$  Hz), 154.64 (d,  $J_{C-F} = 252.0$  Hz), 151.98 (d,  $J_{C-F} = 42.0$  Hz), 150.74 (d,  $J_{C-F} = 8.0$  Hz), 149.44 (d,  $J_{C-F} = 196.0$  Hz), 147.37 (d,  $J_{C-F} = 3.0$  Hz), 147.21, 146.81, 143.54 (d,  $J_{C-F} = 11.0$  Hz), 136.13, 135.09, 132.02, 118.20 (dd,  $J_{C-F} = 3.0$  Hz), 116.24 (dd,  $J_{C-F} = 14.0$  Hz), 111.84, 59.63, 56.19 (2C), 46.44, 38.90, 33.41 (2C), 30.16, 22.21, 16.08, 8.57.

#### 4.2.62. 5-Fluoro-*N*-(5-(4-methylpiperazin-1-yl)pyridin-2-yl)-4-(2'-methylspiro[cyclopentane-1,3'-indol]-5'-yl)pyrimidin-2-amine (**29**)

Starting from **7E** (100.0 mg, 0.32 mmol) and **INT-1** (61.5 mg, 0.32 mmol), 27.3 mg of **29** was obtained as a yellow solid at 18% yield according to the method described for the synthesis of **1**. Purity: 98.6%; retention time: 3.06 min. MP: 213.7–214.3 °C. HRMS-ESI:  $[M+H]^+$  observed 472.2624, calculated 472.2625.  $^1H$  NMR (400 MHz,  $CDCl_3$ )  $\delta$  9.28 (brs, 1H), 8.44 (d, 1H,  $J = 3.6$  Hz), 8.33 (d, 1H,  $J = 9.2$  Hz), 8.18 (d, 1H,  $J = 2.0$  Hz), 8.12–8.09 (m, 2H), 7.64 (d, 1H,  $J = 8.0$  Hz), 7.33 (dd, 1H,  $J = 9.2$  Hz, 2.4 Hz), 3.16–3.14 (m, 4H), 2.59–2.58 (m, 4H), 2.35 (s, 3H), 2.34 (s, 3H), 2.15–2.06 (m, 6H),

1.87–1.83 (m, 2H).  $^{13}C$  NMR (100 MHz,  $CDCl_3$ )  $\delta$  189.74, 156.16, 155.65 (d,  $J_{C-F} = 3.0$  Hz), 152.04, 151.99 (d,  $J_{C-F} = 4.0$  Hz), 149.46 (d,  $J_{C-F} = 192.0$  Hz), 147.03 (d,  $J_{C-F} = 27.0$  Hz), 146.70, 142.72, 136.94, 130.60 (d,  $J_{C-F} = 6.0$  Hz), 129.07 (d,  $J_{C-F} = 8.0$  Hz), 126.31, 121.97 (d,  $J_{C-F} = 6.0$  Hz), 119.66, 112.32, 64.20, 54.97 (2C), 49.75 (2C), 46.13, 35.35 (2C), 26.76 (2C), 16.14.

#### 4.2.63. 4-(3-Ethyl-7-fluoro-2,3-dimethyl-3H-indol-5-yl)-*N*-(5-(1-ethylpiperidin-4-yl)pyridin-2-yl)-5-fluoropyrimidin-2-amine (**30**)

Starting from **2E** (100.0 mg, 0.31 mmol) and **INT-5** (63.5 mg, 0.31 mmol), 25.0 mg of **30** was obtained as a light yellow solid at 16% yield according to the method described for the synthesis of **1**. Purity: 99.3%; retention time: 3.35 min. MP: 145.7–146.3 °C. HRMS-ESI:  $[M+H]^+$  observed 491.2720, calculated 491.2735.  $^1H$  NMR (400 MHz,  $DMSO-d_6$ )  $\delta$  9.99 (brs, 1H), 8.70 (d, 1H,  $J = 3.2$  Hz), 8.19 (s, 1H), 8.14 (d, 1H,  $J = 8.8$  Hz), 7.92 (s, 1H), 7.85 (d, 1H,  $J = 11.2$  Hz), 7.69 (d, 1H,  $J = 8.4$  Hz), 3.04–3.02 (m, 2H), 2.42–2.41 (m, 2H), 2.28 (s, 3H), 2.04–1.99 (m, 3H), 1.89–1.84 (m, 1H), 1.78–1.63 (m, 4H), 1.33 (s, 3H), 1.04 (t, 3H,  $J = 6.8$  Hz), 0.36 (t, 3H,  $J = 7.2$  Hz).  $^{13}C$  NMR (100 MHz,  $DMSO-d_6$ )  $\delta$  191.62, 156.05, 154.13 (d,  $J_{C-F} = 206.0$  Hz), 151.85, 151.64, 150.39 (d,  $J_{C-F} = 201.0$  Hz), 148.24, 147.98, 146.69, 143.47, 143.36, 136.30, 131.87, 118.93, 115.99 (d,  $J_{C-F} = 15.0$  Hz), 112.62, 59.92, 53.40, 52.20, 32.81, 29.54, 22.03 (2C), 16.31 (2C), 12.18, 8.87 (2C).

#### 4.2.64. *tert*-butyl 4-(6-((4-(3-ethyl-7-fluoro-2,3-dimethyl-3H-indol-5-yl)-5-fluoropyrimidin-2-yl)amino)pyridin-3-yl)piperidine-1-carboxylate (**31F**)

Starting from **2E** (321.7 mg, 1.0 mmol) and **INT-6** (277.3 mg, 1.0 mmol), 112.3 mg of **31F** was obtained at 20% yield according to the method described for the synthesis of **1**. ESI-MS:  $m/z$  563.3  $[M+H]^+$ .

#### 4.2.65. 4-(3-Ethyl-7-fluoro-2,3-dimethyl-3H-indol-5-yl)-5-fluoro-*N*-(5-(piperidin-4-yl)pyridin-2-yl)pyrimidin-2-amine (**31**)

Starting from **31F** (40.0 mg, 0.07 mmol), 16.3 mg of **31** was obtained as a light yellow solid at 50% yield according to the method described for the synthesis of **8**. purity: 98.3%; retention time: 3.33 min. MP: 125.1–126.3 °C. HRMS-ESI:  $[M+H]^+$  observed 463.2410, calculated 463.2422.  $^1H$  NMR (400 MHz,  $CDCl_3$ )  $\delta$  8.61 (brs, 1H), 8.46 (d, 1H,  $J = 3.6$  Hz), 8.34 (d, 1H,  $J = 8.8$  Hz), 8.26 (d, 1H,  $J = 1.6$  Hz), 7.93 (d, 1H,  $J = 11.2$  Hz), 7.64 (d, 1H,  $J = 8.0$  Hz), 7.86 (s, 1H), 7.61 (dd, 1H,  $J = 8.4$  Hz, 2.0 Hz), 3.24–3.21 (m, 2H), 2.77 (t, 1H,  $J = 10.8$  Hz), 2.64–2.61 (m, 1H), 2.34 (s, 3H), 2.06–1.91 (m, 4H), 1.89–1.84 (m, 3H), 1.72–1.63 (m, 2H), 1.39 (s, 3H), 0.50 (t, 1H,  $J = 7.2$  Hz).  $^{13}C$  NMR (100 MHz,  $CDCl_3$ )  $\delta$  190.58, 155.43 (d,  $J_{C-F} = 3.0$  Hz), 154.69 (d,  $J_{C-F} = 252.0$  Hz), 151.18, 150.94 (d,  $J_{C-F} = 9.0$  Hz), 149.61 (d,  $J_{C-F} = 219.0$  Hz), 147.09, 146.66, 143.64 (d,  $J_{C-F} = 11.0$  Hz), 136.25, 135.81, 131.96 (d,  $J_{C-F} = 12.0$  Hz), 131.90, 118.17 (dd,  $J_{C-F} = 5.0$  Hz), 116.36 (dd,  $J_{C-F} = 7.0$  Hz), 111.76, 59.69, 47.03 (2C), 39.97, 34.35 (2C), 30.19, 22.26, 16.10, 8.58.

#### 4.2.66. 5-Fluoro-4-(7-fluoro-2,3,3-trimethyl-3H-indol-5-yl)-*N*-(5-(1-methylpiperidin-4-yl)pyridin-2-yl)pyrimidin-2-amine (**32**)

Starting from **1E** (200.0 mg, 0.65 mmol) and **INT-4** (124.3 mg, 0.65 mmol), 60.0 mg of **32** was obtained as a light yellow solid at 20% yield according to the method described for the synthesis of **1**. Purity: 97.9%; retention time: 1.12 min. MP: 124.3–125.1 °C. HRMS-ESI:  $[M+H]^+$  observed 463.2411, calculated 463.2422.  $^1H$  NMR (400 MHz, Methanol- $d_4$ )  $\delta$  8.57 (brs, 1H), 8.37 (d, 1H,  $J = 3.6$  Hz), 8.18 (s, 1H), 8.13 (d, 1H,  $J = 8.8$  Hz), 7.84 (s, 1H), 7.70 (d, 1H,  $J = 11.2$  Hz), 7.51 (d, 1H,  $J = 7.2$  Hz), 3.21–3.18 (m, 2H), 2.60–2.54 (m, 4H), 2.50–2.44 (m, 2H), 2.37 (s, 3H), 1.90–1.79 (m, 4H), 1.38 (s, 6H).  $^{13}C$  NMR (100 MHz, Methanol- $d_4$ )  $\delta$  194.78, 156.97, 155.70 (d,  $J_{C-F} = 201.0$  Hz), 153.41 (d,  $J_{C-F} = 22.0$  Hz), 152.06 (d,  $J_{C-F} = 9.0$  Hz),

151.15(d,  $J_{C-F}$  = 11.0 Hz), 151.00 (d,  $J_{C-F}$  = 226.0 Hz), 148.47, 147.30, 142.82(d,  $J_{C-F}$  = 12.0 Hz), 137.64, 134.43, 133.93 (d,  $J_{C-F}$  = 6.0 Hz), 119.66 (d,  $J_{C-F}$  = 5.0 Hz), 117.05 (dd,  $J_{C-F}$  = 6.0 Hz), 113.77, 56.36, 55.82 (2C), 44.06, 37.62, 31.74, 23.22 (2C), 15.72, 15.48.

#### 4.2.67. 5-Bromo-3-ethyl-2,3-dimethyl-3H-indole (**33C**)

Starting from (4-bromophenyl)hydrazine (22.00 g, 117.6 mmol) and 1-cyclopentylethanone (11.82 g, 117.6 mmol), 19.31 g of **33C** was obtained at 65% yield according to the method described for the synthesis of **7C**. ESI-MS:  $m/z$  251.0  $[M+H]^+$ .

#### 4.2.68. 3-Ethyl-2,3-dimethyl-5-(4,4,5,5-tetramethyl-1,3,2-dioxaborolan-2-yl)-3H-indole (**33D**)

Starting from **33C** (13.0 g, 51.8 mmol) and bis(pinacolato)diboron (13.20 g, 51.8 mmol), 9.53 g of **33D** was obtained at 61% yield according to the method described for the synthesis of **7D**. ESI-MS:  $m/z$  300.2  $[M+H]^+$ .

#### 4.2.69. 5-(2-Chloro-5-fluoropyrimidin-4-yl)-3-ethyl-2,3-dimethyl-3H-indole (**33E**)

Starting from **33D** (9.5 g, 31.9 mmol) and 2,4-dichloro-5-fluoropyrimidine (5.30 g, 31.9 mmol), 3.22 g of **33E** was obtained at 33% yield according to the method described for the synthesis of **7D**. ESI-MS:  $m/z$  304.1  $[M+H]^+$ .

#### 4.2.70. tert-butyl 4-(6-((4-(3-ethyl-2,3-dimethyl-3H-indol-5-yl)-5-fluoropyrimidin-2-yl)amino)pyridin-3-yl)piperazine-1-carboxylate (**33F**)

Starting from **33E** (303.7 mg, 1.0 mmol) and **INT-3** (278.3 mg, 1.0 mmol), 120.0 mg of **33F** was obtained at 22% yield according to the method described for the synthesis of **1**. ESI-MS:  $m/z$  546.3  $[M+H]^+$ .

#### 4.2.71. 4-(3-Ethyl-2,3-dimethyl-3H-indol-5-yl)-5-fluoro-N-(5-(piperazin-1-yl)pyridin-2-yl)pyrimidin-2-amine (**33**)

Starting from **33F** (50.0 mg, 0.09 mmol), 36.0 mg of **33** was obtained as a yellow solid at 90% yield according to the method described for the synthesis of **8**. Purity: 99.7%; retention time: 1.12 min. MP: 124.5–125.8 °C. HRMS-ESI:  $[M+H]^+$  observed 446.2457, calculated 446.2468.  $^1H$  NMR (400 MHz,  $CDCl_3$ )  $\delta$  9.68 (brs, 1H), 8.44 (d, 1H,  $J$  = 3.6 Hz), 8.32 (d, 1H,  $J$  = 8.8 Hz), 8.18 (d, 1H,  $J$  = 2.4 Hz), 8.11 (d, 1H,  $J$  = 8.0 Hz), 7.98 (s, 1H), 7.64 (d, 1H,  $J$  = 8.0 Hz), 7.30 (d, 1H,  $J$  = 2.8 Hz), 3.05–3.04 (m, 4H), 3.00–2.98 (m, 4H), 2.26 (s, 3H), 2.00–1.90 (m, 2H), 1.83–1.74 (m, 1H), 1.32 (s, 3H), 0.45 (t, 1H,  $J$  = 7.2 Hz).  $^{13}C$  NMR (100 MHz,  $CDCl_3$ )  $\delta$  189.87, 156.91, 155.73 (d,  $J_{C-F}$  = 2.0 Hz), 152.10 (d,  $J_{C-F}$  = 9.0 Hz), 151.90, 149.3 (d,  $J_{C-F}$  = 239.0 Hz), 146.82 (d,  $J_{C-F}$  = 10.0 Hz), 143.89, 143.17, 136.90, 130.54 (d,  $J_{C-F}$  = 6.0 Hz), 129.26 (d,  $J_{C-F}$  = 6.0 Hz), 126.51, 122.41 (d,  $J_{C-F}$  = 7.0 Hz), 119.85, 112.34, 58.66, 51.02 (2C), 46.01 (2C), 30.05, 22.17, 15.94, 8.59.

#### 4.2.72. tert-butyl 4-(6-((4-(3-ethyl-2,3-dimethyl-3H-indol-5-yl)-5-fluoropyrimidin-2-yl)amino)pyridin-3-yl)piperidine-1-carboxylate (**34F**)

Starting from **33E** (303.7 mg, 1.0 mmol) and **INT-6** (277.3 mg, 1.0 mmol), 98.0 mg of **34F** was obtained at 18% yield according to the method described for the synthesis of **33F**. ESI-MS:  $m/z$  545.3  $[M+H]^+$ .

#### 4.2.73. 4-(3-Ethyl-2,3-dimethyl-3H-indol-5-yl)-5-fluoro-N-(5-(piperidin-4-yl)pyridin-2-yl)pyrimidin-2-amine (**34**)

Starting from **34F** (98.0 mg, 0.18 mmol), 72.6 mg of **34** was obtained as a light yellow solid at 91% yield according to the method described for the synthesis of **8**. Purity: 96.7%; retention time: 3.40 min. MP: 113.5–114.8 °C. HRMS-ESI:  $[M+H]^+$  observed

445.2508, calculated 445.2516.  $^1H$  NMR (400 MHz, Methanol- $d_4$ )  $\delta$  8.33 (d, 1H,  $J$  = 2.8 Hz), 8.16–8.13 (m, 2H), 7.95–7.93 (m, 2H), 7.48–7.41 (m, 2H), 3.18–3.15 (m, 2H), 2.73 (t, 1H,  $J$  = 11.6 Hz), 2.59–2.53 (m, 1H), 2.30 (s, 3H), 2.01–1.96 (m, 1H), 1.89–1.83 (m, 1H), 1.79–1.76 (m, 2H), 1.66–1.58 (m, 2H), 1.32 (s, 3H), 0.42 (t, 1H,  $J$  = 6.8 Hz).  $^{13}C$  NMR (100 MHz, Methanol- $d_4$ )  $\delta$  193.08, 157.18, 156.98, 153.64 (d,  $J_{C-F}$  = 31.0 Hz), 153.24 (d,  $J_{C-F}$  = 213.0 Hz), 153.00, 148.38 (d,  $J_{C-F}$  = 27.0 Hz), 147.24, 145.28, 137.65, 136.61, 132.19 (d,  $J_{C-F}$  = 5.0 Hz), 130.60 (d,  $J_{C-F}$  = 7.0 Hz), 123.87 (d,  $J_{C-F}$  = 7.0 Hz), 120.23, 113.66, 60.25, 47.04 (2C), 40.28, 34.07 (2C), 30.92, 22.65, 15.87, 8.95.

#### 4.2.74. 4-(3-Ethyl-2,3-dimethyl-3H-indol-5-yl)-5-fluoro-N-(5-(4-methylpiperazin-1-yl)pyridin-2-yl)pyrimidin-2-amine (**35**)

Starting from **33E** (303.7 mg, 1.0 mmol) and **INT-1** (192.2 mg, 1.0 mmol), 115.0 mg of **35** was obtained as a yellow solid at 20% yield according to the method described for the synthesis of **1**. Purity: 97.2%; retention time: 3.09 min. MP: 199.4–200.8 °C. HRMS-ESI:  $[M+H]^+$  observed 460.2615, calculated 460.2625.  $^1H$  NMR (400 MHz, Methanol- $d_4$ )  $\delta$  8.42 (d, 1H,  $J$  = 3.2 Hz), 8.18 (d, 1H,  $J$  = 8.8 Hz), 8.09–8.01 (m, 3H), 7.57 (d, 1H,  $J$  = 8.0 Hz), 7.42–7.37 (m, 1H), 3.22–3.15 (m, 4H), 2.61–2.60 (m, 4H), 2.35 (s, 3H), 2.32 (s, 3H), 2.07–2.02 (m, 1H), 1.94–1.89 (m, 1H), 1.38 (s, 3H), 0.43 (t, 1H,  $J$  = 7.2 Hz).  $^{13}C$  NMR (100 MHz, Methanol- $d_4$ )  $\delta$  192.95, 157.08, 153.35 (d,  $J_{C-F}$  = 241.0 Hz), 153.12 (d,  $J_{C-F}$  = 9.0 Hz), 148.33, 148.07, 147.85, 145.20, 144.14, 137.16, 132.31 (d,  $J_{C-F}$  = 6.0 Hz), 130.57 (d,  $J_{C-F}$  = 7.0 Hz), 127.81, 123.83 (d,  $J_{C-F}$  = 6.0 Hz), 120.20, 114.41, 60.21, 55.89 (2C), 50.24 (2C), 46.14, 30.92, 22.62, 15.85, 8.98.

#### 4.2.75. 4-(3-Ethyl-2,3-dimethyl-3H-indol-5-yl)-N-(5-(1-ethylpiperidin-4-yl)pyridin-2-yl)-5-fluoropyrimidin-2-amine (**36**)

Starting from **33E** (303.7 mg, 1.0 mmol) and **INT-5** (205.3 mg, 1.0 mmol), 103.8 mg of **36** was obtained as a light yellow solid at 22% yield according to the method described for the synthesis of **1**. Purity: 97.3%; retention time: 1.13 min. MP: 137.2–138.4 °C. HRMS-ESI:  $[M+H]^+$  observed 473.2817, calculated 473.2829.  $^1H$  NMR (400 MHz,  $CDCl_3$ )  $\delta$  9.17 (brs, 1H), 8.48 (d, 1H,  $J$  = 3.6 Hz), 8.39 (d, 1H,  $J$  = 8.8 Hz), 8.31 (d, 1H,  $J$  = 1.6 Hz), 8.15 (d, 1H,  $J$  = 8.0 Hz), 8.04 (s, 1H), 7.67 (d, 1H,  $J$  = 8.0 Hz), 7.60 (dd, 1H,  $J$  = 8.8 Hz, 2.0 Hz), 3.11–3.08 (m, 4H), 2.53–2.44 (m, 3H), 2.30 (s, 3H), 2.05–1.97 (m, 3H), 1.86–1.81 (m, 5H), 1.36 (s, 3H), 1.13 (t, 3H,  $J$  = 7.2 Hz), 0.49 (t, 1H,  $J$  = 7.2 Hz).  $^{13}C$  NMR (100 MHz,  $CDCl_3$ )  $\delta$  189.96, 157.09, 155.54 (d,  $J_{C-F}$  = 3.0 Hz), 152.24 (d,  $J_{C-F}$  = 6.0 Hz), 152.15, 151.54, 149.65 (d,  $J_{C-F}$  = 262.0 Hz), 146.79, 143.9, 136.10, 135.15, 130.37 (d,  $J_{C-F}$  = 6.0 Hz), 129.39 (d,  $J_{C-F}$  = 8.0 Hz), 122.35 (d,  $J_{C-F}$  = 7.0 Hz), 119.88, 111.76, 58.72, 53.79 (2C), 52.63, 39.67, 33.39, 30.10, 22.23, 15.97, 12.11, 8.60 (2C).

#### 4.2.76. 4-(3-Ethyl-2,3-dimethyl-3H-indol-5-yl)-5-fluoro-N-(5-(1-methylpiperidin-4-yl)pyridin-2-yl)pyrimidin-2-amine (**37**)

Starting from **33E** (303.7 mg, 1.0 mmol) and **INT-4** (191.2 mg, 1.0 mmol), 73.3 mg of **37** was obtained as a white solid at 16% yield according to the method described for the synthesis of **1**. Purity: 97.3%; retention time: 1.12 min. MP: 204.1–205.3 °C. HRMS-ESI:  $[M+H]^+$  observed 459.2665, calculated 459.2672.  $^1H$  NMR (400 MHz,  $CDCl_3$ )  $\delta$  8.97 (brs, 1H), 8.47 (d, 1H,  $J$  = 3.6 Hz), 8.39 (d, 1H,  $J$  = 8.4 Hz), 8.30 (d, 1H,  $J$  = 2.0 Hz), 8.15 (d, 1H,  $J$  = 8.4 Hz), 8.04 (s, 1H), 7.68 (d, 1H,  $J$  = 8.0 Hz), 7.59 (dd, 1H,  $J$  = 8.8 Hz, 2.4 Hz), 3.01–2.98 (m, 4H), 2.51–2.45 (m, 1H), 2.34 (s, 3H), 2.31 (s, 3H), 2.10–1.97 (m, 3H), 1.85–1.81 (m, 5H), 1.37 (s, 3H), 0.49 (t, 1H,  $J$  = 7.2 Hz).  $^{13}C$  NMR (100 MHz,  $CDCl_3$ )  $\delta$  189.99, 157.10, 155.49 (d,  $J_{C-F}$  = 2.0 Hz), 152.27 (d,  $J_{C-F}$  = 6.0 Hz), 152.18, 151.52, 149.68 (d,  $J_{C-F}$  = 268.0 Hz), 146.77 (d,  $J_{C-F}$  = 3.0 Hz), 144.00, 136.11, 135.07, 130.34 (d,  $J_{C-F}$  = 5.0 Hz), 129.39 (d,  $J_{C-F}$  = 8.0 Hz), 122.36 (d,  $J_{C-F}$  = 7.0 Hz), 119.90, 111.77, 58.73, 56.22 (2C), 46.45, 38.92, 33.43 (2C), 30.10, 22.23, 15.98, 8.60.

#### 4.2.77. 4-(3-Ethyl-2,3-dimethyl-3H-indol-5-yl)-N-(5-(4-ethylpiperazin-1-yl)pyridin-2-yl)-5-fluoropyrimidin-2-amine (**38**)

Starting from **33E** (303.7 mg, 1.0 mmol) and **INT-2** (206.3 mg, 1.0 mmol), 47.6 mg of **38** was obtained as a yellow solid at 19% yield according to the method described for the synthesis of **1**. Purity: 96.3%; retention time: 3.40 min. MP: 112.3–113.9 °C. HRMS-ESI:  $[M+H]^+$  observed 474.2773, calculated 474.2781.  $^1H$  NMR (400 MHz,  $CDCl_3$ )  $\delta$  8.93 (brs, 1H), 8.44 (d, 1H,  $J = 3.6$  Hz), 8.33 (d, 1H,  $J = 9.2$  Hz), 8.15–8.13 (m, 2H), 8.02 (s, 1H), 7.67 (d, 1H,  $J = 8.0$  Hz), 7.35 (d, 1H,  $J = 8.0$  Hz), 3.19–3.18 (m, 4H), 2.63–2.62 (m, 4H), 2.52–2.47 (m, 2H), 2.30 (s, 3H), 2.02–1.97 (m, 1H), 1.86–1.80 (m, 1H), 1.36 (s, 3H), 1.14 (t, 3H,  $J = 7.2$  Hz), 0.57 (t, 1H,  $J = 7.2$  Hz).  $^{13}C$  NMR (100 MHz,  $CDCl_3$ )  $\delta$  189.89, 157.02, 155.63, 152.21, 152.13 (d,  $J_{C-F} = 10.0$  Hz), 149.51 (d,  $J_{C-F} = 257.0$  Hz), 146.68 (d,  $J_{C-F} = 11.0$  Hz), 143.93, 142.86, 136.84, 130.47, 129.30 (d,  $J_{C-F} = 6.0$  Hz), 126.39, 122.40 (d,  $J_{C-F} = 6.0$  Hz), 119.89, 112.32, 58.71, 52.68 (2C), 52.34, 49.82 (2C), 30.09, 22.22, 15.96, 11.69, 8.60.

#### 4.3. Molecular docking

The X-ray crystal structure of human CDK6-Vcyclin (PDB: 2EUF) was used for docking studies. Before docking simulation, the ligands and proteins were prepared with the standard protocol by Sybyl X V2.0, including the addition of hydrogens, the assignment of bond order, and the assessment of the protonation state. All of the docking calculations were performed using Surflex.

#### 4.4. CDKs inhibition assays

The enzymatic screening assays were performed with ADP-Glo™ Kinase Assay from Promega (Madison, WI, USA). The assays were developed following the assay's technical manual and validated following the *Assay Guidance Manual* (Iversen PW, Beck B, Chen YF et al. HTS Assay Validation. 2012 May 1 [Updated 2012 Oct 1]. In: Sittampalam GS, Coussens NP, Brimacombe K et al., editors. *Assay Guidance Manual* [Internet]. Bethesda (MD): Eli Lilly & Company and the National Center for Advancing Translational Sciences; 2004-. Available from: <https://www.ncbi.nlm.nih.gov/books/NBK83783/>). Kinase  $IC_{50}$  determinations were performed in 384-well microplates (purchased from Corning). The reaction was carried out in a 10  $\mu$ L volume containing 0.031 ng/ $\mu$ L kinase, 10  $\mu$ M ATP, and 0.1  $\mu$ g/ $\mu$ L Histone H1 in assay buffer (200 mM Tris, pH 7.5, 100 mM  $MgCl_2$  and 0.5 mg/mL bovine serum albumin). In brief, the reactions were incubated at 37 °C for 90 min and 10  $\mu$ L ADP-Glo reagent was added to the wells to stop the kinase reaction, followed by incubation at RT for 40 min. The signal was visualized by the addition of 20  $\mu$ L detection solution. After 30 min incubation at RT, the plate was read on an M1000 PRO plate reader (Tecan, Männedorf, Switzerland). To monitor the assay performance over time, a positive control compound was tested in each plate.  $IC_{50}$  were determined with a four-parameter sigmoidal equation. If the curve fitting parameters of the positive control compound showed great variation, the test compounds in the plate were retested. If more than 2 outliers were observed in the fitting curve of a test compound, the compound was retested. Otherwise, each test compound was tested once. The positive control compound for the CDK4/6 assay was amebaciliclib and for the CDK1/2 assay, AZD5438. The positive control compounds, palbociclib and ribociclib, were purchased from Selleck Chemicals.

#### 4.5. 85 Kinase assays

PI3K $\alpha$ , PI3K $\beta$ , PI3K $\delta$ , and PI3K $\gamma$  were purchased from Millipore (Billerica, MA, USA); ALK, ALK(C1196M), and ALK(C1156Y) were purchased from Carina Biosciences, Inc. (Tokyo, Japan); and the

other kinases were purchased from ThermoFisher. The Z-lyte screening method was used for 56 kinases including ABL, ACVR1B/ALK4, AurA, AURKB, AXL, CAMK2B, CDC42(BPB), CHEK2, CHK1, CK1 $\alpha$ , CK1 $\gamma$ 1, CK2 $\alpha$ 1, CLK1, cMET, DYRK3, EphA2, EPHB2, ERBB2(HER2), ERK2, FGFR1, Grk2, Grk3, Grk4, Grk5, Grk6, GSK3 $\beta$ , INSR, JNK1, KDR, Lck, LOK1, Lyn A, NIK, MAPKAPK2, MARK1, MerTK, MINK, MLK1, MST4, p38 $\alpha$ , PAK1 FL, PAK2, PAK4, PDGFRB, PDK1, PKA, PKC $\beta$ II, PLK1, RET, Ret(V804L), SRC, SYK, TAOK2, TIE2, TRKA, and TYRO3, and staurosporine was the positive control compound, each assay was duplicated two times, and the average value was recorded. The time-resolved fluorescence resonance energy transfer screening method was used for 23 kinases including AKT1, AKT2, AKT3, ALK, ALK(C1156Y), ALK(L1196M), BMX, BTK, CDK4/cyclinD1, CDK6/cyclinD1, EGFR, d746-750/T790M, EGFR T790M/L858R, EGFR WT, ITK, JAK1, JAK2, JAK3, PTK6, RAF1, SRMS, TAK1, TEC, LRRK2, and TAK1, and staurosporine was the positive control compound, each assay was duplicated two times, and the average value was recorded. The LanthaScreen Eu Kinase Binding method was used for two kinases including CDK8/cyclin C and SLK, and staurosporine was the positive control compound, each assay was duplicated two times, and the average value was recorded. The ADP-Glo screening method was used for four kinases, namely PI3K $\alpha$ , PI3K $\beta$ , PI3K $\delta$ , and PI3K $\gamma$ , and PI-103 was the positive control compound, each assay was duplicated two times, and the average value was recorded.

#### 4.6. $IC_{50}$ determination for JAK3 and NIK

JAK3 and NIK were purchased from ThermoFisher. Compound **11** and the positive control compounds were dissolved in 5 mM DMSO solution and we put them in a nitrogen hood at room temperature for long-term storage. The compounds were diluted into 1 mM DMSO, and we used Echo (Labcyte-Echo555) to dilute the compounds in DMSO with a 3-fold factor, for a total of 11 concentrations, and the final concentrations varied from 10  $\mu$ M to 0.17 nM. We transferred a 5- $\mu$ L volume containing enzyme (0.08 nM for JAK3; 1.25 nM for NIK) and substrate (50 nM ULight-JAK-1peptide for JAK3; 2  $\mu$ M ser/thr 7 for NIK) in assay buffer (50 Hepes, 1mM EGTA, 10mM  $MgCl_2$ , 0.01% Brij-35) into the assay plate and incubated the assay plate for 15 min at room temperature (23 °C); 5  $\mu$ L ATP (4  $\mu$ M for JAK3; 13  $\mu$ M for NIK) in assay buffer were transferred into the assay plate and we incubated the assay plate for a certain time (90 min for JAK3; 60 min for NIK) at room temperature (23 °C). We transferred 10  $\mu$ L detection reagent (2nM Eu-W1024 anti-phosphotyrosine for JAK3 in 1  $\times$  detection buffer and 10 mM EDTA; 1:65536 development reagent A in development reagent buffer for NIK) into the assay plate and we incubated the assay plate for a certain time (90 min for JAK3; 60 min for NIK) at room temperature (23 °C). We read the assay plate in Envision (PerkinElmer-2104). Each compound was tested once, Z factors of all of the plates were more than 0.5, and all of the data passed QC criteria.

The positive control compound for JAK3 assay was tofacitinib, and the positive control compound for NIK assay was staurosporine.

#### 4.7. Anti-proliferation assay

The U87MG glioblastoma cell line was obtained from the China Infrastructure of Cell Line Resources (Beijing, China) and maintained at 37 °C, 5%  $CO_2$  in Dulbecco's Modified Eagle's Medium containing 10% fetal bovine serum. Cells were seeded at 4000 cells/100  $\mu$ L/well in a 96-well plate, and the plates were incubated overnight to allow the cells to adhere. Compound **11** and the positive control compound (amebaciclib, purchased from Selleck Chemicals) were serially diluted in the plate (100  $\mu$ L/well) and

incubated for 72 h at 37 °C. Then the medium was removed, 4% paraformaldehyde (50 µL/well) was added to the wells, and the cells were fixed for 30 min at RT. Cells were washed twice with phosphate-buffered saline (PBS) solution, and permeabilized in 0.2% Triton-X100 for 5 min. Cells were washed twice with PBS, after which 50 µL DAPI (1 µg/mL) was added to the wells, followed by incubation of the cells in the dark for 20 min. After washing three times with PBS, PBS (100 µL/well) was added to the wells. The plates were scanned using IN Cell Analyzer 2200 (GE Healthcare, Little Chalfont, UK). Each compound was tested three times independently and replicated one time.

#### 4.8. Flow cytometry

The U87MG glioblastoma cell line was obtained from the China Infrastructure of Cell Line Resources (Beijing, China) and maintained at 37 °C, 5% CO<sub>2</sub> in Eagle's minimal essential medium (EMEM) containing 10% fetal bovine serum. Cells were seeded at 2E+5 cells/2 mL/well in a 6-well plate, and the plates were incubated for 24 h in a humidified incubator at 37 °C, 5% CO<sub>2</sub>. Compound **11** was serially diluted in the plate and incubated for 24 h at 37 °C. DMSO served as negative control. The medium was removed, then the cells were trypsinized, centrifuged and washed once with phosphate-buffered saline (PBS) solution. The cells are fixed with pre-cold Ethanol at 4 °C, centrifuged to remove the supernatant, and washed once with PBS. The cell were suspended in staining solution containing 100 µg/ml RNase A (Cat#EN0531, Thermo Scientific) and 50 µg/ml Propidium iodide (Cat#P4170-10MG, Sigma), incubated at room temperature for 20 min. Data were collected using Accuri C6 flow cytometer (BD bioscience).

#### 4.9. Stability study in mouse liver microsomes

CD-1 mouse liver microsomes (20 mg/mL) were obtained from Xenotech (Kansas City, KS, USA). The study was performed in a 96-well plate. Then 10 µL/well compound solution (10 µM) was added to the wells. The CD-1 mouse liver microsomes (20 mg/mL) were incubated for 5 min at RT, after which 80 µL/well was added to the plate. Next, 10 µL/well nicotinamide adenine dinucleotide phosphate (NADP) cofactor was added to the wells to start the reaction. At each time point, 300 µL/well solution (cold acetonitrile [ACN], 100 ng/mL tolbutamide, and 100 ng/mL labetalol) was added to the wells to stop the reaction. Then the protein was precipitated by centrifugation at 4000 rpm for 20 min, and the supernatant was analyzed by LC/MS/MS (API 4000, ESI: positive, Mobile Phase A: 0.1% formic acid [FA] in water; Mobile Phase B: 0.1% FA in ACN).

#### 4.10. Bidirectional flux assay in transfected MDCK cells

MDCK II and MDR1-MDCK II cells (obtained from Piet Borst at the Netherlands Cancer Institute) were seeded onto polyethylene membranes in 96-well BD Insert Plates (BD Biosciences, Franklin Lakes, NJ, USA) at  $2.3 \times 10^5$  cells/cm<sup>2</sup> until confluent cell monolayer formation occurred (4–7 days). Compound **11** and reference compounds were diluted in Transport Buffer (Hank's Balanced Salt Solution [HBSS] with 10 mM HEPES with and without the P-gp inhibitor GF120918, pH 7.4) to 2 µM (DMSO <1%), and were applied to the apical or basolateral side of the cell monolayer. Permeation of compound **11** and reference compounds from the A to B or B to A direction was determined in duplicate with or without the GF120918 P-gp inhibitor (10 µM) in a 150 min incubation at 37 °C and 5% CO<sub>2</sub> at a relative humidity of 95%. In addition, the ER of each compound was also determined. Compound **11** and reference compounds were quantified by LC/MS/MS analysis based on the peak area ratio of analyte/IS (the LC pump used was Shimadzu LC

20-AD; the MS system used was API 4000; the column used was ACE Phenyl, 50 × 2.1 mm; Mobile Phase A was 0.1% FA in Water; Mobile Phase B was 0.1% FA in ACN). Six wells per 96-well plate were randomly selected for the Lucifer Yellow Permeability Assay to determine the cell monolayer integrity at the same duration as the test compounds. A total of 75 µL of 100 µM Lucifer Yellow diluted in Transport Buffer and 250 µL Transport Buffer were added to the apical and basolateral chambers respectively. After a 120 min incubation, 20 µL Lucifer Yellow samples were taken from the apical sides, followed by the addition of 60 µL Transport Buffer. Then 80 µL Lucifer Yellow samples were taken from the basolateral sides. The relative fluorescence unit (RFU) of Lucifer Yellow was measured at 425/528 nm (excitation/emission) with a Molecular Device M2e plate reader. To lyse the cells for the determination of total recovery, the remaining transport solutions were removed by gently tapping the cell plate on a paper towel. Stop Solution (200 µL) was added to the apical well and mixed by pipetting up and down 5 times before the lysed sample was taken from each apical well. The  $P_{app}$  (cm/s) was calculated by the following equation:

$$P_{app} = (dC_r/dt) \times V_r / (A \times C_0)$$

where  $dC_r/dt$  is the cumulative concentration of the compound in the receiver chamber as a function of time (µM/s),  $V_r$  is the volume in the receiver chamber (0.075 mL on the apical side and 0.25 mL on the basolateral side),  $A$  is the surface area for transport (i.e., 0.0804 cm<sup>2</sup> for the area of the monolayer), and  $C_0$  is the initial concentration in the donor chamber (µM).

The ER was calculated as follows:  $ER = P_{app}(BA)/P_{app}(AB)$ .

The net efflux ratio was calculated as follows:

$$Net\ RE_a = RE_a(MDR1-MDCK\ II)/RE_a(Wild-type\ MDCK\ II)\ and$$

$$Net\ RE_i = RE_i(MDR1-MDCK\ II)/RE_i(Wild-type\ MDCK\ II),$$

where  $RE_i$  and  $RE_a$  represent the ERs of the test compound with or without an inhibitor of efflux transport respectively.

Percent recovery was calculated as follows:

$$\% Recovery = 100 \times [(V_r \times C_r) + (V_d \times C_d)] / (V_d \times C_0)\ and$$

$$\% Total\ Recovery = 100 \times [(V_r \times C_r) + (V_d \times C_d) + (V_c \times C_c)] / (V_d \times C_0),$$

where  $V_d$  is the volume in the donor chambers (0.075 mL on the apical side and 0.25 mL on the basolateral side); and  $C_d$  and  $C_r$  are the final concentrations of the transport compound in the donor and receiver chambers respectively;  $C_c$  is the compound concentration in the cell lysate solution (µM); and  $V_c$  is the volume in the insert well (0.075 mL in this assay).

Percentage of Lucifer Yellow in the basolateral well was calculated as follows:

$$Lucifer\ Yellow = \frac{V_{Basolateral} \times RFU_{Basolateral}}{V_{Apical} \times RFU_{Apical} + V_{Basolateral} \times RFU_{Basolateral}} \times 100$$

where  $RFU_{Apical}$  and  $RFU_{Basolateral}$  are the relative fluorescence unit values of Lucifer Yellow in the apical and basolateral wells, respectively; and  $V_{Apical}$  and  $V_{Basolateral}$  are the volume in the apical and basolateral wells, respectively (0.075 mL and 0.25 mL). The % Lucifer Yellow should be less than 2.

#### 4.11. Bidirectional flux assay in Caco-2 cells

Caco-2 cells purchased from American Type Culture Collection (Manassas, VA, USA) were seeded onto polyethylene membranes in 96-well BD Insert Plates at a density of  $1 \times 10^5$  cells/cm<sup>2</sup>. The medium was refreshed every 4–5 days until confluent cell monolayer formation occurred (21–28 days). The Transport Buffer in the study was HBSS with 10 mM HEPES at a pH of  $7.40 \pm 0.05$ . Compound **11** was tested at 2  $\mu$ M bi-directionally in triplicate, in the presence or absence of 30  $\mu$ M novobiocin. The final DMSO concentration was adjusted to less than 1%. The plate was incubated for 2 h at  $37 \pm 1$  °C with 5% CO<sub>2</sub> at saturated humidity. After mixing with ACN containing IS (Tolbutamide), samples were centrifuged at 4000 rpm for 20 min. Subsequently, 100  $\mu$ L supernatant was diluted with 100  $\mu$ L distilled water for LC/MS/MS analysis. Concentrations of compound **11** in the starting solution, donor solution, receiver solution, and cell lysate were quantified by LC/MS/MS, using peak the area ratio of analyte/IS (the LC pump used was Shimadzu LC 20-AD; the MS system used was API 4000; the column used was OPTI-LYNX,  $1.5 \times 5.0$  mm; Mobile Phase A was 2 mM NH<sub>4</sub>OAC in Water/50% MeOH in ACN = 95:5; Mobile Phase B was 2 mM NH<sub>4</sub>OAC in Water/50% MeOH in ACN = 10:90). Then six wells per 96-well plate were randomly selected for The Lucifer Yellow Assay Permeability Assay to determine the cell monolayer integrity at the same duration of the test compounds. To lyse the cells for determination of total recovery, the remaining transport solutions were removed by gently tapping the cell plate on a paper towel. Stop Solution (200  $\mu$ L) was added to the apical well and mixed by pipetting up and down five times before the lysed sample was taken from each apical well. The  $P_{app}$  (cm/s) was calculated using the equation:

$$P_{app} = (dC_r/dt) \times V_r / (A \times C_0)$$

where  $dC_r/dt$  is the cumulative concentration of compound **11** in the receiver chamber as a function of time ( $\mu$ M/s);  $V_r$  is the solution volume in the receiver chamber (0.075 mL on the apical side and 0.25 mL on the basolateral side);  $A$  is the surface area for transport (i.e., 0.0804 cm<sup>2</sup>) for the area of the monolayer; and  $C_0$  is the initial concentration in the donor chamber ( $\mu$ M).

The efflux ratio was calculated using the equation:  $ER = P_{app}(BA)/P_{app}(AB)$ .

Percent recovery was calculated using the equation:

$$\% \text{ Recovery} = 100 \times [(V_r \times C_r) + (V_d \times C_d)] / (V_d \times C_0)$$

$$\% \text{ Total recovery} = 100 \times [(V_r \times C_r) + (V_d \times C_d) + (V_c \times C_c)] / (V_d \times C_0),$$

where  $V_d$  is the volume in the donor chamber (0.075 mL on the apical side and 0.25 mL on the basolateral side);  $C_d$  and  $C_r$  are the final concentrations of the transport compound in the donor and receiver chambers, respectively;  $C_c$  is the concentration in the cell lysate ( $\mu$ M); and  $V_c$  is the volume in the insert well (0.075 mL in this assay).

#### 4.12. Measurement of logD at a pH of 7.4

A 10 mM stock solution of compound **11** and controls (nadolol, mexiletine, propranolol, quinidine, amitriptyline, chlorpromazine) in DMSO were prepared, and 100 mM phosphate buffer including 1% DMSO (pH 7.4) was also prepared. Then 100 mL 1-Octanol was added to 10 mL of the phosphate buffer, vigorously shaken, and left standing overnight at room temperature before use. Then 1-Octanol Saturated Buffer was taken and stored at room temperature for a maximum of 1 week. Next, 10 mL phosphate buffer (pH 7.4) was added to 100 mL 1-Octanol, vigorously shaken, and left

standing overnight at RT before use, after which Octanol Saturated Buffer was taken and stored at room temperature for a maximum of 1 week. The IS was dissolved in ACN to a concentration of 0.5 mg/mL, after which 250  $\mu$ L IS and 5 mL 1-Octanol Saturated Buffer were added to 1 L 50% methanol/50% water to obtain an IS buffer solution. Compound **11** (10 mM in DMSO; 2  $\mu$ L/well) and control samples (10 mM in DMSO; 2  $\mu$ L/well) were transferred in duplicate from storage tubes to 96-well polypropylene cluster tubes. Then buffer-saturated 1-Octanol (150  $\mu$ L/well) and 1-Octanol Saturated Buffer (150  $\mu$ L/well) were added to each well. Each tube was vigorously mixed for 3 min, shaken for 1 h at 880 rpm at 26 °C, and centrifuged at 2500 rpm for 2 min. The buffer layer sample was diluted by 20-fold and the 1-Octanol layer sample was diluted 200-fold with IS solution. Then the concentration of the filtrate for compound **11** and the controls was determined by LC/MS/MS (LC/MS used was API 3000; aqueous solvent was water distilled with 2 mM ammonium acetate: Methanol (95%:5%); organic solvent was methanol:Water:FA (90%:10%:0.1%); the column used was a small molecule trap of  $1.5 \times 5$  mm from Optimize Technologies Inc. [Oregon City, OR, USA] and the Xbridge C18 Column ( $2.1 \times 50$  mm, 5  $\mu$ m) from Waters Corporation [Milford, MA, USA]). The logD value for compound **11** was calculated using the following equation:

#### 4.13. PK analysis

ICR male mice or SD male rats (Age: 6–8 weeks; Animal supplier: JOINN Laboratories, Inc.) were randomly divided into two groups ( $n = 3$  in each group) and were administered a single 2 mg/kg i.v. dose or single 5 mg/kg p.o. dose. The i.v. dose was administered as a solution in 10% NMP/90% (18% Captisol pH 3) vehicle, and the p.o. dose was administered as a solution in 0.1% HEC/0.5% Tween-80 vehicle. Serial blood samples were collected up to 24 h post-dose. Plasma samples were analyzed by LC/MS/MS (Acquity UPLC BEH C18 1.7  $\mu$ m,  $2.1 \times 50$  mm column; Mobile Phase A: 10 mM AA + 0.5% NH<sub>4</sub>OH + 5% MeOH in H<sub>2</sub>O; Mobile Phase B: 10 mM AA in 90% MeOH); ionization: ESI. PK parameters for compound **11** were determined from the plasma concentration-time data using non-compartmental methods.

#### 4.14. Blood-brain distribution studies

Male CD-1 mice (age: 6–8 weeks; animal supplier: JOINN (Suzhou) Laboratory Animal Co., Ltd.) were randomly divided into 7 groups ( $n = 3$  in each group) and were administered a single 10 mg/kg p.o. dose. For plasma samples, a 50  $\mu$ L aliquot sample was protein precipitated with 250  $\mu$ L ACN (500 ng/mL dexamethasone as internal standard in ACN), after which the mixture was thoroughly vortexed and centrifuged at 4000 rpm for 20 min at 4 °C. The 150  $\mu$ L supernatant was mixed with 150  $\mu$ L water with 0.1% FA, thoroughly vortexed, and centrifuged at 4 °C. Then 10  $\mu$ L sample was injected for LC/MS/MS analysis (LC/MS/MS-X [API 4000]; ESI: positive; Mobile Phase A: 0.1% FA in water; Mobile Phase B: 0.1% FA in ACN). To prepare brain homogenate samples, the brain tissue sample was homogenized for 2 min with 5 vol (w:v) of homogenizing solution (PBS [pH 7.4] buffer:MeOH [v:v, 2:1]). A 50  $\mu$ L aliquot protein sample was precipitated with 250  $\mu$ L ACN (500 ng/mL dexamethasone as internal standard in ACN), the mixture was thoroughly vortexed and centrifuged at 4000 rpm for 20 min at 4 °C. The 150  $\mu$ L supernatant was mixed with 150  $\mu$ L water with 0.1% FA, thoroughly vortexed, and centrifuged at 4 °C. Then the 10  $\mu$ L sample was injected for LC/MS/MS analysis (LC/MS/MS-X [API 4000]; ESI: positive; Mobile Phase A: 0.1% FA in water; Mobile Phase B: 0.1% FA in ACN).

#### 4.15. Determination of plasma protein binding

CD-1 mouse plasma was purchased from Bioreclamation IVT (Baltimore, MD, USA), the HT-Dialysis plate (Model HTD 96 b, Cat. #1006) and the dialysis membrane (MW cut off 12–14 kDa, Cat. #1101) were purchased from HT Dialysis LLC (Gales Ferry, CT, USA). A total of 28.56 g  $\text{Na}_2\text{HPO}_4 \cdot 12\text{H}_2\text{O}$  (AR grade) and 3.12 g  $\text{NaH}_2\text{PO}_4 \cdot 2\text{H}_2\text{O}$  (AR grade) were dissolved in 1000 mL ultrapure water, mixed, and adjusted to a final solution of 1% phosphoric acid or 1 M sodium hydroxide at a pH  $7.4 \pm 0.1$ ; it was stored at  $2-8^\circ\text{C}$  refrigerator. Pooled plasma (frozen at  $<-70^\circ\text{C}$ ) was thawed in a water bath at  $37^\circ\text{C}$  for 10–20 min and centrifuged at 4000 rpm for 5 min to remove any clots. The pH value was checked and adjusted to  $7.4 \pm 0.1$  if required. The dialysis membrane was soaked in ultrapure water at RT for approximately 1 h, separated into two strips, and then soaked in ethanol:water (20:80 v:v) at  $2-8^\circ\text{C}$  overnight. Prior to the experiment, the membrane was rinsed with ultrapure water. A concentration of 400  $\mu\text{M}$  working solution was made by diluting the appropriate volume of stock solution with DMSO. Then 2  $\mu\text{M}$  final solution was made by diluting 4  $\mu\text{L}$  of working solution (400  $\mu\text{M}$ ) with 796  $\mu\text{L}$  blank plasma, followed by thorough mixing. Each well of the dialysis plate was incubated with 150  $\mu\text{L}$  plasma solution (in triplicate) and then loaded and dialyzed against an equal volume of dialysis buffer. Before dialysis, 50  $\mu\text{L}$  aliquots of spiked plasma (in triplicate) were removed ( $T_0$  sample) and stored at  $-40^\circ\text{C}$ . The dialysis plate was sealed and placed in an incubator at  $37^\circ\text{C}$  for 4 h with rotation at 150 rpm. After dialysis, aliquots of dialysate (50  $\mu\text{L}$ ) and retenate (50  $\mu\text{L}$ ) were removed and transferred to a new 96-well polypropylene plate (sample collection plate). All of the samples in each well were incubated with an equal volume of blank matrix to obtain a final 50:50 ratio of plasma:dialysis buffer in each well. The samples were diluted with 300  $\mu\text{L}$  of 50% ACN/MeOH (containing 200 ng/mL Tolbutamide and 20 ng/mL Buspirone) to precipitate the protein in the plasma. The samples in the collection plate were shaken at 800 rpm for 5 min to mix the samples and were centrifuged at 4000 rpm for 20 min. An aliquot of supernatant (100  $\mu\text{L}$ ) in each well was transferred and mixed with 200  $\mu\text{L}$  ultrapure water before it was subjected to LC/MS/MS analysis (LC system used was Shimadzu LC 20-AD; MS system used was API 4000; column used was ACE Phenyl,  $50 \times 2.1$  mm; Mobile Phase A was 0.1% FA in Water; Mobile Phase B was 0.1% FA in CAN). The concentration was calculated using the peak area ratio of analyte and IS. The results were calculated by the following equations:

$$\% \text{ Unbound} = 100 * F_C / T_C, \% \text{ Bound} = 100 - \% \text{ Unbound}$$

and

$$\% \text{ Recovery} = 100 * (F_C + T_C) / T_0,$$

where  $T_C$  is the total compound concentration as determined by the calculated concentration on the retenate side of the membrane,  $F_C$  is the free compound concentration as determined by the calculated concentration on the dialysate side of the membrane, and  $T_0$  is the total compound concentration as determined before dialysis.

#### 4.16. Determination of brain binding

CD-1 mouse brain homogenate was prepared in a WuXi AppTec Co. Ltd. HT-Dialysis plate (Model HTD 96b, Cat. #1006) and the dialysis membrane (MW cut off of 12–14 kDa, Cat. #1101) were purchased from HT Dialysis LLC. A total of 28.56 g  $\text{Na}_2\text{HPO}_4 \cdot 12\text{H}_2\text{O}$  (AR grade) and 3.12 g  $\text{NaH}_2\text{PO}_4 \cdot 2\text{H}_2\text{O}$  (AR grade) were dissolved to a final volume of 1000 mL ultrapure water and mixed, resulting in 1% phosphoric acid or 1 M sodium hydroxide solutions at a pH of

$7.4 \pm 0.1$ . The final solution was stored in a  $2-8^\circ\text{C}$  refrigerator. CD-1 mouse brain homogenate was thawed in a water bath at RT before use. The dialysis membrane was soaked in ultrapure water at RT for approximately 1 h, separated into two strips, and soaked in ethanol:water (20:80 v:v) at  $2-8^\circ\text{C}$  overnight. Prior to the experiment, the membrane was rinsed with ultrapure water. Working solutions (400  $\mu\text{M}$ ) of compound **11** were prepared by diluting the appropriate volume of stock solutions with DMSO. Aliquots of 5  $\mu\text{L}$  of working solutions (400  $\mu\text{M}$ ) were spiked into 995  $\mu\text{L}$  blank plasma/brain homogenate (matrix) to achieve 2  $\mu\text{M}$  final concentrations as loading solutions. The plates containing loading solution were shaken. The concentration of organic solvent in the final solution was 0.5% DMSO. Aliquots of 50  $\mu\text{L}$  loading solution were transferred in triplicate to sample collection plates at time zero ( $T_0$ ) for recovery calculation. The samples were immediately incubated with blank buffer to obtain a final volume of 100  $\mu\text{L}$  with a 50:50 ratio of matrix:dialysis buffer in each well. The  $T_0$  samples were added to 500  $\mu\text{L}$  stop solution containing 50% ACN/Methanol containing IS (200 ng/mL tolbutamide and 20 ng/mL buspirone). Then the sample plates were oscillated thoroughly and stored at  $2-8^\circ\text{C}$  until being further processed along with other post-dialysis samples. Aliquots of 150  $\mu\text{L}$  loading solution were loaded in triplicate to the donor side of each dialysis well and dialyzed against an equal volume of dialysis buffer. Then the plate was sealed with cap strips and rotated at approximately 100 rpm in a humidified incubator with 5%  $\text{CO}_2$  at  $37^\circ\text{C}$  for 4 h. At the end of dialysis, aliquots of dialysate (50  $\mu\text{L}$ ) and retenate (50  $\mu\text{L}$ ) were placed into sample collection plates. Each sample was matched with blank buffer or matrix to obtain a final volume of 100  $\mu\text{L}$  with a 50:50 vol ratio of matrix:dialysis buffer in each well and 500  $\mu\text{L}$  of stop solution. All samples in the collection plates were shaken at 800 rpm for 5 min to mix the samples and centrifuged at  $20^\circ\text{C}$  at 4000 rpm for 20 min. Aliquots of supernatant (150  $\mu\text{L}$ ) in each well were transferred into new 96-well sample plates before being subjected to LC/MS/MS analysis (LC system was Shimadzu LC 20-AD; MS was API 4000; column was ACE Phenyl,  $50 \times 2.1$  mm; Mobile Phase A was 0.1% FA in Water; Mobile Phase B was 0.1% FA in ACN). The concentration was calculated using the peak area ratio of analyte and IS. The results were calculated by the following equations:

$$\% \text{ Unbound} = 1 / D / (1 / (F_C / T_C) - 1) + 1 / D * 100$$

and

$$\% \text{ Recovery} = 100 * (F_C + T_C) / T_0,$$

where  $T_C$  is the total compound concentration as determined by the calculated concentration on the retenate side of the membrane,  $F_C$  is the free compound concentration as determined by the calculated concentration on the dialysate side of the membrane, and  $T_0$  is the total compound concentration as determined before dialysis; Dilution factor (D) was determined to be 10 in this assay.

#### 4.17. Inhibition of Rb phosphorylation in nude mice bearing subcutaneous COLO 205 human colon tumors

COLO 205 tumor cells were maintained *in vitro* as a monolayer culture in RPMI 1640 medium supplemented with 10% fetal bovine serum at  $37^\circ\text{C}$  in an atmosphere of 5%  $\text{CO}_2$  in air. The tumor cells were routinely sub-cultured twice weekly. Cells in an exponential growth phase were harvested and counted after tumor inoculation. Each of the female nude mice (age: 8–10 weeks; animal supplier: Beijing HFK Bio-Technology Co. Ltd.) was inoculated subcutaneously at the right flank with COLO 205 tumor cells ( $5 \times 10^6$ ) in 0.1 mL PBS for tumor development. Tumor volumes were measured



in two dimensions using a caliper, and the volume was expressed in mm<sup>3</sup> using the formula:  $V = 0.5 a \times b^2$  where  $a$  and  $b$  are the long and short diameters of the tumor, respectively. The treatments were started when the mean tumor size reached approximately 489 mm<sup>3</sup>. Before commencement of treatment, all animals were weighed and the tumor volumes were measured using a caliper. Since tumor volume could affect the effectiveness of any given treatment, mice were assigned to groups using the randomized block design based on their tumor volumes to ensure that all groups had comparable baselines. After animals were randomized into groups (three mice/group) by tumor volume, compound **11** was formulated in 0.1% HPC/0.25% Tween 80 and administered orally by gavage (final volume 0.2 mL) once daily with the scheduled dose. For biomarker analysis, the animals were asphyxiated with CO<sub>2</sub> and tumors were quickly removed, weighed, homogenized in lysis buffer, and centrifuged. The lysates were stored at –80 °C until subsequent analysis.

#### 4.18. Western blot analysis

The protein samples were heated at 95 °C for 10 min, and clarified by centrifugation at 12000 rpm for 10 min at 4 °C. Proteins were resolved on 10% SDS-PAGE gels (10 µg cell lysate per lane), transferred to nitrocellulose membranes, and blocked for 1 h at 37 °C in 5% dry milk in TBST (137 mM sodium chloride, 20 mM Tris, 0.05% Tween-20). Then membranes were incubated in the same buffer with primary antibodies overnight at 4 °C, incubated for 1 h with horseradish peroxidase-conjugated secondary antibody, washed again with TBST, and developed using chemiluminescent substrate. Band intensity was determined using Image J. Molecular Imager with Amersham Imager 600 (GE Healthcare).

#### 4.19. Orthotopic nude mouse model

Female nude mice (age: 6–8 weeks; bodyweight: 18–22 g; Animal supplier: Shanghai Sino-British SIPPR/BK Laboratory Animal Co., Ltd.) were anesthetized by intraperitoneal (i.p.) injection of 80 mg/kg pentobarbital sodium. For pain relief, the animals were dosed subcutaneously (s.c.) 30 min before surgery with 0.1 mg/kg of buprenorphine and 6 h post-surgery. Animals were observed post-anesthesia until recovery. The anesthetized mouse was properly positioned. The head skin of the mouse was sterilized with 70% alcohol and draped in a sterile fashion. An incision of around ~10 mm was made just at the right of the midline and anterior to the interaural line. Each mouse was inoculated intracranially with  $3 \times 10^5$  U87-Luc cells mixed with Matrigel in 3 µL (PBS:Matrigel = 4:1) at the right frontal lobe, 2 mm lateral from the bregma, and 0.5 mm from the anterior at a depth of 3.5 mm. The incision was stitched using No. 6 suture and then sterilized with povidone-iodine solution. The mice were kept warm until they recovered from anesthesia. The animals were randomized to treatment groups (8 mice/group) based on their bioluminescence density on day 6 after tumor implantation, and the average bioluminescence reached  $2.812 \times 10^7$  photons/sec. The mice were treated daily for 35 days with compound **11**. Body weights were measured once every 2 days. The surgically inoculated mice were weighed and administered luciferin at a dose of 150 mg/kg i.p. Then, 10 min after luciferin injection, the animals were pre-anesthetized with a gas mixture of oxygen and isoflurane. When the animals were in a complete anesthetic state, the mice were moved into the imaging chamber for bioluminescence measurements with an IVIS (Lumina II) imaging system. Bioluminescence of the whole animal body was measured and recorded once per week. Then tumor bioluminescence was used for the calculation of TGI value (in percent). Animals were checked daily and animals that

showed deteriorating and moribund condition (animals that had lost significant [ $>20\%$ ] body weight) and those that were unable to consume adequate amounts of food or water were euthanized with CO<sub>2</sub>. Body weights were measured once every 2 days. The survival of all animals was followed and the MST was calculated for each group. The increase in life span was calculated by dividing the difference in MST of the treatment group from the control group by the MST of the vehicle-treated animals, (i.e., the percent increase over the life span of the control animals).

#### Compliance with ethical standards

All protocols requiring the use of mice were approved by the Animal Care Committee of Beijing Normal University.

#### Conflicts of interest

The authors have no competing financial interests to declare.

#### Acknowledgments

We gratefully acknowledge the financial support from the Development of Significant New Drugs program (Grant No. 2014ZX09507007001), the Natural Science Foundation of China (No. 201371026), and the Science and Technology Support Program (No. 2014BAA03B03). The authors are grateful to Xin Cai from FenDi Technology Co. Ltd. for the support in calculational chemistry, and Zhenhua Chen for providing many key intermediates.

#### Appendix A. Supplementary data

Supplementary data related to this article can be found at <https://doi.org/10.1016/j.ejmech.2017.12.003>.

#### References

- [1] S. Roy, D. Lahiri, T. Maji, J. Biswas, Recurrent glioblastoma: where we stand, *South Asian J. Cancer* 4 (2015) 163–173.
- [2] R. Stupp, W.P. Mason, M.J. van den Bent, M. Weller, B. Fisher, M.J.B. Taphoorn, K. Belanger, A.A. Brandes, C. Marosi, U.M.D. Bogdahn, J. Curschmann, R.C. Janzer, S.K. Ludwin, T. Gorlia, A. Allgeier, D. Lacombe, J.G. Cairncross, E. Eisenhauer, R.O. Mirimanoff, Radiotherapy plus concomitant and adjuvant temozolomide for glioblastoma, *N. Engl. J. Med.* 352 (2005) 987–996.
- [3] M.H. Cohen, J.R. Johnson, R. Pazdur, Food and Drug Administration Drug approval summary: temozolomide plus radiation therapy for the treatment of newly diagnosed glioblastoma multiforme, *Clin. Cancer Res.* 11 (2005) 6767–6771.
- [4] S.A. Chowdhary, T. Ryken, H.B. Newton, Survival outcomes and safety of carmustine wafers in the treatment of high-grade gliomas: a meta-analysis, *J. Neurooncol.* 122 (2015) 367–382.
- [5] H. Wang, X. Zhang, L. Teng, R.J. Legerski, DNA damage check point recovery and cancer development, *Exp. Cell Res.* 334 (2015) 350–358.
- [6] J.W. Harbour, R.X. Luo, A. DeiSanti, A.A. Postigo, D.C. Dean, CDK phosphorylation triggers sequential intramolecular interactions that progressively block Rb functions as cells move through G1, *Cell* 98 (1999) 859–869.
- [7] C.J. Sherr, G1 phase progression: cycling on cue, *Cell* 79 (1994) 551–555.
- [8] M. Malumbres, M. Barbacid, Cell cycle, CDKs and cancer: a changing paradigm, *Nat. Rev. Cancer* 9 (2009) 153–166.
- [9] S. Ortega, M. Malumbres, M. Barbacid, Cyclin D-dependent kinases, INK4 inhibitors and cancer, *Biochim. Biophys. Acta* 1602 (2002) 73–87.
- [10] G.I. Shapiro, Cyclin-dependent kinase pathways as targets for cancer treatment, *J. Clin. Oncol.* 24 (2006) 1770–1783.
- [11] (a) The Cancer Genome Atlas Network, Comprehensive genomic characterization defines human glioblastoma genes and core pathways, *Nature* 455 (2008) 1061–1068; (b) D.W. Parsons, S. Jones, X. Zhang, J.C.-H. Lin, R.J. Leary, P. Angenendt, P. Mankoo, H. Carter, I.-M. Siu, G.L. Gallia, A. Olivi, R. McLendon, B.A. Rasheed, S. Keir, T. Nikolskaya, Y. Nikolsky, D.A. Busam, H. Tekleab, L.A. Diaz, J. Hartigan, D.R. Smith, R.L. Strausberg, S.K.N. Marie, S.M.O. Shinjo, H. Yan, G.J. Riggins, D.D. Bigner, R. Karchin, N. Papadopoulos, G. Parmigiani, B. Vogelstein, V.E. Velculescu, K.W. Kinzler, An integrated genomic analysis of human glioblastoma multiforme, *Science* 321 (2008) 1807–1812.
- [12] (a) B.S. Paugh, A. Broniscer, C. Qu, C.P. Miller, J. Zhang, R.G. Tatevosian, J.M. Olson, J.R. Geyer, S.N. Chi, N.S. da Silva, A. Onar-Thomas, J.N. Baker,

- A. Gajjar, D.W. Ellison, Z.J. Baker, Genome-wide analyses identify recurrent amplifications of receptor tyrosine kinases and cell-cycle regulatory genes in diffuse intrinsic pontine glioma, *J. Clin. Oncol.* 29 (2011) 3999–4006;
- (b) K.E. Warren, K. Killian, M. Suuriniemi, Y. Wang, M. Quezado, P.S. Meltzer, Genomic aberrations in pediatric diffuse intrinsic pontine gliomas, *Neuro-Oncology* 14 (2012) 326–332.
- [13] (a) C. McInnes, Progress in the evaluation of CDK inhibitors as anti-tumor agents, *Drug Discov. Today* 13 (2008) 875–881;
- (b) F. Graf, B. Mosch, L. Koehler, R. Bergmann, F. Wuest, J. Pietzsch, Cyclin-dependent kinase 4/6 (CDK4/6) inhibitors: perspectives in cancer therapy and imaging, *Mini Rev. Med. Chem.* 10 (2010) 527–539;
- (c) V. Krystof, S. Uldrijan, Cyclin-dependent kinase inhibitors as anticancer drugs, *Curr. Drug Targets* 11 (2010) 291–302;
- (d) J. Cienas, K. Kalyan, A. Sorokinas, A. Jatulyte, D. Valiunas, A. Kaupinis, M. Valius, Highlights of the latest advances in research on CDK inhibitors, *Cancers (Basel)* 6 (2014) 2224–2242.
- [14] (a) P.L. Toogood, P.J. Harvey, J.T. Repine, D.J. Sheehan, S.N. VanderWel, H. Zhou, P.R. Keller, D.J. McNamara, D. Sherry, T. Zhu, J. Brodfuehrer, C. Choi, M.R. Barvian, D.W. Fry, Discovery of a potent and selective inhibitor of Cyclin-dependent kinase 4/6, *J. Med. Chem.* 48 (2005) 2388–2406;
- (b) S. Dhillon, Palbociclib: first global approval, *Drugs* 75 (2015) 543–551.
- [15] L.M. Gelbert, S. Cai, X. Lin, C. Sanchez-Martinez, M. del Prado, M.-J. Lallena, R. Torres, R.T. Ajamie, G.N. Wishart, R.S. Flack, B.L. Neubauer, J. Young, E.M. Chan, P. Iversen, D. Cronier, E. Kreklau, A. de Dios, Preclinical characterization of the CDK4/6 inhibitor LY2835219: in-vivo cell cycle-dependent/independent anti-tumor activities alone/in combination with gemcitabine, *Invest. New Drugs* 32 (2014) 825–837.
- [16] Yogesh Patel, Abigail Davis, Ashish Kala, Jessica Roberts, Megan Jacus, Suzanne Baker, Martine Roussel, Clinton Stewart, PDTB-12, CNS penetration of the CDK4/6 inhibitor ribociclib (LEE011) in non-tumor bearing mice and mice bearing orthotopic pediatric brain tumors, *Neuro Oncol.* 18 (2016) vi152.
- [17] (a) <https://clinicaltrials.gov/ct2/show/NCT02896335?term=palbociclib&rank=13>.
- (b) <https://clinicaltrials.gov/ct2/show/NCT02981940?term=abemaciclib&rank=2>.
- (c) <https://clinicaltrials.gov/ct2/show/NCT02345824> (Accessed 25 March, 2017).
- [18] K.L. Barton, K. Misuraca, F. Cordero, E. Dobrikova, H.D. Min, M. Gromeier, D.G. Kirsch, O.J. Becher, PD-0332991, a CDK4/6 inhibitor, significantly prolongs survival in a genetically engineered mouse model of brainstem glioma, *PLoS One* 8 (2013), e77639.
- [19] T.J. Raub, G.N. Wishart, P. Kulanthaivel, B.A. Staton, R.T. Ajamie, G.A. Sawada, L.M. Gelbert, H.E. Shannon, C. Sanchez-Martinez, A. De Dios, Brain exposure of two selective dual CDK4 and CDK6 inhibitors and the antitumor activity of CDK4 and CDK6 inhibition in combination with Temozolomide in an intracranial glioblastoma xenograft, *Drug Metab. Dispos.* 43 (2015) 1360–1371.
- [20] K. Michaud, D.A. Solomon, E. Oermann, J.-S. Kim, W.-Z. Zhong, M.D. Prados, T. Ozawa, C.D. James, T. Waldman, Pharmacologic inhibition of cyclin-dependent kinases 4 and 6 arrests the growth of glioblastoma multiforme intracranial xenografts, *Cancer Res.* 70 (2010) 3228–3238.
- [21] T.P. Heffron, Small molecule kinase inhibitors for the treatment of brain cancer, *J. Med. Chem.* 59 (2016) 10030–10066.
- [22] J.-A. Rader, M. Russell, L.S. Hart, M.S. Nakazawa, L.T. Belcastro, L. Martinez, Y. Li, E.L. Carpenter, E.F. Attiyeh, S.J. Diskin, S.S. Parasuraman, G. Caponigro, R.W. Schnepf, A.C. Wood, B. Pawel, K.A. Cole, J.M. Maris, Dual CDK4/CDK6 inhibition induces cell cycle arrest and senescence in neuroblastoma, *Clin. Cancer Res.* 19 (2013) 6173–6182.
- [23] D.W. Fry, P.J. Harvey, P.R. Keller, W.L. Elliott, M.-A. Meade, E. Trachet, M. Albassam, X.-X. Zheng, W.R. Leopold, N.K. Pryer, P.L. Toogood, Specific inhibition of cyclin-dependent kinase 4/6 by PD 0332991 and associated antitumor activity in human tumor xenografts, *Mol. Cancer Ther.* 3 (2004) 1427–1438.
- [24] (a) H. Sun, H. Dai, N. Shaik, W.F. Elmquist, Drug efflux transporters in the CNS, *Adv. Drug Deliv. Rev.* 55 (2003) 83–105;
- (b) H. He, K.A. Lyons, X. Shen, Z. Yao, K. Bleasby, G. Chan, M. Hafey, X. Li, S. Xu, G.M. Salituro, L.H. Cohen, W. Tang, Utility of unbound plasma drug levels and P-glycoprotein transport data in prediction of central nervous system exposure, *Xenobiotica* 39 (2009) 687–693;
- (c) H. Kodaira, H. Kusuhara, T. Fujita, J. Ushiki, E. Fuse, Y. Sugiyama, Quantitative evaluation of the impact of active efflux by p-glycoprotein and breast cancer resistance protein at the blood-brain barrier on the predictability of the unbound concentrations of drugs in the brain using cerebrospinal fluid concentration as a surrogate, *J. Pharmacol. Exp. Ther.* 339 (2011) 935–944.
- [25] Z. Rankovic, CNS Drug design: balancing physicochemical properties for optimal brain exposure, *J. Med. Chem.* 58 (2015) 2584–2608.
- [26] P.V. Desai, G.A. Sawada, I.A. Watson, T.J. Raub, Integration of in silico and in vitro tools for scaffold optimization during drug discovery: predicting P-glycoprotein efflux, *Mol. Pharm.* 10 (2013) 1249–1261.
- [27] S.A. Hitchcock, Structural modifications that alter the P-glycoprotein efflux properties of compounds, *J. Med. Chem.* 55 (2012) 4877–4895.
- [28] Uzma Asghar, Agnieszka K. Witkiewicz, Nicholas C. Turner, Erik S. Knudsen, The history and future of targeting cyclin-dependent kinases in cancer therapy, *Nat. Rev. Drug Discov.* 14 (2015) 130–146.
- [29] Young Shin Cho, Maria Borland, Christopher Brain, Christine H.-T. Chen, Hong Cheng, Rajiv Chopra, Kristy Chung, James Groarke, Guo He, Ying Hou, Sunkyu Kim, Steven Kovats, Yipin Lu, Marc O'Reilly, Junqing Shen, Troy Smith, Gary Trakshel, Markus Vogtle, Mei Xu, Ming Xu, Moo Je Sung, 4-(Pyrazol-4-yl)-pyrimidines as selective inhibitors of Cyclin-dependent kinase 4/6, *J. Med. Chem.* 53 (2010) 7938–7957.
- [30] Heshu Lu, Ursula Schulze-Gahmen, Toward understanding the structural basis of Cyclin-dependent kinase 6 specific inhibition, *J. Med. Chem.* 49 (2006) 3826–3831.
- [31] (a) T.T. Wager, R.Y. Chandrasekaran, X. Hou, M.D. Troutman, P.R. Verhoest, A. Villalobos, Y. Will, Defining desirable central nervous system drug space through the alignment of molecular properties, in vitro ADME, and safety attributes, *ACS Chem. Neurosci.* 1 (2010) 420–434;
- (b) T.T. Wager, X. Hou, P.R. Verhoest, A. Villalobos, Moving beyond rules: the development of a central nervous system multiparameter optimization (CNS MPO) approach to enable alignment of druglike properties, *ACS Chem. Neurosci.* 1 (2010) 435–449.
- [32] G. Bellec, Y. Dréano, P. Lozach, J.F. Ménez, F. Berthou, Cytochrome P450 metabolic dealkylation of nine N-nitrosodialkylamines by human liver microsomes, *Carcinogenesis* 17 (1996) 2029–2034.
- [33] M.R. Finlay, D.G. Acton, D.M. Andrews, A.J. Barker, M. Dennis, E. Fisher, M.A. Graham, C.P. Green, D.W. Heaton, G. Karoutchi, S.A. Loddick, R. Morgentin, A. Roberts, J.A. Tucker, H.M. Weir, Imidazole piperazines: SAR and development of a potent class of cyclin-dependent kinase inhibitors with a novel binding mode, *Bioorg. Med. Chem. Lett.* 18 (2008) 4442–4446.
- [34] (a) S. Tadesse, M. Yu, M. Kumarasiri, B.T. Le, S. Wang, Targeting CDK6 in cancer: state of the art and new insights, *Cell Cycle* 14 (2015) 3220–3230;
- (b) S. Muller, A. Chaikuad, N.S. Gray, S. Knapp, The ins and outs of selective kinase inhibitor development, *Nat. Chem. Biol.* 11 (2015) 818–821.
- [35] Christopher A. Lipinski, Drug-like properties and the causes of poor solubility and poor permeability, *J. Pharmacol. Toxicol. Methods.* 44 (2000) 235–249.
- [36] H. Van de Waterbeemd, G. Camenisch, G. Folkers, J.R. Chretien, O.A. Raevsky, Estimation of blood–brain barrier crossing of drugs using molecular size and shape, and H-bonding descriptors, *J. Drug Target.* 6 (1998) 151–165.
- [37] M.J. Waring, Defining optimum lipophilicity and molecular weight ranges for drug candidates - molecular weight dependent lower logD limits based on permeability, *Bioorg. Med. Chem. Lett.* 19 (2009) 2844–2851.
- [38] S.A. Hitchcock, Structural modifications that alter the P-glycoprotein efflux properties of compounds, *J. Med. Chem.* 55 (2012) 4877–4895.
- [39] H. Pajouhesh, G.R. Lenz, Medicinal chemical properties of successful central nervous system drugs, *NeuroRx* 2 (2005) 541–553.
- [40] Ji Jianguo, Li Tao, William H. Bunnelle, Selective amination of polyhalopyridines catalyzed by a palladium–xantphos complex, *Org. Lett.* 5 (24) (2003) 4611–4614.
- [41] P. Brett, Fors Nicole, R. Davis, Stephen L. Buchwald, A highly active catalyst for palladium-catalyzed cross-coupling reactions: room-temperature suzuki couplings and amination of unactivated aryl chlorides, *J. Am. Chem. Soc.* 120 (1998) 9722–9723.